

**AN INVESTIGATION INTO PRESSURE DROP ACROSS
BENDS FOR FLUIDISED DENSE PHASE PNEUMATIC
CONVEYING SYSTEMS**

**A
THESIS**

Submitted in partial fulfillment of the requirements for the award of degree of

Master of Engineering (M.E.)

**In
Thermal Engineering**

**Submitted by
NAVEEN MANI TRIPATHI
(ROLL NO. 801283018)**



UNDER THE GUIDANCE OF

**Dr. S.S. MALLICK
(Assistant Professor)**

**DEPARTMENT OF MECHANICAL ENGINEERING
THAPAR UNIVERSITY, PATIALA – 147004**

JULY 2014

CERTIFICATION

I, Naveen Mani Tripathi, hereby declare that this thesis report entitled "*An Investigation into pressure drop across bends for fluidised dense phase pneumatic conveying systems*" submitted in the partial fulfilment of the requirements for the award of degree of Master of Engineering in Thermal Engineering, in the Mechanical Department, Thapar University, Patiala, is wholly my own work. This matter embodied in this report has not been submitted in part or full to any other university or institute for the award of any degree.

Date: 24/06/2014

Place: Patiala



Naveen Mani Tripathi

801283018

Thapar University, Patiala

This is to certify that above statement made by the student concerned is correct and true to the best of my knowledge & belief.



Supervisor:

Dr. S.S. Mallick

Assistant Professor

Mechanical Engineering Department

Thapar University, Patiala

Countersigned by



Dr. Ajay Batish

Professor and Head

Mechanical Engineering Department

Thapar University, Patiala



Dr. S.K. Mohapatra

Dean

Academic Affairs

Thapar University, Patiala

ACKNOWLEDGEMENT

This work grew out of a series of dialogues with Dr. S.S. Mallick whose capacity to combine critique with an immediate empathy and commitment towards the research will always inspire me. His advice on interpreting the case study results and productive comments on an earlier draft directly contributed to this study.

Most of the results described in this thesis would not have been obtained without the experimental data of University of Wollongong laboratories. I owe a great deal of appreciation and gratitude to Prof. P.W. Wypych, University of Wollongong, Australia, for providing me the valuable information and relevant experimental data.

The opportunity, support, exposure and atmosphere provided by the Thapar University, Patiala, to carry out my studies are highly appreciated.

The financial support provided by the Department of Science and Technology (DST) and Council of Scientific and Industrial Research (CSIR) to carry out my studies is greatly appreciated.

A special debt of gratitude is owed to the authors whose works I have consulted and quoted in this work.

Last but not least, I am forever grateful to my parents for their unconditional support and best wishes.

ABSTRACT

An accurate estimation of the total pipeline pressure drop is of significant importance for the reliable design of a pneumatic conveying system. This report presents results from an investigation into the modelling of bend pressure drop for pneumatic conveying of fly ash. Seven existing bend models were used (in conjunction with solids friction models for straight pipes, verticals and initial acceleration losses) to predict the total pipeline pressure drop for conveying of two fly ash (median particle diameter: 30 μm ; particle density: 2300 kg/m^3 ; loose-poured bulk density: 700 kg/m^3 and median particle diameter: 45 μm ; particle density: 1950 kg/m^3 ; loose-poured bulk density: 950 kg/m^3) in five test rigs: 69 mm I.D. x 168 m long; 105 mm I.D. x 168 m long; 69 mm I.D. x 554 m; 63.5 mm I.D. x 24 m; 50 mm I.D. x 70 m long pipes. A comparison amongst the predicted pneumatic conveying characteristics (PCC) using all seven bend models (and the experimental plots) indicated that the values of predicted total pipeline PCC and trends significantly depend to the choice of bend models. While some models have provided trends confirming to the experimental plots, some other models resulted in prediction of higher bend pressure drop values in dense-phase than in dilute-phase. Pan (1992), Pan and Wypych (1998) and Chambers and Marcus (1986) models are found to be suitable to reliably predict the bend losses for fly ash conveying systems over a large range of air flows.

The comparisons demonstrated the limitations of “existing” models. A large number of pneumatic conveying tests has been conducted for two different pipeline configurations to develop a solid friction factor model for pressure drop prediction in closely coupled bend.

TABLE OF CONTENTS

	Page No.
CERTIFICATION	i
ACKNOWLEDGEMENT	ii
ABSTRACT	iii
TABLE OF CONTENTS	iv
LIST OF FIGURES	vi
LIST OF TABLES	xi
LIST OF SYMBOLS AND ABBRIVIATIONS	xii
CHAPTER 1: Introduction and Objectives	1
1.1 Introduction	2
1.2 Objectives	5
CHAPTER 2: Literature Review	7
2.1 Pneumatic conveying	8
2.2 Modes of pneumatic conveying systems	9
2.3 Basic components of pneumatic conveying system	15
2.4 Bends	16
2.5 Properties of bulk solids	19
2.6 Material classification	24
2.7 Design consideration of pneumatic conveying system	27
2.8 Models to predict bend pressure drop	31
CHAPTER 3: Test facility and procedures	40
3.1 Introduction	41
3.2 Experimental program	41

CHAPTER 4: Evaluation of different bend models	53
4.1 Introduction	54
4.2 Model for solid friction factor of horizontal straight pipe	54
4.3 Evaluation of bend models based on UoW data	56
4.4 Evaluation of bend models based on TU data	65
CHAPTER 5: Modelling and validation of solid friction factor model for closely coupled bend	73
5.1 Introduction	74
5.2 General power function format	75
CHAPTER 6: Conclusion and future scope of work	79
6.1 Conclusion	80
6.2 Future scope of work	81
REFERENCES	83
APPENDIX: A1	89
APPENDIX: A2	92
APPENDIX: A3	113
LIST OF PUBLICATIONS	116

LIST OF FIGURES

	Page No.
Figure 1.1: Typical PCC for Fluidised Dense-Phase	4
Figure 2.1: Dilute phase pneumatic conveying	10
Figure 2.2: Dense phase pneumatic conveying	11
Figure 2.3: Fluidised dense phase	12
Figure 2.4: Low velocity slug flow	13
Figure 2.5: Low velocity plug flow	13
Figure 2.6: Internal bypass and external bypass	14
Figure 2.7: Single slug conveying	14
Figure 2.8: Air-assisted gravity conveying	15
Figure 2.9: Component of pneumatic conveying system	15
Figure 2.10: Short radius bend	17
Figure 2.11: Blind tee and blind bend	18
Figure 2.12: Gamma bend	18
Figure 2.13: An ideal fluidization curve showing a typical test chamber and parameters $\Delta p/h$, V_f , and U_{mf}	23
Figure 2.14: Geldart's fluidization diagram	25
Figure 2.15: Pressure drop in double bends	38
Figure 3.1: Layout of the 69 mm I.D. x 168 m long pipeline Test Rig (for fly ash)	45
Figure 3.2: Layout of the 63.5 mm I.D. x 24 m long pipeline Test Rig (for fly ash)	47
Figure 3.3: Test Bend of 1 m bend radius	48

Figure 3.4: Piping and Instrumentation diagram for compressed air of 63.5 mm I.D. x 24 m Test Rig (for fly ash)	48
Figure 3.5 (a): Calibration factor for pressure transducer (P4)	50
Figure 3.5 (b): Calibration factor for pressure transducer (P6)	51
Figure 4.1: Comparison of experimental versus predicted values of total pipeline pressure drop (fly ash, D = 69 mm, L = 168 m, $m_s = 19$ t/h)	57
Figure 4.2: Comparison of experimental versus predicted values of total pipeline pressure drop (fly ash, D = 105 mm, L = 168 m, $m_s = 28$ t/h)	58
Figure 4.3: Comparison of experimental versus predicted values of total pipeline pressure drop (fly ash, D = 69 mm, L = 554 m, $m_s = 11$ t/h)	59
Figure 4.4: Bend loss PCC based on different bend models (fly ash, D = 69 mm, L = 168 m, $m_s = 19$ t/h)	62
Figure 4.5: Comparison of bend only pressure drop between low velocity flow and high velocity (fly ash, D = 105 mm, L = 168 m, $m_s = 28$ t/h)	63
Figure 4.6: Comparison of bend only pressure drop between low velocity flow and high velocity (fly ash, D = 69 mm, L = 554 m, $m_s = 11$ t/h)	64
Figure 4.7: Comparison of experimental versus predicted values of total pipeline pressure drop (fly ash, D = 63.5 mm, L = 24 m, $m_s = 4.5$ t/h)	66
Figure 4.8: Comparison of experimental versus predicted values of total pipeline pressure drop (fly ash, D = 63.5 mm, L = 24 m, $m_s = 3.5$ t/h)	67
Figure 4.9: Comparison of experimental versus predicted values of total pipeline pressure drop (fly ash, D = 50 mm, L = 70 m, $m_s = 2.5$ t/h)	68

Figure 4.10: Comparison of experimental versus predicted values of total pipeline pressure drop (fly ash, $D = 50$ mm, $L = 70$ m, $m_s = 1.5$ t/h)	69
Figure 4.11: Bend loss PCC based on different bend models in dense to dilute phase (fly ash, $D = 63.5$ mm, $L = 24$ m, $m_s = 4.5$ t/h)	71
Figure 5.1: Experimental versus predicted PCC for fly ash and 38.1 mm I.D. x 24 m long Pipeline	76
Figure 5.2: Experimental versus predicted PCC for fly ash and 38.1 mm I.D. x 24 m long Pipeline	77
Figure 5.3: Experimental versus predicted PCC for fly ash and 63.5 mm I.D. x 24 m long Pipeline	77
Figure A1.1: Schematic of the 105 mm I.D. x 168 m Long Test Rig (for Fly Ash)	89
Figure A1.2: Schematic of the 69 mm I.D. x 554 m Long Test Rig (for Fly Ash)	90
Figure A1.3: Schematic of the 50 mm I.D. x 70 m Long Test Rig (for Fly Ash)	91
Figure A2.1: Comparison of experimental and predicted values of total pipeline pressure drop (fly ash, $D = 69$ mm, $L = 168$ m, $m_s = 14$ t/h)	92
Figure A2.2: Comparison of experimental and predicted values of total pipeline pressure drop (fly ash, $D = 69$ mm, $L = 168$ m, $m_s = 9$ t/h)	93
Figure A2.3: Comparison of experimental and predicted values of total pipeline pressure drop (fly ash, $D = 105$ mm, $L = 168$ m, $m_s = 23$ t/h)	94
Figure A2.4: Comparison of experimental and predicted values of total pipeline pressure drop (fly ash, $D = 105$ mm, $L = 168$ m, $m_s = 18$ t/h)	95

Figure A2.5: Comparison of experimental and predicted values of total pipeline pressure drop (fly ash, $D = 69$ mm, $L = 554$ m, $m_s = 9$ t/h)	96
Figure A2.6: Comparison of experimental and predicted values of total pipeline pressure drop (fly ash, $D = 69$ mm, $L = 554$ m, $m_s = 7$ t/h)	97
Figure A2.7: Comparison of bend only pressure drop between low velocity flow and high velocity (fly ash, $D = 69$ mm, $L = 168$ m, $m_s = 19$ t/h)	98
Figure A2.8: Comparison of bend only pressure drop between low velocity flow versus high velocity flow (fly ash, $D = 69$ mm, $L = 168$ m, $m_s = 14$ t/h)	99
Figure A2.9: Comparison of bend only pressure drop between low velocity flow and high velocity flow (fly ash, $D = 69$ mm, $L = 168$ m, $m_s = 9$ t/h)	100
Figure A2.10: Comparison of bend only pressure drop between low velocity flow versus high velocity flow (fly ash, $D = 105$ mm, $L = 168$ m, $m_s = 23$ t/h)	101
Figure A2.11: Comparison of bend only pressure drop between low velocity flow and high velocity flow (fly ash, $D = 105$ mm, $L = 168$ m, $m_s = 18$ t/h)	102
Figure A2.12: Comparison of bend only pressure drop between low velocity flow and high velocity flow (fly ash, $D = 69$ mm, $L = 554$ m, $m_s = 9$ t/h)	103
Figure A2.13: Comparison of bend only pressure drop between low velocity flow and high velocity (fly ash, $D = 69$ mm, $L = 554$ m, $m_s = 7$ t/h)	104

Figure A2.14: Bend loss PCC based on different bend models (fly ash, $D = 69$ mm, $L = 168$ m, $m_s = 14$ t/h)	105
Figure A2.15: Bend loss PCC based on different bend models (fly ash, $D = 69$ mm, $L = 168$ m, $m_s = 9$ t/h)	106
Figure A2.16: Bend loss PCC based on different bend models (fly ash, $D = 105$ mm, $L = 168$ m, $m_s = 28$ t/h)	107
Figure A2.17: Bend loss PCC based on different bend models (fly ash, $D = 105$ mm, $L = 168$ m, $m_s = 23$ t/h)	108
Figure A2.18: Bend loss PCC based on different bend models (fly ash, $D = 105$ mm, $L = 168$ m, $m_s = 18$ t/h)	109
Figure A2.19: Bend loss PCC based on different bend models (fly ash, $D = 69$ mm, $L = 554$ m, $m_s = 11$ t/h)	110
Figure A2.20: Bend loss PCC based on different bend models (fly ash, $D = 69$ mm, $L = 554$ m, $m_s = 9$ t/h)	111
Figure A2.21: Bend loss PCC based on different bend models (fly ash, $D = 69$ mm, $L = 554$ m, $m_s = 7$ t/h)	112

LIST OF TABLES

	Page No.
Table 2.1: Common radius bends dimension	16
Table 2.2: Common method of size analysis	19
Table 2.3: Terminology to characterise particles shapes	20
Table 2.4: Moh's scale of hardness	21
Table 2.5: B factor for bends	30
Table 3.1: Physical Properties of fly ash	42
Table A3.1: Closely coupled bend data (P7-P8)	113
Table A3.2: Summary output of Regression Analysis of Closely coupled bend data (P7-P8)	115

LIST OF SYMBOLS AND ABBREVIATIONS

B	Bend loss factor
D	Internal diameter of pipe [m]
$Fr = V/(gD)^{0.5}$	Froud number of flow
g	Acceleration due to gravity [m/sec ²]
L	Length of pipe [m]
m_f	Mass flow rate of air [kg/sec]
m_s	Mass flow rate of solids [kg/sec]
$m^* = m_s/m_f$	Solid loading Ratio
K	Constant of power function
N	Number of bends
ΔP	Pressure drop through a straight horizontal pipe [Pa]
ΔP_{bo}	Pressure drop through bend [Pa]
$(\Delta P_z)_{solid}$	Pressure drop due to solids for an equivalent straight length of the bend [Pa]
R_B	Radius of curvature bend [m]
r	Radius of bend pipe [m]
$Re = \rho VD/\mu$	Reynolds number
V	Superficial air velocity [m/sec]
V_o	Velocity at bend outlet [m/sec]
ρ	Density of air [kg/m ³]
ρ_o	Density of air at bend outlet
λ_f	Air/gas only friction factor

λ_{bs}	Solid friction factor at bend
λ_s	Solid friction factor
μ	Fluid viscosity [Pa.sec]

Subscripts

b	Bend
f	Fluid (air)
i	Inlet condition
o	Outlet condition
s	Solids
sus	Suspension
z	Straight Horizontal Pipe

Abbreviations

BD	Bottom Discharge
I.D.	Internal diameter of pipe
PCC	Pneumatic conveying characteristics

CHAPTER 1: INTRODUCTION AND OBJECTIVES

1.1 Introduction

Pneumatic conveying is the process of transportation of dry bulk materials through pipelines with the help of air or other non-reacting gases. This process is being used in several industries, such as in thermal power plants to convey pulverised coal and fly ash, cement, chemical, food, petrochemical industries etc. Some reasons to use this process are ease of automation and control, dust free, totally enclosed system, flexible layout, hygienic and being environmental friendly. Klinzing et al. (1997) presented that conventional mode of conveying as “dilute phase” (suspension flow), where the velocity of gas is sufficiently high to suspend the particles in the pipeline. However, to obtain the increasingly demand of industries such as new product and process, improved quality etc, several modes of “dense phase” (non-suspension flow) have been developed to take the advantage of particular product properties (e.g. rheological and aeration characteristics). An accurate estimation of minimum transport boundary and total pipeline pressure drop are important criteria for reliable design of pneumatic conveying systems. Under prediction of minimum transport boundary (i.e. minimum conveying air requirement to avoid lack of aeration of fluidised powders) would result in either reduced throughput or line blockage. Total pipeline pressure drop consists of losses due to horizontal straight pipes, bends, verticals and initial acceleration of particles from rest. Accurate prediction of each element pressure drop, especially the horizontal pipe and bend losses, is very important as they form the significant share of total pipeline losses. For straight pipe losses Barth (1958) proposed equation (1) for pressure drop (ΔP) for solid-gas flow. This equation is believed to be originally proposed for dilute phase transport of coarse particles. However, various researchers

such as Stegmaier (1978), Weber (1981), Pan (1992), Pan and Wypych (1998) and Jones et al. (2003) employed this expression to predict the pressure loss for dense-phase flow of fine powders (such as fly ash, cement, pulverised coal etc) through straight pipes.

$$\Delta p = (\lambda_f + m^* \lambda_s) \frac{\rho_s L V^2}{2D} \quad (1.1)$$

Pneumatic conveying systems are easy to install and provide flexible layout due to presence of bends. In past few decades, there have been number of research efforts (Schuchart, 1968; Singh and Wolf, 1972; Rossetti, 1983; Chamber and Marcus, 1986; Pan, 1992; Pan and Wypych, 1998; and Das and Meloy, 2002) on the pressure drop due to gas-solid flow in bends. Most of the models on bend losses are related to the specific product and laboratory conditions for example location/orientation of the test bend, flow conditions etc. Schuchart (1968) was one of the first researchers to study the gas-solids flow through pipe bends. Bradley and Mills (1988) proposed that a more accurate prediction of the overall pressure loss can be achieved by predicting the pressure drop through the straight pipes and bends separately because upon exit from a bend, velocity of solid reduces significantly, due to which solids drop out from the gas stream and would then try to re-accelerate to be again in flow. This re-acceleration of particles causes pressure drop of the gas. Bradley (1990) conducted experiments on the bend pressure drop with test set up similar to that presented by Bradley (1989) using wheat flour and with seven different types of bends. It was concluded that different radius bends produce similar loss (i.e. pressure drop is irrespective of the radius of curvature of the bends) but this result contradicts with the findings of Mills and Mason (1985).

Chaudhry et al. (2001) did experiments on 10 materials using the setup, which was referred by Bradley (1989) and developed a model having 50 % accuracy in prediction of bend pressure drop. All these existing models are empirical and have shown reliable results for total pipeline pressure drop when applied to the researchers own data, but have not been adequately examined for accuracy and reliability for their scale-up and different products and experimental set up.

Typical Pneumatic Conveying Characteristics (PCC) of Fluidised dense phase (FDP) is as follows-

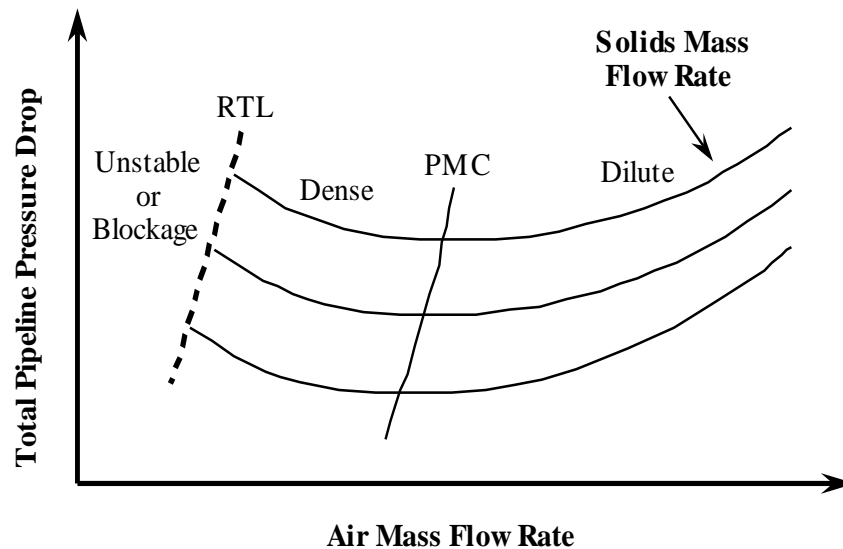


Figure 1.1: Typical PCC for Fluidised Dense-Phase (PMC - Pressure Minimum Curve, RTL - Reliable Transport Limit) (Wypych, Hastie, J. Yi, UOW, 2005)

According to Marcus et al. (1984) there are large amount of conflicting theories that there need for a structured research program to facilitate the monitoring of following parameters:

- Influence of particle size
- Bend attitude

- Bend radius
- Bend cross-section (square, rectangular or round)
- Pressure loss across bend and system
- Acceleration length required from exit of bend
- Determination of an “equivalent length” for a bend.

As the suspended particles approaches the bend in the pipeline, a number of factors come into play. Some particles move through bends in zig-zag fashion. On each impact the velocity of suspension reduced. Several researchers have examined the flow of solid-gas mixture in pipe bends such as Schuchart (1968), Singh and Wolf (1972), Rossetti (1983), Chamber and Marcus (1986), Pan (1992), Pan and Wypych (1998) and Das and Meloy (2002) etc. All these existing models are empirical and have shown reliable results when applied to the researchers own data, but have not been adequately examined for accuracy and reliability for their scale-up and different experimental setup. Hence, there is requirement to examine the accuracy of the models under different conditions that are different pipe length and/or diameter and also scale-up conditions of pipe diameter and/or length by using different conveying material.

1.2. Objectives

Specific objectives include:

- i. To develop a solid friction factor model to predict the straight pipe pressure drop;

- ii. Evaluating the existing bend models for predicting the total pipeline pressure drop for different pipelines.
- iii. To develop a solid friction factor model to predict the bend pressure drop;

CHAPTER 2: LITERATURE REVIEW

This chapter exhibit different studies and research carried out by many researchers on pressure drop for dense-phase pneumatic conveying of bulk solids since last many years. Initial studies was related to understand the general concepts and operating conditions for pneumatic conveying after that studies regarding the dense phase conveying. In all pneumatic conveying system bends are reality. In spite of that in most of literature there has pay a little attention to the influence of bends. Bends are easy to install and provide flexibility to the layout of a pneumatic conveying system, but it also introduce additional pressure loss in the system. On exit from a bend, the velocity of solids reduced significantly, sometimes resulting in drop out of the solids from the conveying gas stream (Marcus et al., 1990). The solids would then try to extract kinetic energy from the gas-stream to be again in suspension. This re-acceleration of particles causes pressure drop of the conveying gas-stream and that zone is called reacceleration zone. Also there will be losses due to the change in direction of the solids-gas stream going through the bend. Mallick (2010), for accurate estimation of pressure losses in the system, loss due to the bends was first realised by Rizk (1982), when he has provided his λ model for fly ash for horizontal straight pipe lengths. Here, conscious efforts have been made to present the review more confined to bend pressure drop in fluidised dense phase pneumatic conveying

2.1 Pneumatic conveying

It is defined as the conveying of bulk solids such as powders (cement, fly ash), granular products (crushed coal, grain) or bulk commodities (cans, live chickens, paper rolls) through a confined flow channel (pipeline, porous membrane) at positive or negative gaseous pressure i.e. nitrogen and hydrogen (Wypych, 1999).

Advantages of pneumatic conveying: Some of the advantages of pneumatic conveying are listed below:

- Clean environment
- Simple system consists of compressed gas source, feeding device, conveying pipe and receiver to separate the products from gas (Wypych, 1999).
- Low maintenance and manpower.
- Flexible routing (Wypych, 1999).
- Easy to automate and control pneumatic conveying systems (Yi, 2001).

Disadvantages of pneumatic conveying: Some of the disadvantages of pneumatic conveying are listed below:

- Relatively high power consumption.
- Limited conveying distance means there is a maximum limit of pipe length up to which pipe length can be increased (Wypych, 1999).
- Damage to the product (Yi, 2001).
- High level of skills to design, operate and maintain a system (Yi, 2001).

2.2 Modes of pneumatic conveying systems

Wypych (1989), there is two modes of pneumatic conveying. Ratio of mass of solid (m_s) and mass of air (m_f) is called solid loading ratio (m^*).

$$m^* = \frac{m_s}{m_f} \quad (2.1)$$

(1) Dilute phase

It is traditional pneumatic conveying system which provides sufficient air to entrain, suspend and transport particles along the pipeline. Several terms are employed to describe this mode of flow, such as dilute-phase, lean-phase or suspension-flow. Dilute phase conveying is the most common used method of transporting materials. Many different feeders can be employed for dilute-phase pneumatic conveying systems, such as venturies, rotary valves, screw pumps and blow tanks. There is virtually no limit to the range of materials that can be conveyed with dilute-phase system. Products commonly conveyed in dilute phase systems include flour, resins, specialty chemicals, ground feeds, and granular and palletized products. Of the various types of pneumatic systems, a dilute phase system will generally be lowest in capital cost.

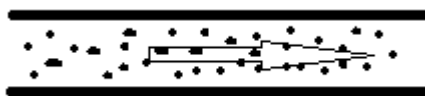


Figure 2.1: Dilute-phase pneumatic conveying

Limitations

This process uses a relatively large amount of air to convey a relatively small amount of material and at lower pressures than dense phase systems. So power requirements are also high. Higher air velocities will have the following other disadvantages:

- The wear caused by the product on the pipe is considerably higher therefore this process is not suitable for materials which are susceptible to degradation and/or are abrasive in nature.
- The products can get deformed or crushed therefore this process is not recommended for friable products.

(2) Dense phase

Dense-phase conveying, also referred to as non-suspension flow. It have been developed mainly to eliminate/minimise the problems generally occurs in dilute phase systems and hence, expand the future potential of pneumatic conveying. Due to the product being the dominant phase in dense-phase conveying, test work and experience usually are necessary to confirm dense-phase suitability accurate operating conditions and product quality. The dense-phase classification diagram is useful in providing an initial indicator of dense-phase suitability.



Figure 2.2: Dense-phase pneumatic conveying.

Solid gas transportation process can be described by pneumatic conveying characteristics (PCC). PCC for given pipeline are plot of pressure drop (Δp) or pressure gradient ($\Delta p/L$) versus the superficial gas velocity (V_f) or mass flow rate of gas (m_f) (Wypych 2006).

Types of Dense Phase Systems: The following different modes of dense-phase conveying are in use:

- i. Fluidised dense phase
- ii. Low velocity slug flow
- iii. Low velocity plug flow
- iv. Bypass conveying
- v. Single slug conveying
- vi. Air assisted gravity conveying

i. Fluidised dense phase

Fluidised dense-phase is considered often as the most reliable and efficient method of conveying certain powders or fine granular bulk solids over distances ranging from only a few metres up to 2 km. It takes advantage of the fluidisation and air retention properties of the bulk material (Mainwaring et al., 1987).

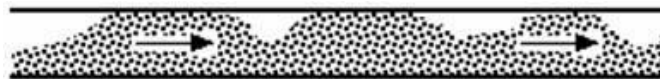


Figure 2.3: Fluidised dense-phase (FDP). (Wypych and Hauser, 1990)

ii. Low velocity slug flow

This mode of dense-phase pneumatic conveying has been developed to allow friable and/or granular products to be conveyed with extremely low levels of particle damage (e.g. sugar, poly pellets, wheat and duralina) and also system damage (e.g. bend wear) (Pan et al., 1994).



Figure 2.4: Low velocity slug flow (LVSF). (Pan et al., 1994)

iii. Low velocity plug flow

The low velocity conveying systems typically transport the product as a series of discrete plugs. At first glance, this mode of flow (Wypych et al., 1990) appears similar to low velocity slug flow. However, the main differences are that low velocity plug flow does not produce a stationary layer of material. It is most suited to cohesive or sticky powders.



Figure 2.5: Low velocity plug flow (LVPF).

iv. Bypass conveying

The gritty bulk materials (e.g. alumina, poly powder, fine sand, coarse fly ash) usually display good fluidisation behaviour, they also deaerate quite quickly (especially compared with the powders suited to FDP) and generate high friction forces when allowed to build up inside the pipeline. Hence, it is usually necessary to employ dilute-phase for such materials and also purge the pipeline prior to any shut-down operation. However, by employing specially designed bypass technology, it is still possible to convey such materials in dense-phase. Various types of bypass technology are available (Klintworth and Marcus, 1985).

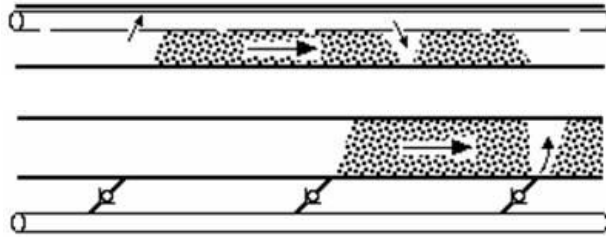


Figure 2.6: (At top) internal bypass and (below) external bypass.

(J. Klintworth and R.D. Marcus, 1985)

v. Single slug conveying

This dense-phase mode involves the transportation of a limited batch of material per conveying cycle. A detailed description of this method of transport together with typical performance results has been presented by Wypych and Arnold (Wypych and Arnold, 1989).

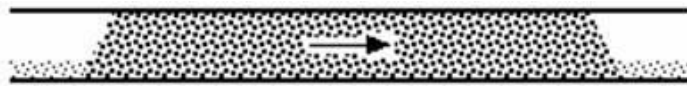


Figure 2.7: Single-slug conveying. (Wypych and Arnold 1989)

vi. Extrusion flow

Occasionally, it may be beneficial to maintain the total conveying pipeline full of material and produce an extrusion mode of flow. Usually, specially designed blow tank feeders are employed for this purpose. It is used to convey meat lumps for canned dog food, chopped fish chunks and gravy (Wypych and Arnold, 1989).

vii. Air assisted gravity conveying

Air-assisted gravity conveying (Ashenden et al., 1995) is actually one of the most efficient modes of dense-phase due to its relatively high solids loadings, low conveying

velocities and low specific air power requirements. For example, a Roots-type blower or even a centrifugal fan is only required, as opposed to a compressor that quite often is selected for the other modes of dense-phase

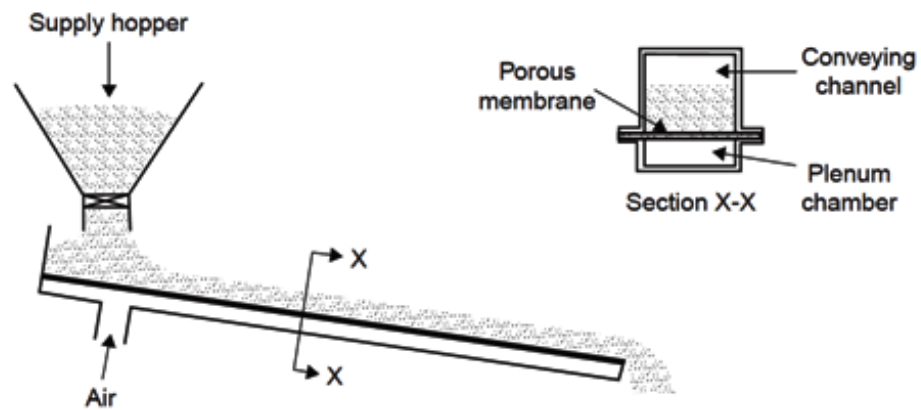


Figure 2.8: Air-assisted gravity conveying (Mills 2004)

2.3 Basic components of pneumatic conveying system

This system consists of four different zones (Kennedy & Wypych 1990). Which are as follows:-

- (a) Prime movers to supply conveying gas **ex.** Fan blower reciprocating and rotary screw compressor.
- (b) Feeding, mixing and acceleration **ex.** Venture, rotary valve, screw, blow tank
- (c) Conveying zone **ex.** Piping, bends, diverters, coupling or flange
- (d) Separating zone **ex.** Cyclone and bag filter

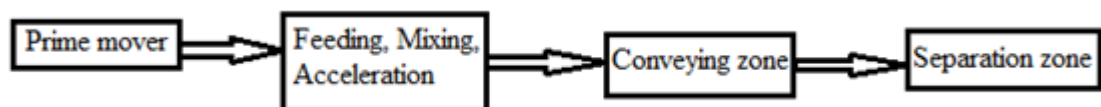


Figure 2.9: Components of pneumatic conveying system

2.4 Bends

Bends are section of pipe which enables convenient change of direction in the flow of the conveyed bulk solids.

2.4.1 Types of bends

According to Dhodapkar and Solt (2009) Bends can be broadly classified into three major categories:-

- a) Common-radius bends (including elbows, short-radius, long-radius and long-sweep bends)
- b) Common fittings (including tee bends, metered bends and elbows)
- c) Specialized bends and innovative designs (such as the Gamma bend, Hammertek Smart Elbow, Pell bow, wear back designs, and lined bends)

a) Common-radius bends

Common radius bends are made by bending standard tubes or pipes. The radius of curvature (R_b) may range from $1D$ to $24D$ (where D is the diameter of the tube or pipe). Common radius bends can be loosely classified as follows.

Table 2.1: Common-radius bends dimension (Dhodapkar & Solt 2009).

Elbow	R_b / D	1 to 2.5
Short radius	R_b / D	3 to 7
Long radius	R_b / D	8 to 14

Long sweep	R_b / D	15 to 24
------------	-----------	----------

These bends are available in wide range of materials of construction and thicknesses, similar to the straight section of pipe (tangent) that is provided on either side of the curved section. The conveyed material may undergo multiple impacts with the pipe wall, or may slide along the outer radius, depending on material properties, solids loading and gas velocity. Bend wear and material attrition commonly occur at the impact zones (Dhodapkar and Solt 2009).

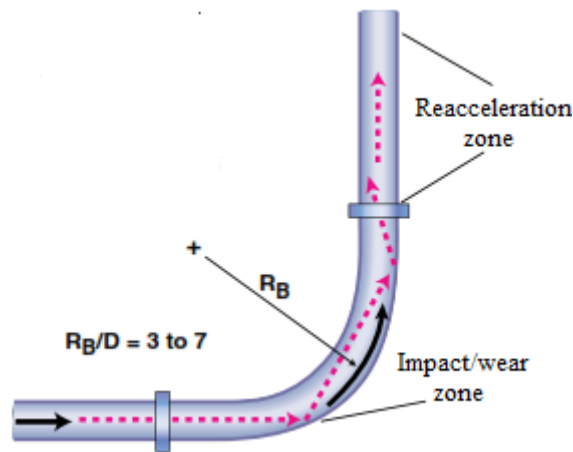


Figure 2.10: Short radius bend (Dhodapkar & Solt 2009).

b) Common fittings

The most commonly used fitting to accomplish a change in flow direction is a blind tee bend. In this design, one of the outlets is plugged thereby allowing conveyed solids to accumulate in the pocket the benefit of this design is that the accumulated pocket of material cushions the impact of the incoming material, significantly reducing the potential for wear and product attrition. The extent of accumulation in the pocket will depend on the orientation of the bend, solids loading, gas velocity and material

properties (such as particle size and cohesiveness). However, in a tee bend, the conveyed solids lose most of their momentum during the impact and thus must be reaccelerated downstream of the bend. As a result, pressure drop across a blind tee can be as much as three times that of a long-radius bend (Dhodapkar and Solt 2009).



Figure 2.11: Blind tee and Blinded bend (Dhodapkar & Solt 2009).

c) Specialized bends

Today, a variety of specialized designs are available to control flow within the bend, in order to minimize attrition and wear. This is often achieved by creating a self-cleaning or replenishing pocket or layer of material, upon which the incoming stream impinges. Wear inside the piping is minimized by redirecting the gas-solid suspension away from typical wear points (Dhodapkar and Solt 2009).

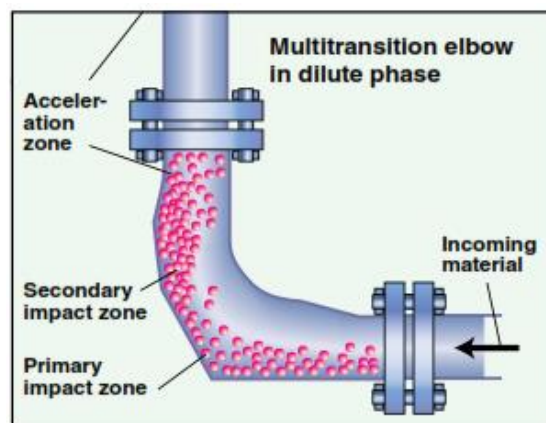


Figure 2.12: Gamma Bend (Dhodapkar & Solt 2009).

2.5 Properties of bulk solids

Bulk solids are mixture of components comprises of at least 2 (solid, liquid, gas) and usually all of 3 states (Kennedy and Wypych, 1990). The properties related to individual particle are known as particle properties i.e. particle size, shape, density, hardness elasticity and the properties related to mixture (bulk solid) as a whole are termed as bulk properties i.e. bulk density, moisture content, wall friction, angle of repose, fluidisation, deaeration and permeability etc). Some important properties are as follows:

1. *Particle size / size distribution*: To predict the PCC the particle size is of very significant. An irregularly shaped particle will present different dimension depending on the orientation that it is observed from, which makes the determination of particle size difficult. That is why results obtained by different methods of size measurement vary generally. Particle shape is an important characteristic as it influences flow ability, packing, interaction with fluids and hence suitability for pneumatic conveying. However, the understanding of this influence is still limited (Wypych, 2006).

Table 2.2: Common methods of size analysis (Wypych, 2006)

Methods Of Size Analysis	Approximate Size Range
Mechanical Sieving	125 mm – 38 μm
Sedimentation	100 μm – 2 μm
Microscope	100 μm – 1 μm
Electron microscope	5 μm – .001 μm
Scanning Electron Microscope	100 μm – 0.1 μm
Classification	50 μm – 2 μm

Laser Diffraction	1.8 mm – 1 μ m
-------------------	--------------------

From the above listed methods, mechanical sieving is perhaps the most widespread. It is a straight forward method. Sieves are manufactured in a range of standard apertures (6.7 μ m – 125 mm) to carry out the analysis a set of sieves is arranged in a stack in order of decreasing aperture from top to bottom with a pan enclosing the bottom and a lid at the top. A sample is placed on the top sieve and the assembly is shaken (usually mechanically) for a set of period of time. The mass retained on each sieve is then recorded, allowing a particle size distribution for the sample to be determined. At small particle sizes, and particularly for low density substances, normal dry sieving becomes ineffective. Below 75 μ m, wet sieving is recommended to improve the reliability and repeatability of the results (Wypych, 1989).

2. *Particle shape*: It is an important characteristic as it influences “flow ability”, packing, interaction with fluids and hence their handle ability in silo and hoppers, suitability for pneumatic conveying etc. Following table lists standard set of terminology to characterise the particle shape (Kennedy and Wypych, 1990). But these terminologies are only relative because everyone has their own ideas regarding the meaning of terms.

Table 2.3: Terminology to characterise particle shape (Kennedy and Wypych, 1990)

Term	Description
Acicular	Needle shape
Angular	Sharp edged or having roughly polyhedral shape
Crystalline	Of geometric shape, freely developed in fluid medium

Dendritic	Having a branched crystalline shape
Fibrous	Regularly or irregularly threadlike
Flaky	Plate like
Granular	Having approximately equi-dimensional, but irregular shape
Irregular	Lacking any symmetry
Nodular	Having a round irregular shape
Spherical	Globule shape

3. *Particle density*: This term represents the actual density of a solid. It is of significance in pneumatic conveying systems because of its effect on minimum transport velocities and air pressure requirements. The particle density can be determined from a specific gravity bottle (respect to water) or by using an air-comparison pycnometer to determine the true volume of a known mass of particles (Wypych, 2006).

4. *Hardness*: It gives indication of the need of avoid excessive abrasion and erosion of key components (e.g. Valves, clutches, hopper linings, elbows, ducting, cyclones). Moh scale proposed in 1822 is still in use with ten selected minerals ranging from talc with a Moh hardness 1, to diamond with a scratch hardness of covering the range of scale. It can be converted to equivalent Vickers, Rockwell and Brinell hardness values.

Table 2.4: Moh scale of hardness (Kennedy and Wypych, 1990)

Moh's scale of hardness	Material	Explanation
1	Talc	Very soft, can be powdered between fingers

2	Gypsum	Moderately soft, can scratch lead
3	Calcite	Can scratch a fingernail
4	Fluorite	Can scratch copper
5	Apatite	Can scratch a knife blade
6	Feldspar	Can scratch a knife blade
7	Quartz	All particles harder than 6 can scratch glass
8	Topaz	
9	Corundum	
10	Diamond	

5. *Bulk density*: Solid density denotes the actual density of the constituents of bulk solid. The bulk density of the material is a measure of the average density of the material. This is a function of not only the particle density of the constituents but also the particle size (and size distribution) and shape, the packing arrangement adopted by the particles (the amount of voids between the particles), the degree to which the particle is compacted (or aerated), the moisture content etc. In terms of storage capacity (silos, hoppers etc.) and through-put capacity (rotary valves, pressure vessels, pipelines etc.) the bulk density is a critical parameter. Since bulk solids are generally a random arrangement of arrange of particle sizes and shapes, it is usually possibly to obtain a number of bulk densities depending on the consolidation that has been experienced by the sample (Wypych, 2006). Generally bulk density is of following types:

- i. Aerated bulk density
- ii. Loose poured bulk density
- iii. Tapped bulk density

iv. Consolidated bulk density

6. *Moisture content*: It has major impact on behaviour of bulk solid. The addition of moisture in fine particles of the sample tends to increase the internal and cohesive strength of the material (Kennedy and Wypych, 1990).

7. *Fluidization*: It refers to the action of a bulk solid being mixed with a gas (usually air) to make it behave like fluid. The minimum superficial velocity of gas (V_f) required to fluidise a given product is referred to as the minimum fluidisation velocity (U_{mf}) determined at atmospheric conditions. Minimum fluidisation velocity is obtained from a fluidisation curve which represents the variation of pressure gradient across a section of fluidised bed (viz. bed pressure drop per unit bed height) with respect to superficial velocity (Wypych, 2006). An ideal fluidisation curve is presented in Figure 2.2.

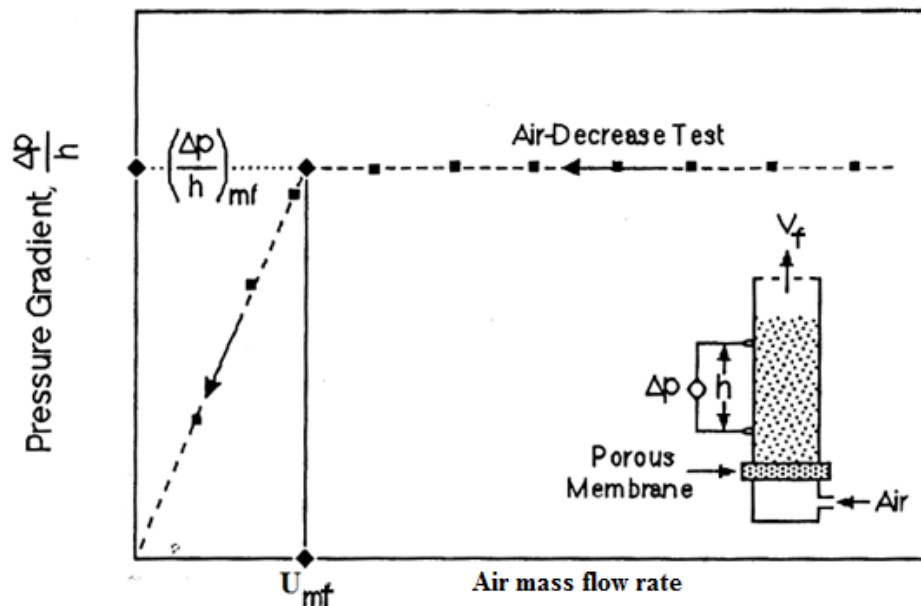


Figure 2.13: An ideal fluidization curve showing a typical test chamber and parameters $\Delta p/h$, V_f and U_{mf} (Wypych, 2006).

8. *Permeability*: In many cases a linear relationship is observed between the pressure gradient across the bed and the superficial air velocity, as is noted at the low velocity end of the fluidisation curve as shown in Figure 2.4. The slope of the curve is commonly known as the permeability factor. Where the fluidisation curve flattens out and little change to the pressure gradient across the bed occurs with increasing superficial air velocity, It is generally found that the pressure gradient is sufficient to support the mass of bulk solids within the fluidising column (Wypych, 2006).

9. *Deaeration*: Deaeration refers to the action of gas leaving a fluidised bed after the gas supply has been turned off. It may be measured by either observing the collapse in bed height as the gas escapes, or more conveniently by recording the drop in pressure gradient over the same process. The behaviour provides a useful measure of the materials ability to retain air, which is a complex function of factors such as particle shape, density, porosity, packing, drag etc. Many materials show an exponential rate of decay in this pressure gradient. This in turn allows a characteristic time constant to be determined for each material (Wypych, 2006).

2.6 Material classification

By using fluidisation data obtained from several researchers, Geldart (1973) was one of the first who classify the materials into four groups. This classification is in terms of the mean particle size, and the difference in density between the particles and the fluidizing medium (Kennedy and Wypych, 1990).

These four groups can be given as:

- *Group A:* This includes the powders having a limited tendency to form bubbles and generally exhibit considerable bed expansion between the minimum fluidization velocity and the minimum bubbling velocity. When the gas is turned off these powders retain aeration and the fluidised bed collapse very slowly.
- *Group B:* Materials belonging to this group fluidize readily and tend to form bubbles, which grow rapidly by coalescence. However, bed expansion is small. The minimum bubbling velocity is approximately equal to (or only slightly greater than) the minimum fluidizing velocity. The fluidised bed does not retain its aeration and collapses quickly when the gas supply is turned off.

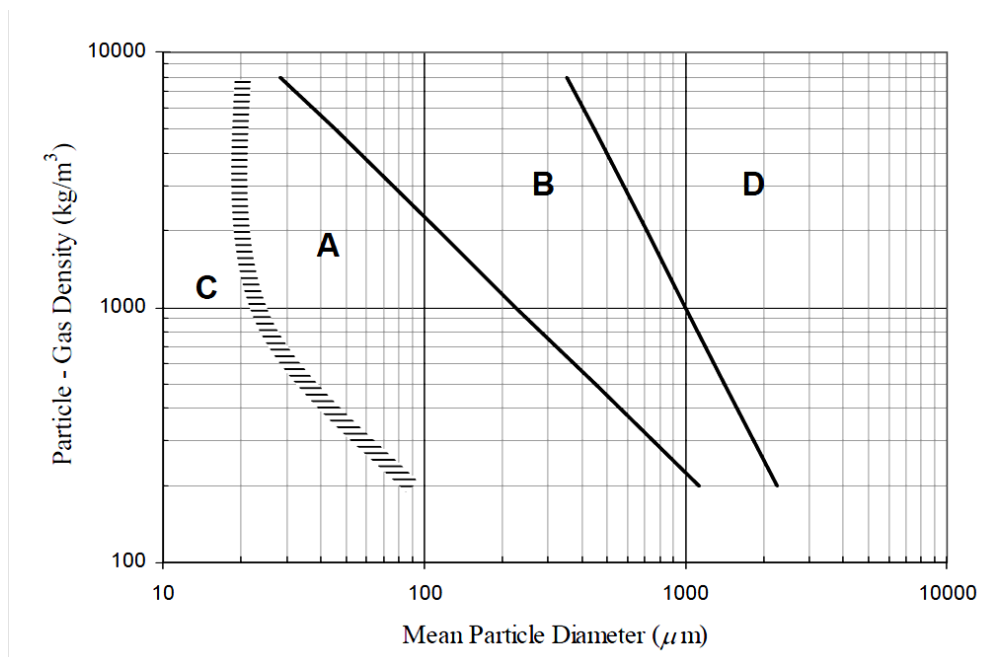


Figure 2.14: Geldart's fluidization Diagram (Kennedy and Wypych, 1990)

- *Group C:* This group contains powders, which are of small particle size and cohesive in nature. As a result normal fluidization is very difficult. The powder lifts as a plug in small diameter tubes.

- *Group D:* This group contains large and/or high-density particles. It is believed that the bubble sizes may be similar to those in Group B, although higher gas velocities are required for fluidization.

It is generally accepted that fluidization and deaeration characteristics are significant in assessing the suitability of bulk solid for pneumatic conveying. Hence, Geldart's classification, though not developed to classify the pneumatic conveying performance of materials, has been used as a useful guide to dense-phase suitability of powders and granular materials.

Marcus (1983) suggested the following:

- Group A materials are the Air Retentive materials and hence potentially suited for fluidised dense-phase, FDP conveying.
- Group B deaerate readily and hence troublesome in dense-phase. These materials generally require higher superficial air velocities.
- Group C includes cohesive materials that are difficult to fluidize satisfactorily and consequently generally unsuited to dense phase conveying .(The dividing line between groups C and A is very indistinct and the only way of properly assessing the suitability of doubtful materials for air-assisted gravity conveying is by practical experiment in a small scale test rig)
- Group D covers materials of larger particle size and high density granular materials. Depending on size, shape and solid density, some of these materials readily form plugs and perform well in dense phase systems. (e.g. plastic pellets, grains)

In later investigations, in 1979 Dixon revealed that the convey ability of a product in dense phase is significant depends to the fluidization properties of that product. His theoretical description enabled boundaries between expected flow conditions to be drawn on the same axes as Geldart's classification. It can be seen that the boundaries between strong axisymmetric slugging, weak asymmetric slugging and no slugging relate well to Geldart's boundaries between groups D, B and A. Dixon concludes that group A products are the best candidates for dense phase conveying. Group D products are also good candidates because of their strong natural slugging behaviour. Group B products can cause problems if high solids loading ratios are used and group C products are possibly the least suitable materials for conveying in a dense phase mode.

Pan (1999) developed a flow mode diagram characterised by loose-poured bulk density and mean particle diameter. The flow mode diagram classifies the bulk solid materials into three groups:

- Materials which can be transported smoothly and gently from dilute to fluidised dense-phase (e.g. cement, fly ash, pulverized coal, soap powder, skim milk powder, lead dust, powdered limestone, flour).
- Materials that can be conveyed in dilute phase or slug flow.
- Bulk solids which can be conveyed only in dilute phase.

2.7 Design consideration of pneumatic conveying system

There are two parameters which play major roles during the design of reliable pneumatic conveying systems i.e. "pressure drop along the conveying zone i.e. piping

bends diverters, coupling and flange” and “minimum conveying velocity” which is also called “minimum transport boundary”. So, we should accurately determine the above two parameters before design of pneumatic conveying system.

According to Efstahios E. Michaelides et al. (1987) in past 30 years the subject of pressure drop in gas solid system was examined by several experimentalists. Their experimental data were compiled and about two dozen correlations were developed. Many of the published correlations are difficult to use, either because they contain parameters, which are difficult to measure or evaluate (e.g. particle sphericity or shape factors) or they have not considered some factors. Some of them indicate that these correlations have some limitations. This creates a problem to designers to use those correlations because they don't know what exact limitation of its applicability is as for as loading, particle sizes and diameter of pipe etc.

Mallick et al. (2010), selection of proper bend model for accurately estimating the total system pressure is very important in pneumatic conveying system. He has used appropriate particle wall friction factor equation (based on straight pipe data) and three bend models (Schuchart (1968), Pan and Wypych (1998) and Chambers and Marcus (1986) model, to predict the total pipeline pressure drop for pneumatically conveying of power station fly ash and compared the predicted pneumatic conveying characteristics (PCC) and experimental PCC. But there was much variation in both the characteristics of all models. Hence it can be concluded that estimation of bend pressure drop have considerable impact in correctly predicting the total pressure loss.

Marcus et al. (1983), presented a procedure to predict the total pipeline pressure drop by dividing the whole pipe-line into components, i.e. by individually calculating pressure drop in straight pipes, bend loss, vertical lift loss and losses due to the initial acceleration and finally adding the all components to find out the total pressure drop. They presented the following relationships for different components:

$$\text{Acceleration loss: } \Delta p_{\text{accel}} = \frac{\rho_f V^2 (1 + 2m^* \frac{C}{V_f})}{2} \quad (2.2)$$

$$\text{Vertical loss: } \Delta p_v = \frac{m^* L_v g \rho_f V_f}{C} \quad (2.3)$$

$$\text{Straight pipe loss: } \Delta p = \frac{(\lambda_f + m^* \lambda_s) L \rho_f V_f^2}{2D} \quad (2.4)$$

$$\text{Bend loss: } \Delta p_b = \frac{NB(1 + m^*) \rho_f V_f^2}{2} \quad (2.5)$$

$$\text{Total loss: } \Delta p_T = \Delta p_{\text{accel}} + \Delta p_v + \Delta p + \Delta p_b \quad (2.6)$$

They proposed Stegmaier (1978) model for calculating solid friction factor:

$$\lambda_s = 2.1 m^{*-0.3} Fr^{-1} Frs^{0.25} \left(\frac{D}{d} \right)^{0.1} \quad \text{For } d < 0.5 \text{ mm} \quad (2.7)$$

Chambers and Marcus (1986) did not provide any derivation or reference for the bend model.

Marcus et al. (1983) tells that to overcome the bend problem researchers have often considered that loss through bend should be minimised hence they have used long radius bend all the times. But this is not practical all the time. In 1963 there was a comprehensive relationship for pressure drop across a bend:

$$\Delta p = \frac{B\rho_f V_t^2}{2} \quad (2.8)$$

Where V_t is transport velocity.

$$V_t = \frac{m_s}{(\rho_f m^* A)} \quad (2.9)$$

The factor B is determined from the ratio of the bend radius / pipe diameter (R_B / D).

Table 2.5: B factor for Δp_{bend} (Marcus et al. 1983)

R_B / D	B
2	1.5
4	0.75
6	0.50

But in equation 2.9 altitude of bend was not considered.

By analysing different researcher's data and performing some experiments Marcus et al. (1983) came to the point that there is need of structured research program to monitoring the following parameters:

- Influence of particle size
- Bend altitude
- Bend radius
- Bend cross section (square, round, rectangular)
- Determination of equivalent length of bend

Mills and Mason (1985) had carried out a comprehensive test in which they used seven sets of identical bends in common pipeline then there was significant difference in

pressure drop. The short radius bends with a bend diameter, D_b , to pipe bore, d , and ratio of 6:1 provides the best performance over the wide range of conveying condition. If we reduce this ratio then pressure drop increases. The long radius bends is better at the highest values of flow rates but not sufficiently better to recommend their use.

Das and Meloy (2002) compared pressure drop across coupled 90° bend to the isolated single 90° bend. The location of bends influences the portion of the total pressure drop. Das and Meloy tell that Wypych and Pan (1993) presented the impact of bend radius, bend number and bend location in the pipeline. But this investigation was mostly due to isolated bends. They have not compared the behaviour of closed coupled double bend.

It is clear from studies that major portion of pressure drop occurs in the straight section right after the bends. But if two bends are close coupled then material exiting from the upstream bend enters the downstream bend before it is fully reaccelerated. Hence effect of two closely coupled bend for pressure drop is different from the cumulative effect of two isolated bends.

Hence it is necessary to determine how these two are related to each other. For this relationship Das and Meloy carried out series of experiments by using six ashes from different sources having different chemical and physical properties.

2.8 Models to predict bend pressure drop

In this section it has been tried to summarise the various bend models presented by researchers with some detail about them.

Schuchart (1968) used number of bends (radius of curvature: 60 mm to 350 mm; pipe I.D: 34.35 mm) to convey: quartz beads (d_p : 1490, 1850, 2350 and 2960 μm ; ρ_s : 2610 kg/m^3) and polyamide plastic (d_p : 2180 μm ; ρ_s : 1140 kg/m^3). Volumetric concentrations during flow were limited up to only 5%, thus indicating dilute-phase flow. The solids contribution of the pressure drop due to the solids-gas flow through bends was expressed as:

$$\left(\frac{\Delta p_{bend}}{\Delta p_z}\right)_{solids} = 210\left(\frac{2R_B}{D}\right)^{-1.15} \quad (2.10)$$

Where, $(\Delta p_z)_{solids}$ is the pressure drop due to the solids for an equivalent length of straight pipe (having the same arc length as that of the bend). This is to be obtained using solid friction factor model (for straight pipe). Finally, the total loss through the bend is to be calculated by adding the pressure drop due gas-only friction term with $(\Delta p_z)_{solids}$. Schuchart (1968) mentioned that for pressure drop calculation of straight pipe due to solids only Barth (1958) equation (1.1) and for gas only pressure drop, Ito's (1959) expression (2.11) is to be used:

$$(\Delta p_{bend})_{air} = \left(\frac{0.029+0.304[Re(r/R_B)]^{-0.25}}{(R_B/r)^{1/2}}\right) \frac{L\rho_o V_o^2}{2D} \quad (2.11)$$

Total bend pressure drop due to bend: $\Delta p_{bo} = (\Delta p_{bend})_{solid} + (\Delta p_{bend})_{air}$
(2.12)

It is to be noted that the equation (2.10) includes the $(\Delta p_z)_{\text{solids}}$ term. Therefore, the reliability of Schuchart (1968) bend model would depend on the accuracy of modelling solids friction through straight pipes, which in itself is an area of active research (Mallick, 2010).

Singh and Wolf (1972) performed 108 number of experiments on 3 bends (radius of curvature: 381, 762 and 1220 mm; pipe I.D: 150 mm) by using granular chopped forage as the conveying material. Using non-dimensional approach, in following grouping were arrived at:

$$\frac{\Delta p_{bs}}{\rho_{fo} V_{fo}^2} = f\left(\frac{R}{D}, \frac{m_s}{\rho_{fo} V_{fo} D^2}, \beta_a\right) \quad (2.13)$$

Where, β_a is bend angle. It was assumed that a generalised power function law would be valid; a relationship was developed between $\frac{\Delta p_{bs}}{\rho_{fo} V_{fo}^2}$ and $\frac{m_s}{\rho_{fo} V_{fo} D^2}$, resulting in the following model for bend pressure drop:

$$\Delta p_{b0} = a_c + a_s \frac{m_s V_o}{D^2} \left(\frac{R}{D}\right)^{a_b} \quad (2.14)$$

Where, a_c is the bend loss due to air only. Using least square method and large number of experimental data, the following expression was obtained:

$$\Delta p_{b0} = 0.13 + a_s \frac{m_s V_o}{D^2} \left(\frac{R}{D}\right)^{-0.18} \quad (2.15)$$

For bend angle 45° and 90°, the values of a_s were found to be 0.00334 and 0.00537, respectively.

Rossetti (1983) performed experiments using coarse and fine particles for different bends (pipe diameter to bend diameter ratio 2 to 8.4) and gave equation (2.16) for bend pressure loss. Coarse particles tend to lose energy through wall collisions, resulting in re-acceleration energy loss (Pan, 1992).

$$\Delta p_{bo} = (\lambda_f + \lambda_s) \frac{\rho_o V_o^2}{2} \quad (2.16)$$

The primary contributor to bend loss is believed to be due to re acceleration of particles at the outlet to the bends (Pan, 1992). Re-acceleration loss takes place at the outlet of the bends. Hence, in this equation (8), the use of bend outlet conditions (such as gas density and velocity at outlet of the bend) appear justified. Westman et al. (1987) suggested following correlations of λ_f and λ_s .

$$\lambda_f = 0.167 \left[1 + 17.062 \left(\frac{2R_B}{D} \right)^{-1.219} \right] Re^{-0.17} \left(\frac{2R_B}{D} \right)^{0.84} \quad (2.17)$$

$$\lambda_s = \frac{5.4 m^{*1.293}}{Fr_o^{0.84} \left(\frac{2R_B}{D} \right)^{0.39}} \quad (2.18)$$

Chamber and Marcus (1986) provided expression (2.19) for total bend pressure loss in the conveying pipeline:

$$\Delta p_{bo} = NB(1 + m^*) \frac{\rho V^2}{2} \quad (2.19)$$

This expression (11) was used by Jones and Williams (2003), Williams and Jones (2004) in the back calculation method of deriving an expression for the solid friction factor for straight pipe length. This model does not take into account particle properties, location of bends, etc. Bradley (1989) did experiments using fly ash and wheat flour for pipeline of I.D: 50, 75 and 100 mm and 7 types of bends of different radius of curvature. A wide range of conveying conditions were employed; flow velocity varied from 4 to 45 m/sec and solid loading ratio was up to 130. He proposed the following format (equation 2.20):

$$\Delta p_b = 1/2 K_b \rho_{sus} V^2 \quad (2.20)$$

In the earlier work of Westman et al. (1987), a mass loading ratio (m^*) was used to model solids friction through the bends. However, Bradley (1989) questioned the applicability of using a mass ratio term. According to Bradley (1989), instead of mass ratio, solids volume occupancy (similar to the volumetric concentration in pipeline) is more important for accurate description of the flow phenomenon. According to him, it is the inter-particulate gaps through which the air has to travel and the air creates a slip

for the solids to be dragged in the direction of flow. Therefore, a volumetric term (such as suspension density) has been considered to be more reliable in describing the dense-phase flow conditions. The velocity term in the above equation is believed to be representing suspension or non-suspension condition of flow. Bradley (1989) expressed K_b as a function of suspension density. A review of Bradley (1989) by Pan (1992) mentioned that the pressure drop caused by bend is the sum of two components. One component of the loss happens in the bend itself and other component occurs in the straight section of pipe just after the bend (due to the re-acceleration of the particles). Pan (1992) evaluated Bradley (1989) slope concept of bend loss estimation, in which pressure drop due to bend could be calculated by the difference profiles of pressure transducer values (before and after the bend). Pan (1992) argued that a small fluctuation in measured static pressure is expected to create a great influence on the value of estimated bend pressure drop, e.g. $\pm 1.81\%$ change in static pressure can result in a $\pm 62.8\%$ change in bend pressure drop. Pan (1992) performed experiments on five type of bends: one blind Tee and four radius bends and used fly ash as the conveying material with properties: ρ_s : 634 kg/m³; ρ_b : 2197 kg/m³; mean d_p : 15.5 μ m.

Based on mathematical and dimensional analysis, semi-empirical correlation (2.22) was derived to predict the solids friction factor through bends:

$$\Delta p_{bo} = m^* \lambda_s \frac{\rho_o V_o^2}{2} \quad (2.21)$$

$$\lambda_s = Y_1 m^{*Y_2} Fr_o^{Y_3} \quad (2.22)$$

Values of the exponents Y_1 , Y_2 and Y_3 (equation 2.22) were determined by minimising the sum of squared errors of pressure along the downstream pipe because the bend outlet conditions are the effective for the major portion of bend loss. Based on his empirical data, Pan (1992) proposed the value of Y_1 , Y_2 and Y_3 (for 90° bend angle) as 0.0052, 0.49 and 1.1182 respectively.

Pan and Wypych (1998) did experiments with four samples of fly ash having properties: particle size: 3.5 to 58 μm ; particle density: 2180 to 2540 kg/m^3 ; loose poured bulk density: 634 to 955 kg/m^3 ; velocity range: 3 to 25 m/s; solid loading ratio up to 130. They derived bend loss expression (2.23) due to solids only:

$$\Delta p_{bs} = 0.5m^* \lambda_{bs} \rho_{bo} V_{bo}^2 \quad (2.23)$$

$$\text{Where } \lambda_{bs} = 0.0097m^{*0.5676} Fr_o^{0.9647} \rho_o^{-0.6232} \quad (2.24)$$

Das and Meloy (2002) performed tests with a pipeline of 63.5 mm I.D. x 169.8 m long, with six samples of fly ash and compared the pressure drop across close-coupled to isolated 90° bends. Six ash samples of different properties were used in the test. The following correlation (2.25) was derived for the purpose of comparison between the single and close-coupled bends:

$$\frac{\Delta p_{solids}}{m^*} = X_1 V_o^{X_2} \quad (2.25)$$

Where, X_1 and X_2 are constants specified for a particular ash and bend geometry. For single (isolated) bends and certain type of fly ash, value of X_1 and X_2 was 0.3×10^{-7} and 3.4 respectively and for double (close-coupled) bends value of X_1 and X_2 was 2.2×10^{-7} and 3.0 respectively.

According to Das et al. (2002) under similar flow conditions, the pressure drop in a close-coupled double bend is less than double of that in a single bend.

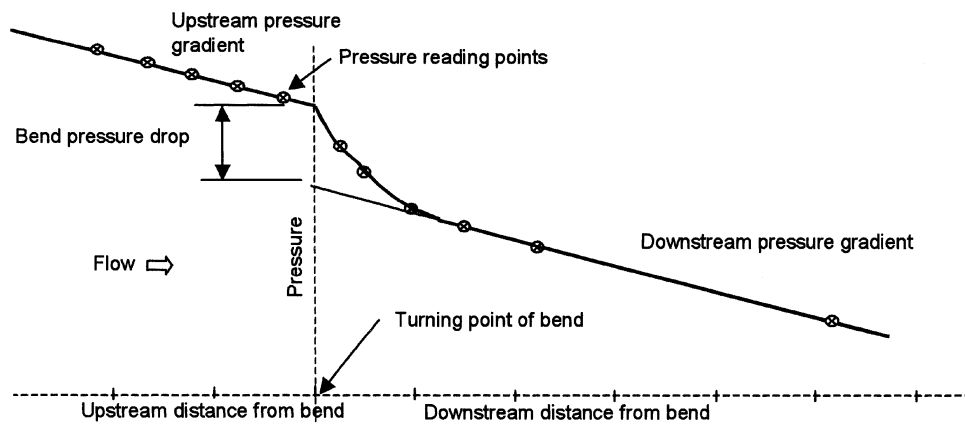


Figure 2.15: Pressure drop in double bends (Das and Meloy, 2002)

From above discussion it was seen that, many researchers (Schuchart, 1968; Singh and Wolf, 1972; Rossetti, 1983; Chamber and Marcus, 1986; Bradley, 1989; Pan, 1992; Pan and Wypych, 1998; and Das and Meloy, 2002 etc) worked on calculating pressure drop due the bends, but every model has validated only for own products and test set up.

From the above studies, it is evident that considerable discrepancies exist between the various models for solids friction derived by the various researchers over the years. Also, the models were not tested under scale-up conditions of length and/or diameters

for their scale-up accuracy and stability. Hence, it is evident that further research is to be conducted to understand solids-gas flow and to predict pressure loss accurately under a wide range of scale-up conditions.

CHAPTER 3: TEST FACILITY AND PROCEDURES

3.1 Introduction

Pneumatic conveying system has been used in industry for several decades. Several theoretical and empirical correlations (Schuchart, 1968; Singh and Wolf, 1972; Rossetti, 1983; Chamber and Marcus, 1986; Bradley, 1989; Pan, 1992; Pan and Wypych, 1998; and Das and Meloy, 2002 etc) have been developed already to predict the pressure drop due to bends. However, most of the correlations are restricted to dilute-phase conveying of coarse particles of relatively narrow size distribution. Also, the empirical correlation are based on given product, pipe materials and conveying conditions. To evaluate the existing correlations and to develop new empirical correlations, it is necessary to conduct experiments in a test rig of appropriate size.

The main purpose of this chapter is to provide a description of test rigs, instrumentation and test materials. Where necessary, a brief explanation of some instruments is provided in detail. Also, a technique used to obtain accurate values of pressure along a pipeline is described. For this thesis, test data from various pipes of different diameter and length were considered to be important for derivation of models for solid friction and their scale up evaluation.

3.2 Experimental Program

The initial plan was to carry out extensive test program with different powders in various pipelines of different diameters and lengths (mainly for the purpose of modelling and scale-up evaluation). However, due to various unforeseen circumstances such as not proper installation of equipment and not proper working of system at first

time only testing with one product using different pipelines could be done and by using data obtained from the test set up (Thapar University) bend model was developed for closely coupled bend and validated with other pipe data. In the meantime of installation of test set up (Thapar University), it was decided that extensive test data of previous experimental programs (Mallick, 2010) carried out in the Bulk Material Handling Laboratory (University of Wollongong) with various powders conveyed in different pipelines would be used for evaluation of different bend models developed by various researchers in past few decades.

3.2.1 Properties of test products

Test data from the following powders were used in this study for the purpose of modelling and Evaluation:

- a) Fly ash (Mallick, 2010)
- b) Fly ash (Thapar University)

Physical properties of these products are listed in the following Table 3.1

Table 3.1: Physical Properties of fly ash

Product	ρ_s Kg/m ³	ρ_{bl} Kg/m ³	d_{50} (μm)
Fly ash (Mallick, 2010)	2300	700	30
Fly ash (Thapar University)	1950	950	45

Particle size distribution was determined using a laser diffraction analyser (Malvern, Mastersizer 2000) and particle density was measured using a pycnometer.

3.2.2 Pneumatic conveying test facility

3.2.2.1 Test facility of University of Wollongong

A schematic test setup of Wollongong for conveying fly ash shown in Figure 3.1. The set up comprised of 0.5 m³ bottom- discharge blow tank feeding system. Single blow tank has been used for 168 m long pipe and twin blow tanks for 554 m long pipe. Pipes and bends were made of mild steel. Three pipelines of different diameter and lengths: 69 mm I.D. x 168 m long, 105 mm I.D. x 168 m long, 69 mm I.D. x 554 m long, were used. Schematic of 105 mm I.D. x 168 m long and 69 mm I.D. x 554 m long pipes are shown in Annexure: Figure A1 and Figure A2, respectively. 168 m pipelines had one vertical lift of 7 m elevation and 5 number of bends (including 2 closely coupled bends). 554 m long pipeline had 17 number of bends (including 8 closely coupled bends). All bends had 1 m radius of curvature and 90° bend angle. For the connection of bends and pipelines, flanges were used with gasket of synthetic material. Compressed air at maximum pressure of approximately 800 kPa was supplied from Ingersoll Rand diesel-powered Model P375-WP, 10.6 m³/min free air delivery rotary screw compressor. Various static pressure measurement points were installed along the pipeline and bends, where P8 was used to measure the total pipeline pressure drop and all other transducers

(i.e. P9, P10, P11 and P12) were installed at out of influence of the bends to measure static pressure at respective points, which were used to model solid friction factor of straight horizontal pipe. Specification of static pressure transducers: manufacturer: Endress & Hauser, model: Cerabar PMC133, pressure range: 0-6 & 0-2 bar, maximum pressure: 40 bar (absolute), current signal: 4-20 mA. Receiver bin of capacity 6 m³ was installed with pulse-jet type dust filter. All other required instruments for such as PRV (pressure reducing valve), flow meter, NRV (non-return valve), blow valve, pressure gauge and load cells (shear beam type) were suitably placed. Calibration of the transducer, load cells & flow meter were performed using the standardized calibration procedure. To record the electrical output signals from the load cells, pressure transducer and flow meters a portable PC compatible data logger (Datataker 800 of Data electronics) was used. That data logger had 24 different channels.

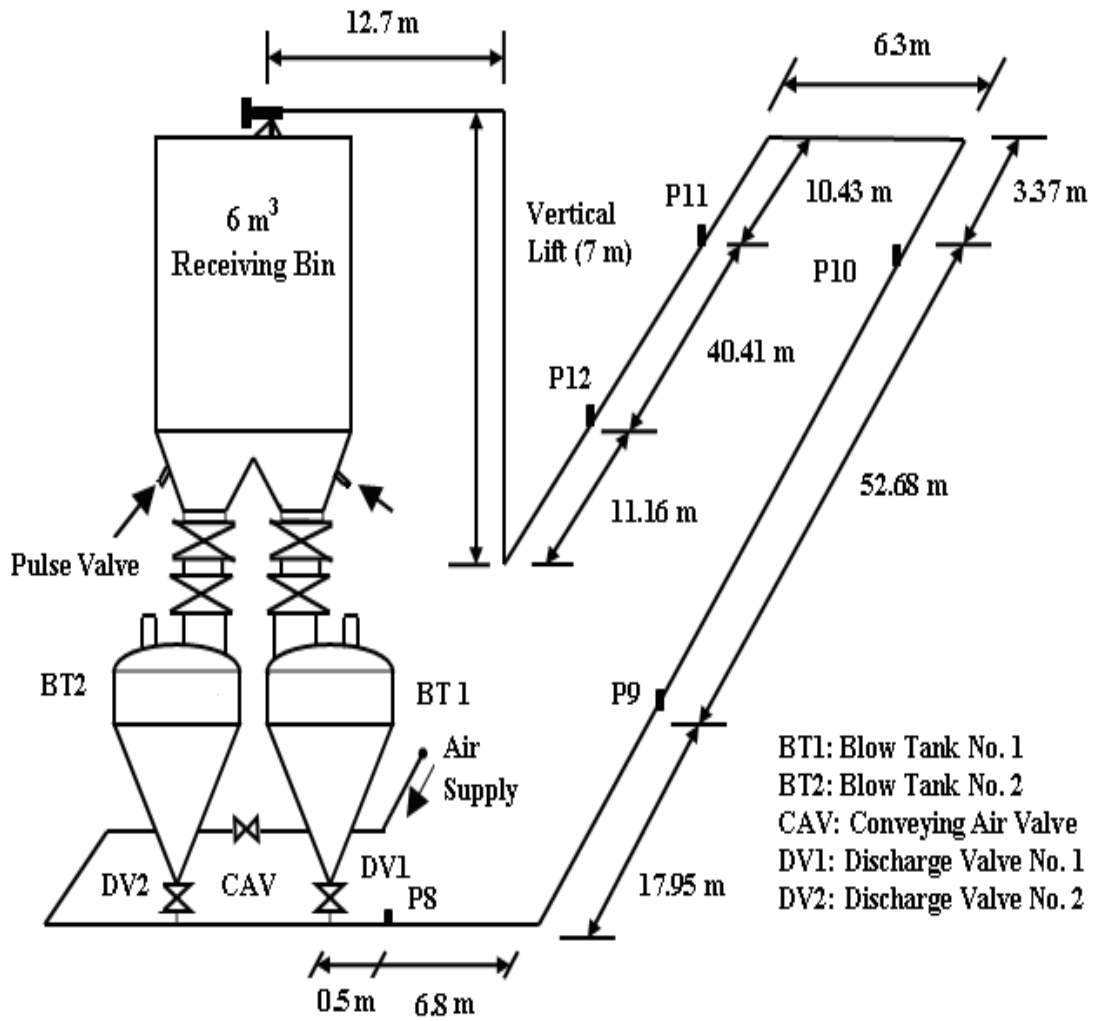


Figure 3.1: Layout of the 69 mm I.D. x 168 m long pipeline Test Rig (for fly ash)

3.2.2.2 Test facility of Thapar University

A schematic test setup of Thapar University for conveying fly ash shown in Figure 3.2.

Major components of experimental setup are listed below.

- Tandem 0.2 m³ capacity blow tank with maximum safe working pressure of 400 kPa;
- 40 mm I.D. x 24 m long mild steel pipeline, including 2 m vertical lift, two 1 m radius 90°, closely coupled bends (test bend is shown in Figure 3.3);
- 0.5 m³ receiving hopper with insertable pulse-jet dust filter;

For the connection of bends and pipelines, flanges were used with gasket of synthetic material. Compressed air at maximum pressure of approximately 750 kPa was supplied from Kirloskar Electric-powered Model KES 18-7.5, 3.37 m³/min free air delivery rotary screw compressor. Various static pressure measurement points were installed along the pipeline and bends, where P4 was used to measure the total pipeline pressure drop and all other transducers (i.e. P6, P7, P8 and P9) were installed at out of influence of the bends to measure static pressure at respective points, which were used to model solid friction factor of straight horizontal pipe. Specification of static pressure transducers: manufacturer: Endress & Hauser, model: Cerabar PMC131, pressure range: 0-4 & 0-2 bar, maximum pressure: 3.5 bar (absolute), current signal: 4-20 mA. Receiver bin of capacity 0.5 m³ was installed with pulse-jet type dust filter. All other required instruments for such as PRV (pressure reducing valve), flow meter, NRV (non-return valve), blow valve, pressure gauge and load cells (shear beam type) were suitably placed. Calibration of the transducer, load cells & flow meter were performed using the standardized calibration procedure. To record the electrical output signals from the load cells, pressure transducer and flow meters a portable PC compatible data logger (NIC Jaipur) was used. That data logger had 16 different channels. Schematic of 50 mm I.D. x 70 m long pipe is shown in Annexure: Figure A3. Piping and Instrumentation (P&I) diagram for Thapar University test rig is shown in Figure 3.4.

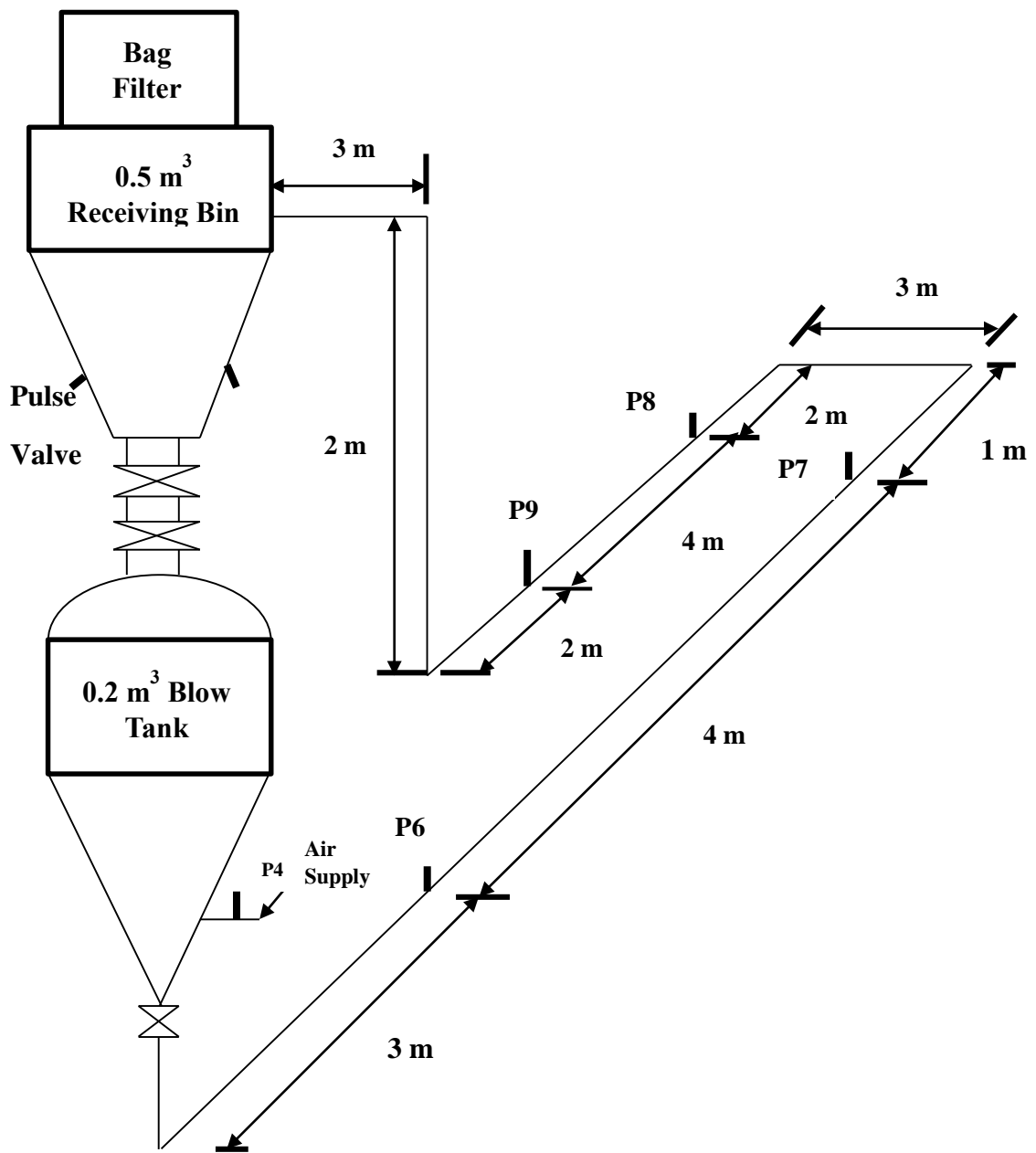


Figure 3.2: Layout of the 63.5 mm I.D. x 24 m long pipeline Test Rig (for fly ash)

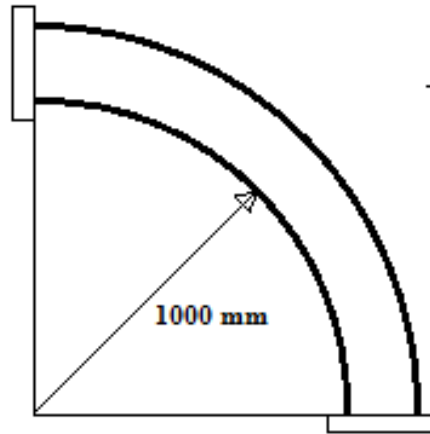


Figure 3.3: Test Bend of 1 m bend radius

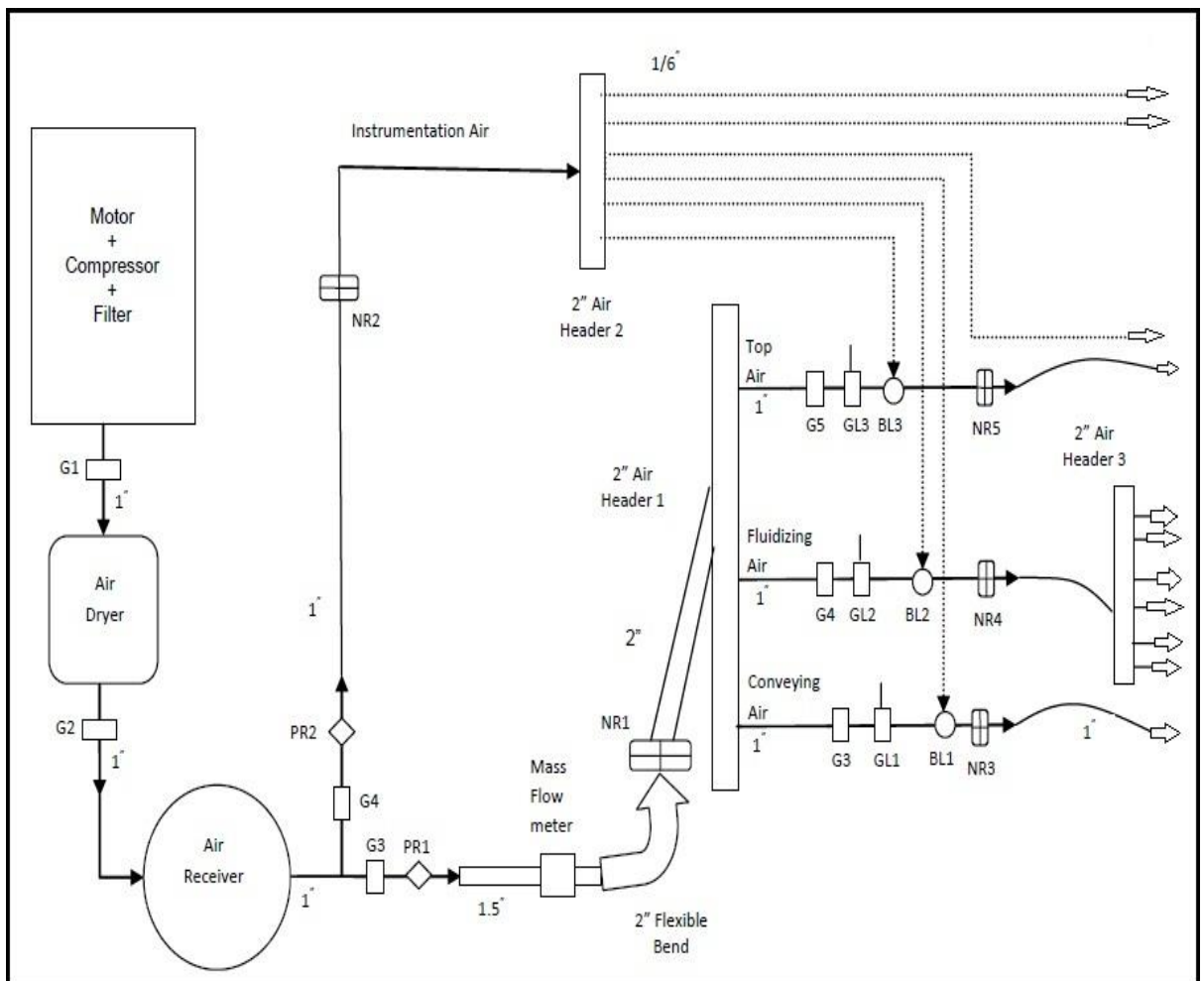


Figure 3.4: Piping and Instrumentation diagram for compressed air of 63.5 mm I.D. x 24 m Test Rig (for fly ash)

3.2.3 Calibrations of load cells (blow tank, receiver bin) and static pressure transducers

Calibrations of the above were performed using the standardised calibration procedure, as described in Pan (1992). However, the procedure for calibration of static pressure transducer is described here. All the pressure transducers in the test program are calibrated by maintaining a constant pressure in the pipeline and simultaneously recording the voltages of the transducers. The calibration procedure is established as below:

- a) Connect all transducers by cable to transducer data logger.
- b) With all material in the receiving hopper (hopper valve and fill valve closed), close the ball valve at the end of the pipeline, vent valve and open the discharge valve.
- c) Close with blind flange upstream of the product feed point and close it until a designated pressure (e.g. 200 kPa) is reached in the pipeline.
- d) Check whether there is a leak on each tapping by manual check. If so, open the vent valve, rectify any leakage point and go back to (c). If not, then go to (e).
- e) Open the vent valve until there is atmospheric pressure in the pipeline. Then close the vent valve.
- f) Adjust the pressure regulator (e.g. 50 kPa), then open the valves to the blow tank top and ring air.

- g) Measure the static pressure in the pipeline by using a pressure meter and record the pressure of all the pressure transducers from data logger simultaneously after the pressure in the pipeline is very stable.
- h) Close the valves to the blow tank top and ring air. Repeat steps (e) to (g) for different static pressures.

Calibration graph of transducers P4 and P6 are shown in Figure 3.5 (a) and (b) respectively.

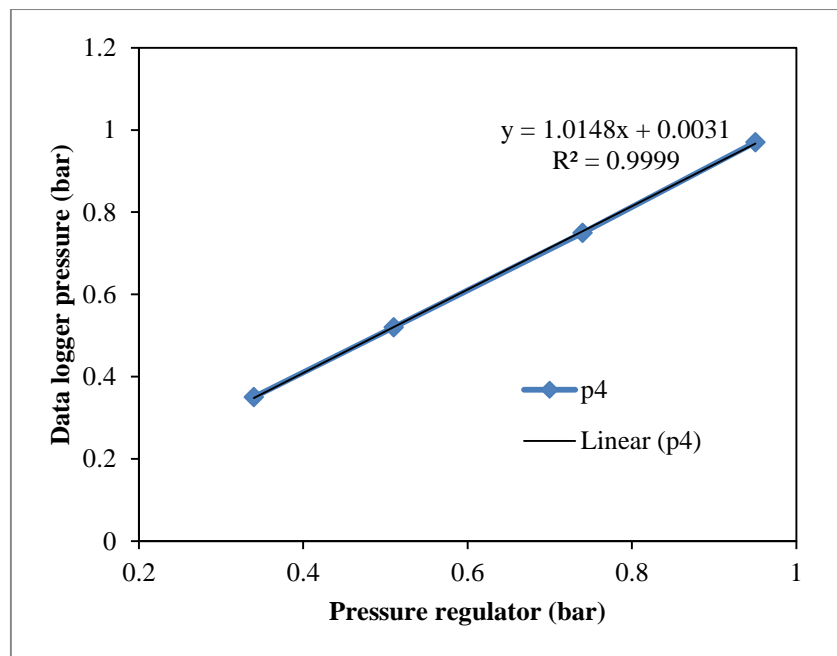


Figure 3.5 (a): Calibration factor for pressure transducer (P4)

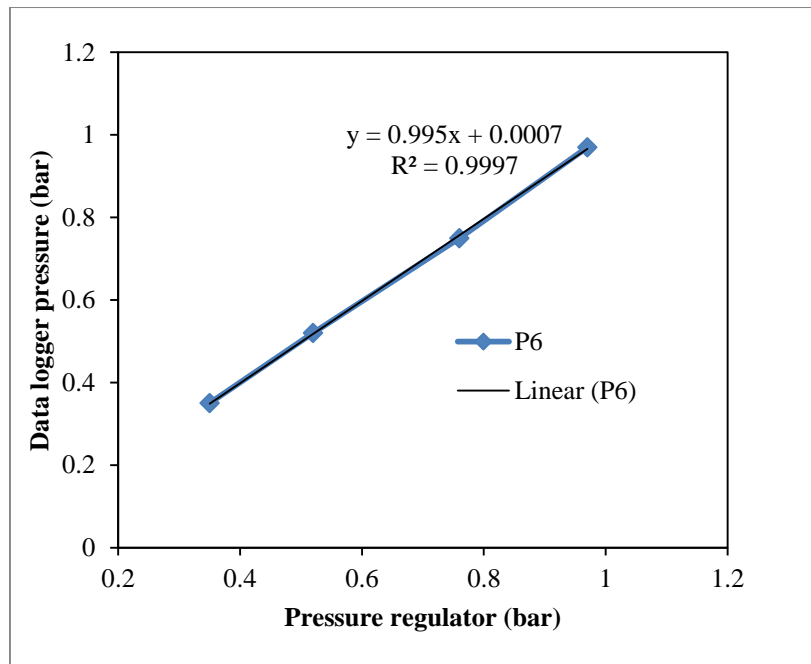


Figure 3.5 (b): Calibration factor for pressure transducer (P6)

Air flow meter is used to measure the amount of air conveyed in a cycle. It is directly connected to the data logger and reading is recorded in the computer with the help of software provided by the company (NIC Jaipur). This air flow meter also have a digital display on it which will show the amount of air passes through it and also the cumulative amount of air flow through it. It's a vortex type of flow meter, a vortex is created by the obstacle present in the path of air flow and is being converted into digital as well as analog signal that are being recorded in the data logger.

Load cells are used for calculating the amount of mass of material accumulated in the receiver bin and the blow tank. Receiver bin and blow tank are placed on shear type load cells, one load cell is placed below each of the four supports and then connected with each other such as, they will give the average reading of the load being transferred. Each load cell is calibrated before using it. The calibration of each load cell is done at the factory itself and at the laboratory.

Blow tank is the device which is used for collection of granular material, the material that has to be transported comes into the blow tank with the opening of inlet valve. This inlet valve is pneumatically controlled and is operated automatically during the conveying cycle. There are two lines of conveying air connected to the blow tank, one is the top air that is required to build up initial pressure in the blow tank so that the bulk material can easily be transported and the other is the fluidization line which ensures that the material in the blow tank would not be settled or stick to any location inside blow tank. When the outlet valve is opened, the material inside the blow tank falls in the conveying line and is being conveyed by the main air/gas. Whereas, the receiver bin is a device that is used for collecting the material at the end of conveying. With the help of bag filter, which was installed at the top of receiver bin material is stored in the tank and air/gas leave the system. It is also provided with fluidization technique.

CHAPTER 4: EVALUATION OF DIFFERENT BEND MODELS

4.1 Introduction

The effects of selecting different bend models on the prediction of total pipeline pressure drop conveying characteristics were evaluated by estimating the total pipeline conveying characteristics for fly ash for different solid flow ranges for the five test rigs: 69 mm I.D. x 168 m, 105 mm I.D. x 168 m, 69 mm I.D. x 554 m, 63.5 mm I.D. x 24 m, 50 mm I.D. x 70 m long pipeline. For the evaluation of bends models using total pipeline PCCs, it was necessary to calculate straight pipe pressure drop and add it with bend pressure drop calculated by different bend models. Accurate prediction of straight pipe pressure drop depends on the accuracy of solid friction factor.

4.2 Model for solid friction factor of horizontal straight pipe

For the purpose of solid friction factor modelling of straight pipe, following general power function format (4.1) was employed. This format has been used by Pan and Wypych (1998), Jones and Williams (2003) and Williams and Jones (2004).

$$\lambda_s = K(m^*)^a (Fr)^b \quad (4.1)$$

For the test set up (69 mm I.D. x 168 m long pipeline), Mallick (2010) conducted a wide range of experiments for dilute and dense phase by using thermal power plant fly ash as test material through a set up (Figure 3.1). Properties of fly ash has been given in Table 3.1.

Static pressure data obtained from straight pipe points (P9-P10) across straight horizontal pipe section of length 52.68 m, following power function correlation (4.1) for solid friction factor has been derived using least square method.

$$\lambda_s = 20.807(m^*)^{-0.71}(Fr_m)^{-2.1131} \quad [R^2 = 0.998] \quad (4.2)$$

This high value of R^2 suggests that the model of solid friction factor is good fit with experimental data. This solid friction factor model (4.2) has been considered by the author, for straight pipe pressure drop investigation and also for Schuchart model (1968) in 69 mm I.D. x 168 m, 105 mm I.D. x 168 m, 69 mm I.D. x 554 m long pipeline. Similarly for the test set up (63.5 mm I.D. x 24 m long pipeline) it was conducted a large number of experiments by author for dilute, dense and blockage by using Ropar (Punjab) thermal power plant fly ash as tested material through a set up (Figure 3.2). Properties of this fly ash has been given in Table 3.1. Static pressure data obtained from straight pipe points (P6-P7) across straight horizontal pipe section of length 4 m, following power function correlation (4.1) for solid friction factor has been derived using least square method.

$$\lambda_s = 1.431(m^*)^{-0.48488}(Fr_m)^{-1.04523} \quad [R^2 = 0.9542] \quad (4.3)$$

This high value of R^2 suggests that the model of solid friction factor is good fit with experimental data. This solid friction factor model (4.3) has been considered by the

author, for straight pipe pressure drop investigation and also for Schuchart model (1968) in 63.5 mm I.D. x 24 m, 50 mm I.D. x 70 m long pipeline.

4.3 Evaluation of bend models based on UoW data

Bend models were evaluated with the help of prediction of total pipeline pressure drop conveying characteristics (PCC) for fly ash and different solid flow ranges for the three test rigs: 69 mm I.D. x 168 m long, 105 mm I.D. x 168 m long, 69 mm I.D. x 554 m, by using each of seven bend models (equation: 2.10, 2.15, 2.16, 2.19, 2.21, 2.23, 2.25) and comparing the predicted PCC with each other and against experimental data. The model (equation 4.2) was used to calculate the pressure drop in straight pipe lengths. In all losses, losses due to initial acceleration and verticals were calculated as per Marcus et.al. (1990). Same models were used to estimate pressure drop in horizontal pipes, vertical and for initial acceleration, therefore any variation in magnitude (and trend) of the predicted total pipeline conveying characteristics should occur only because of the different selected bend models. Results are shown in Figure 4.1 to 4.3.

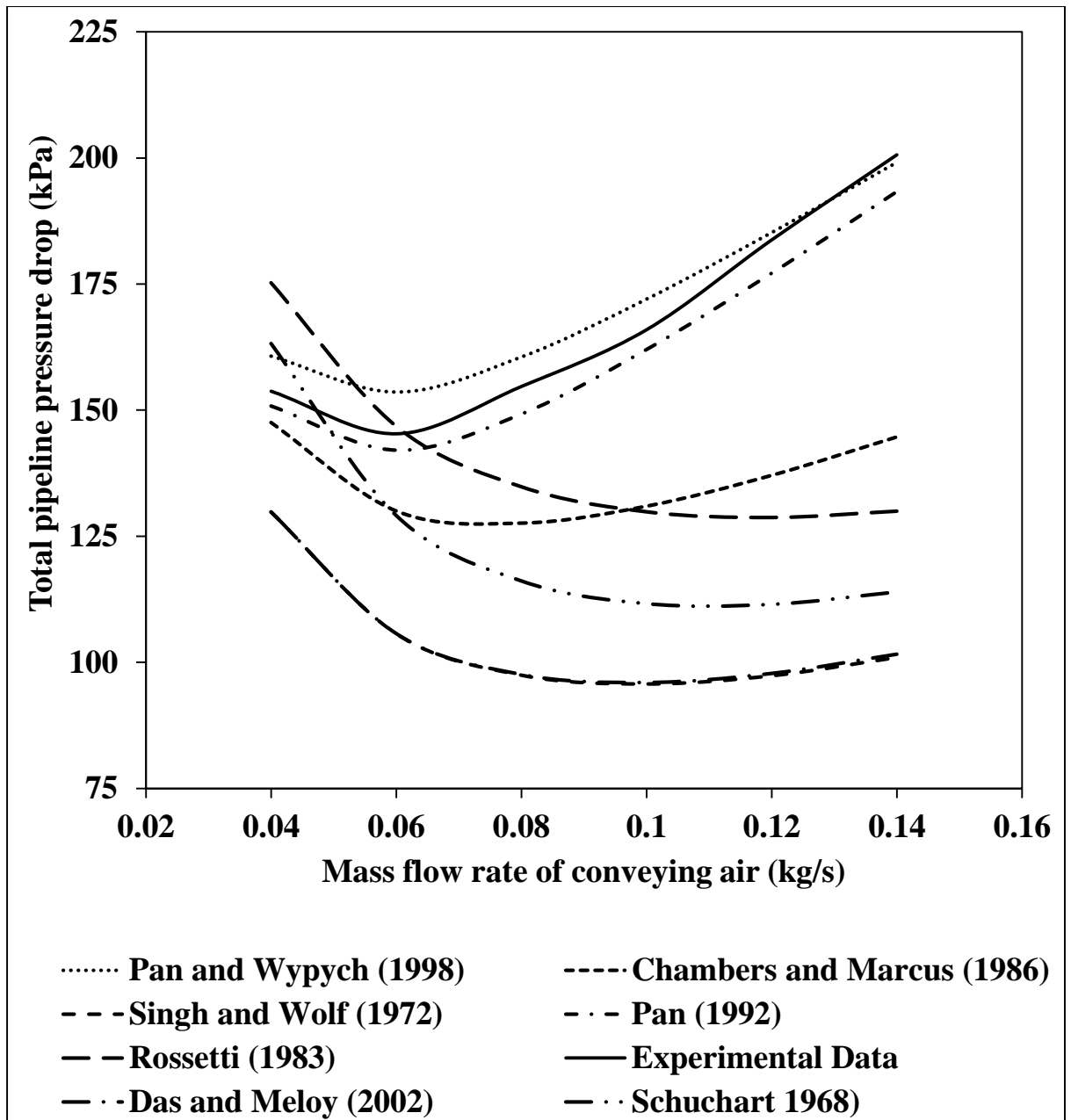


Figure 4.1: Comparison of experimental versus predicted values of total pipeline pressure drop (fly ash, $D = 69$ mm, $L = 168$ m, $m_s = 19$ t/h)

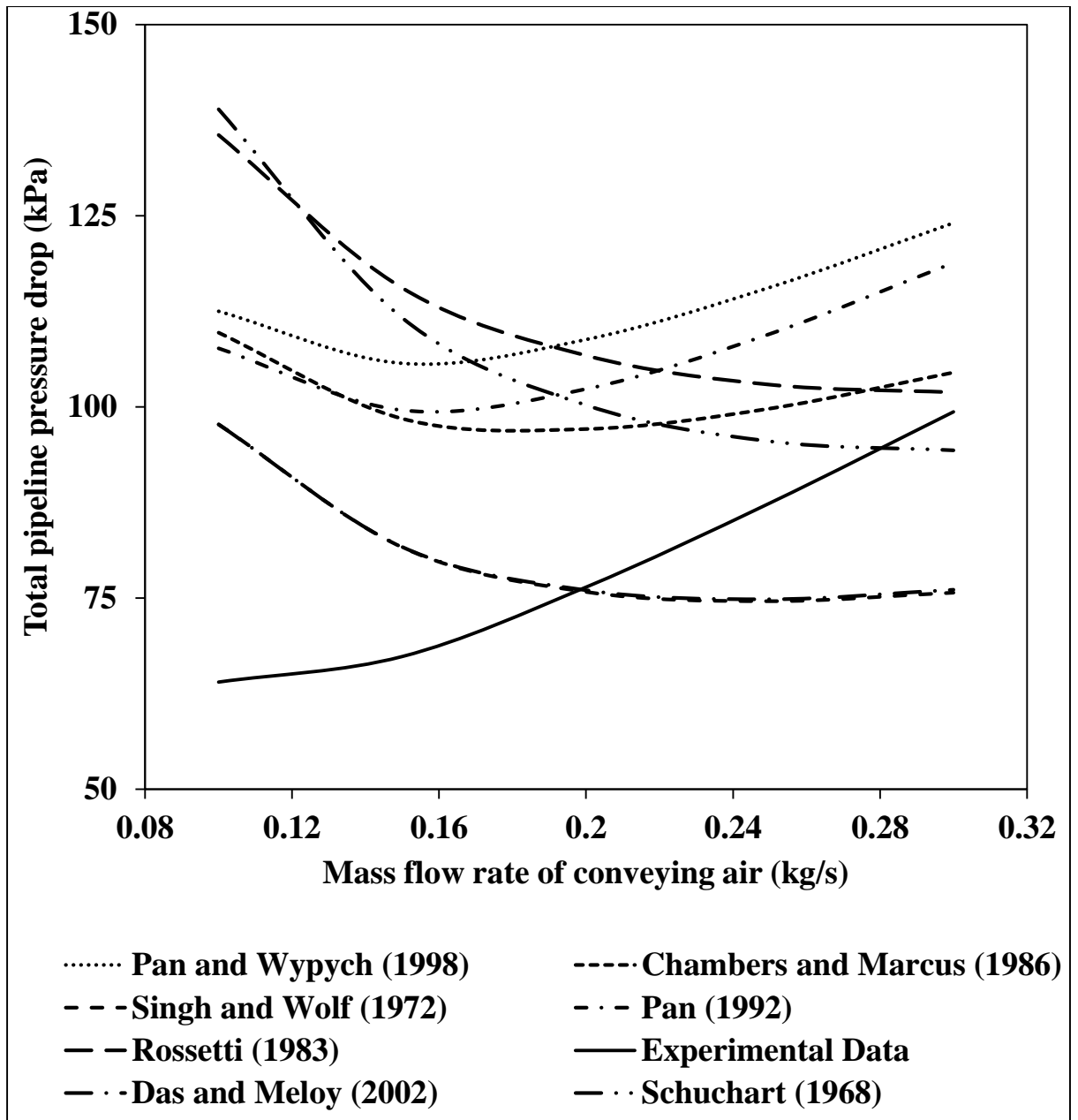


Figure 4.2: Comparison of experimental versus predicted values of total pipeline pressure drop (fly ash, $D = 105$ mm, $L = 168$ m, $m_s = 28$ t/h)

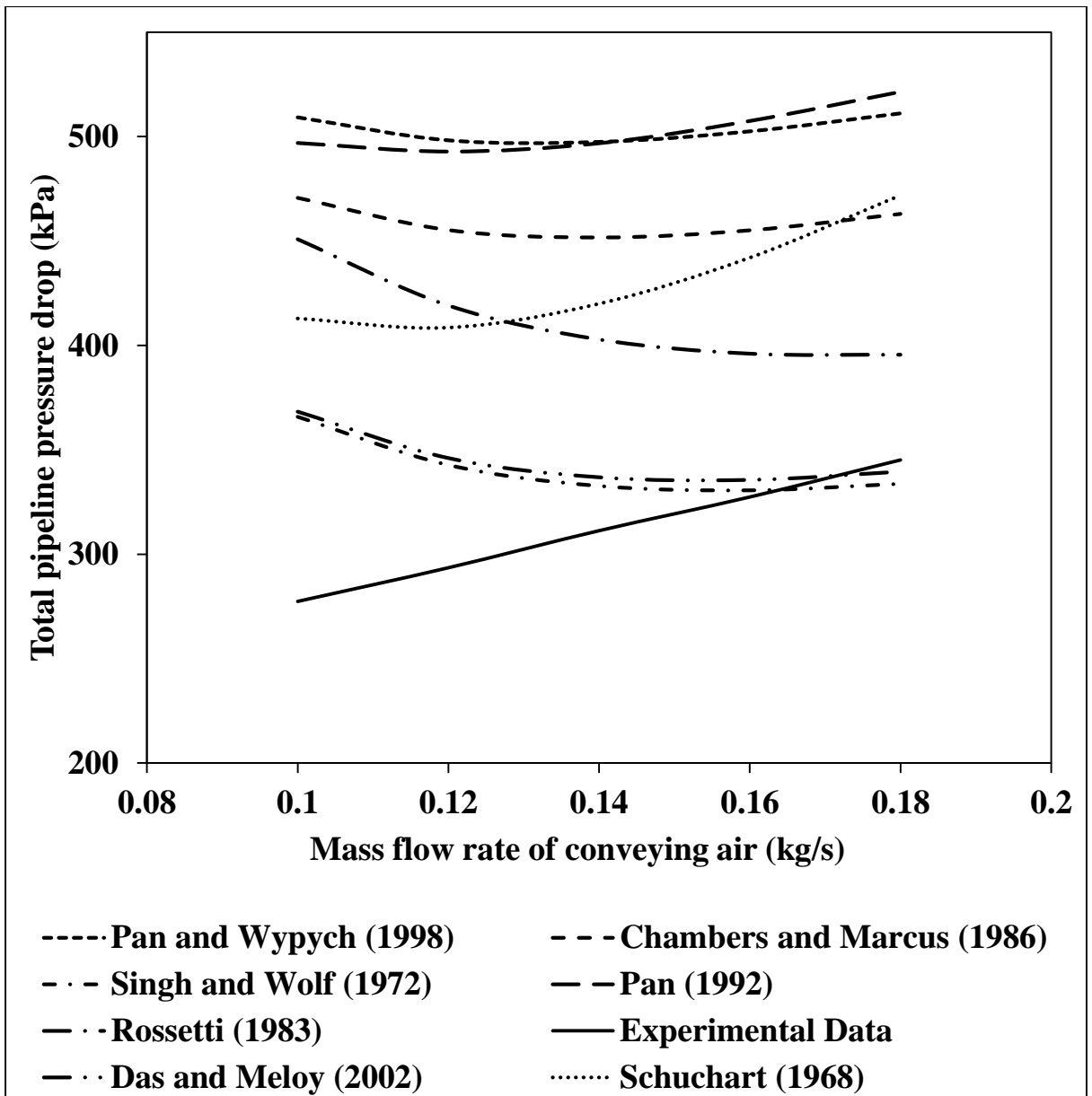


Figure 4.3: Comparison of experimental versus predicted values of total pipeline pressure drop (fly ash, $D = 69$ mm, $L = 554$ m, $m_s = 11$ t/h)

4.3.1 Results and discussion

The above results/comparison plots showed that the selection of different bend models can generate significantly different predicted total pipeline conveying characteristics (even though same solids friction factor model used to calculate pressure drop in straight horizontal pipeline, same initial acceleration and vertical pipe pressure drop model). Figure 4.1 (69 mm I.D x 168 m long), showed that among all bend models Chamber and Marcus (1986), Pan (1992) and Pan and Wypych (1998) model follow the same trend whereas, Rossetti (1983), Schuchart (1968), Singh and wolf (1972) and Das and Meloy (2002) models follow same trend which was different than other three models. There were significant difference in prediction of total pipeline conveying characteristics in dilute phase between Pan and Wypych (1998) and Das and Meloy (2002). On the other hand, the total pipeline PCC of Pan (1992) and Pan and Wypych (1998) seems to follow the experimental trend much better. However, the model presented by other researchers is shown to under-prediction in dilute-phase region. Figure 4.2 (105 mm I.D. x 168 m long), showed that the selection of Pan and Wypych (1998) and Das and Meloy (2002) model create significant difference in total pipeline pressure drop in dilute phase. When compared to experimental pressure drop some models (Pan and Wypych, 1998; Pan, 1992) gives over predicted values and some other models (Das and Meloy, 2002; and Singh and Wolf, 1972) gives under predicted values of total pipeline pressure drop. Whereas, Schuchart (1968), Rossetti (1983) and Chamber and Marcus (1986) are shown to good prediction with experimental pressure drop in dilute phase. Figure 4.3 (69 mm I.D. x 554 m long), showed that the selection of Pan and Wypych (1998) and Das and Meloy (2002) model create significant difference in total pipeline pressure drop in dilute phase. When compared to

experimental total pipeline PCC, all bend models gives over prediction except Das and Meloy (2002) and Singh and Wolf (1972). Das and Meloy (2002) and Singh and Wolf (1972) models gives good prediction of pressure drop in dilute phase. Based on above findings, the differences in total pipeline PCC of different bend models in dilute phase and dense phase were due to bend models only because all other pressure drop which were considered for the calculation of total pipeline pressure drop, used same models. Selection of solid friction factor model of straight pipe also creates difference in total pipeline PCC, because it changes from one location to other location in same test rig. On the basis of this observation it could not said that particular model was inaccurate, because each model was developed in different conveying condition and for different particles. Hence, this evaluation makes it clear that which model should use in a particular condition. Prediction of bend only loss each of seven bend models in low velocity (dense-phase) and high velocity flow (dilute-phase) are comparatively shown in the scattered chart and bar chart with smooth lines form for bend pressure drop only in Figure 4.4 to 4.6 for different solid flow ranges of fly ash for 3 test rigs.

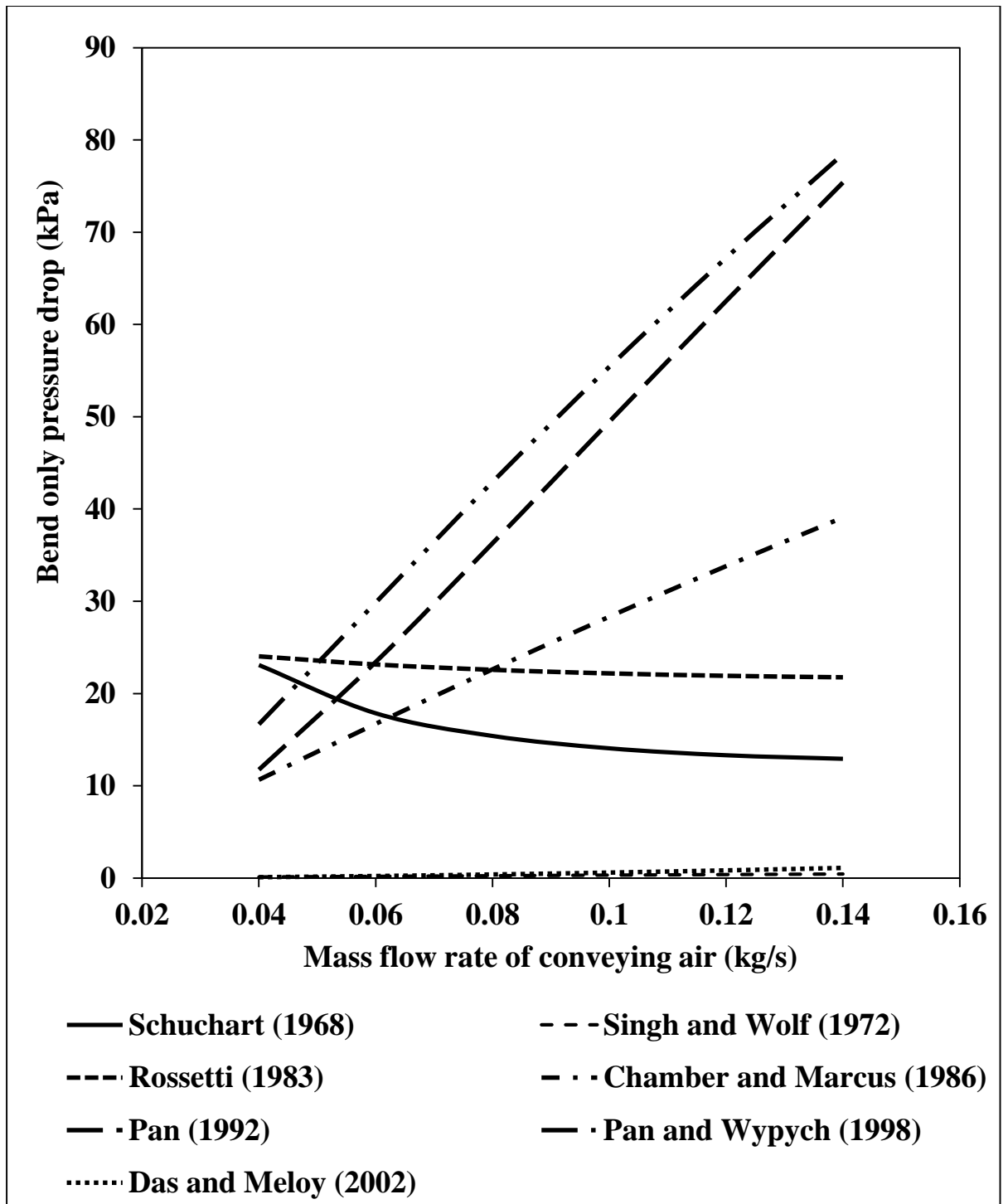


Figure 4.4: Bend loss PCC based on different bend models

(fly ash, $D = 69$ mm, $L = 168$ m, $m_s = 19$ t/h)

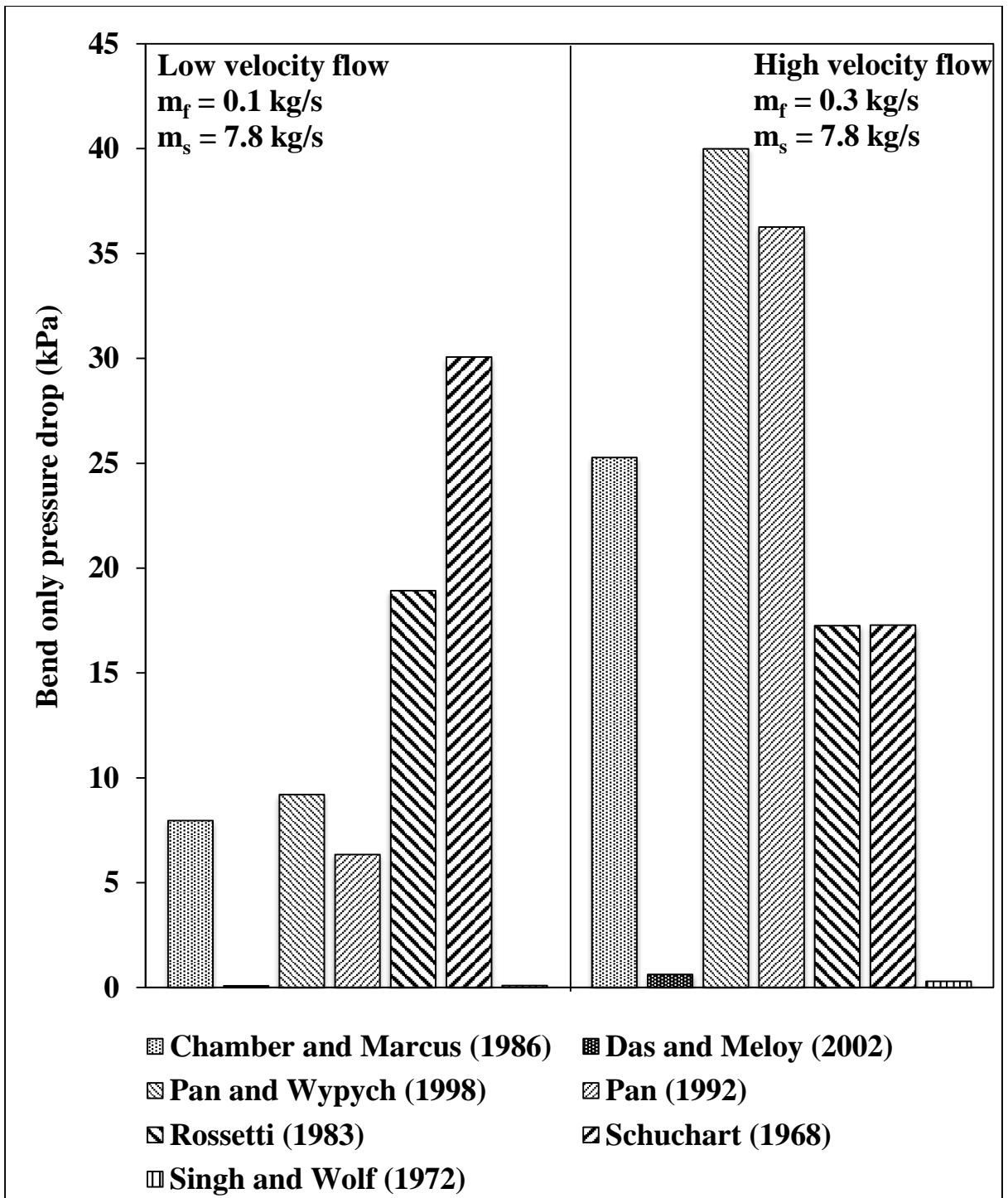


Figure 4.5: Comparison of bend only pressure drop between low velocity flow and high velocity (fly ash, $D = 105 \text{ mm}$, $L = 168 \text{ m}$, $m_s = 28 \text{ t/h}$)

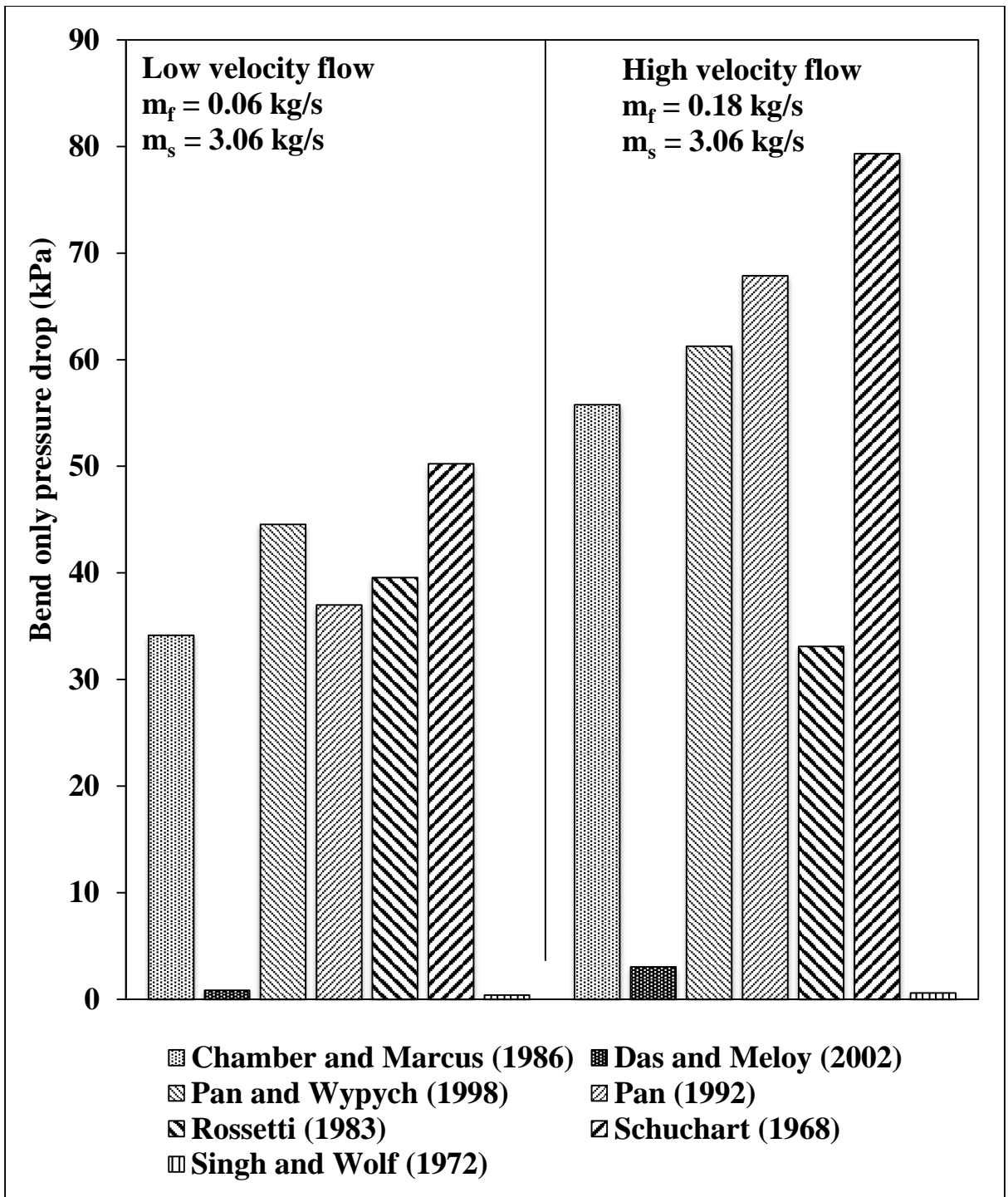


Figure 4.6: Comparison of bend only pressure drop between low velocity flow and high velocity (fly ash, $D = 69 \text{ mm}$, $L = 554 \text{ m}$, $m_s = 11 \text{ t/h}$)

The above comparison plots show that different bend models can generate significantly different predicted total bend pressure drop either in low velocity or high velocity flow.

Low velocity flow have less bend pressure drop compared to high velocity flow. In Figure 4.5 and 4.6 Singh and Wolf (1972) and Das and Meloy (2002) model shows opposite trend that is high bend pressure drop in low velocity flow and vice versa. Figure 4.4 to 4.6, infer that Singh and Wolf (1972) and Das and Meloy (2002) model predict very low bend pressure drop. This indicates that it may not be suitable for this particular application. So for selection of accurate bend model, there should be comparative study of different models for a specific conveying product and test setup.

4.4 Evaluation of bend models based on TU data

The effects of selecting different bend models on the prediction of total pipeline pressure drop conveying characteristics were evaluated by estimating the total pipeline conveying characteristics for fly ash for different solids flow rates for the three test rigs (63.5 mm I.D. x 24 m long, 50 mm I.D. x 70 m long pipelines) by using each of seven bend models (equation: 2.10, 2.15, 2.16, 2.19, 2.21, 2.23, 2.25) and comparing the predicted PCC against experimental data. The model (equation 4.3) was used to calculate the pressure drop in straight pipe lengths. In all losses, losses due to initial acceleration and verticals were calculated as per Marcus et al. (1990). As the same set of models were used to estimate pressure drop in horizontal pipes, vertical and for initial acceleration, therefore any variation in magnitude (and trend) of the predicted total pipeline conveying characteristics should have occurred only due to the difference in selection of bend models. Results are shown in Figure 4.7 to 4.10.

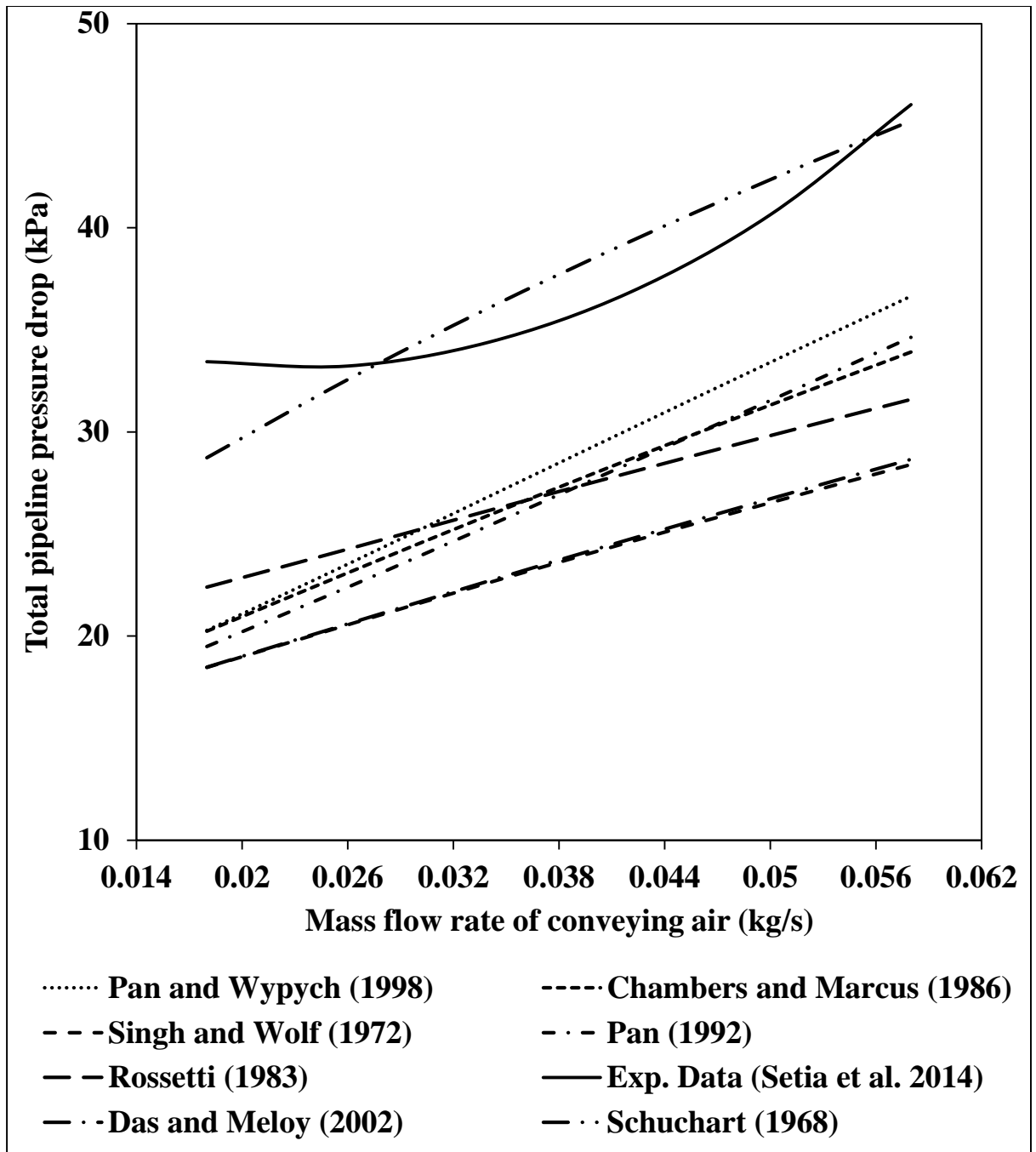


Figure 4.7: Comparison of experimental versus predicted values of total pipeline pressure drop (fly ash, $D = 63.5$ mm, $L = 24$ m, $m_s = 4.5$ t/h)

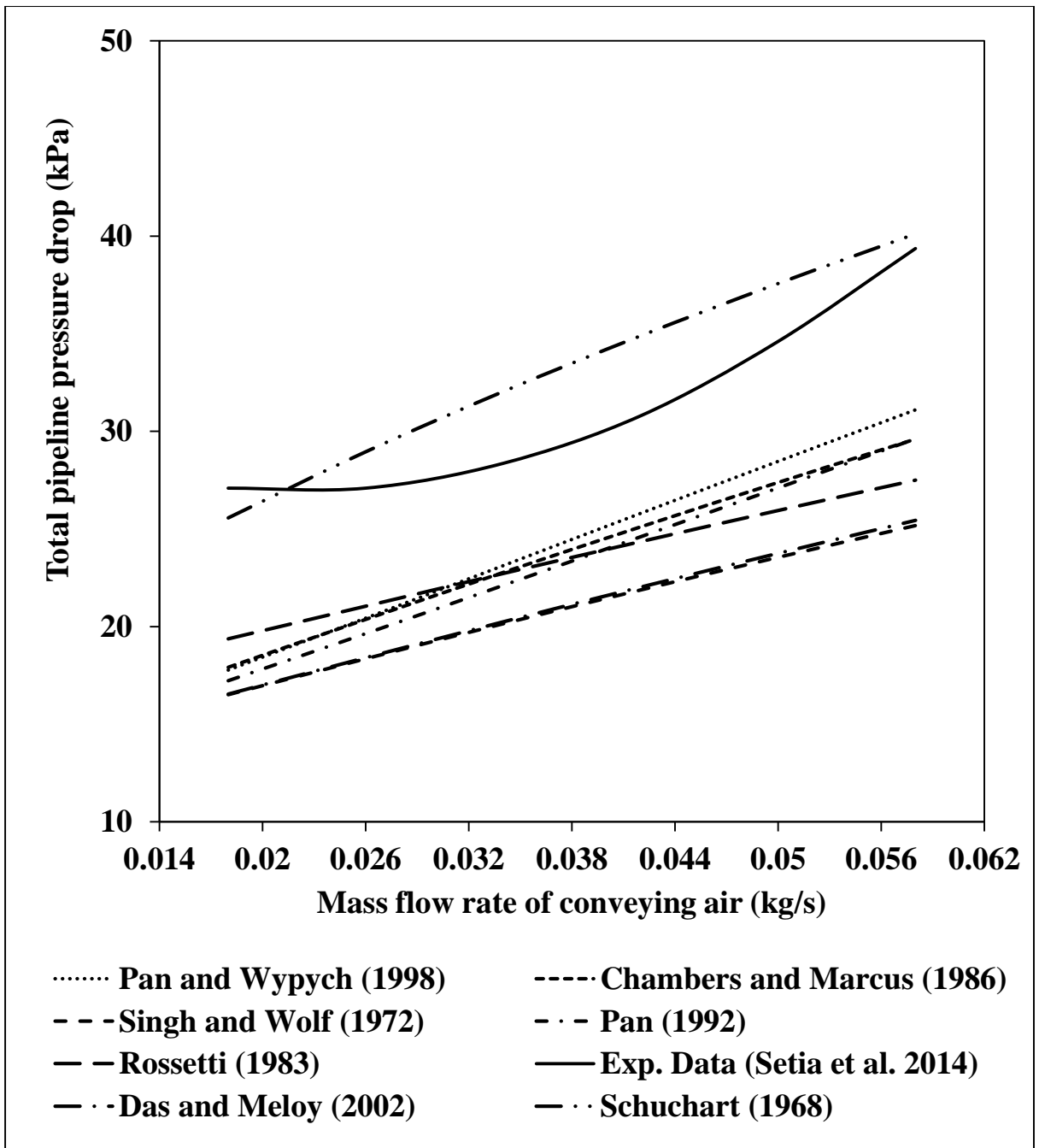


Figure 4.8: Comparison of experimental versus predicted values of total pipeline pressure drop (fly ash, $D = 63.5$ mm, $L = 24$ m, $m_s = 3.5$ t/h)

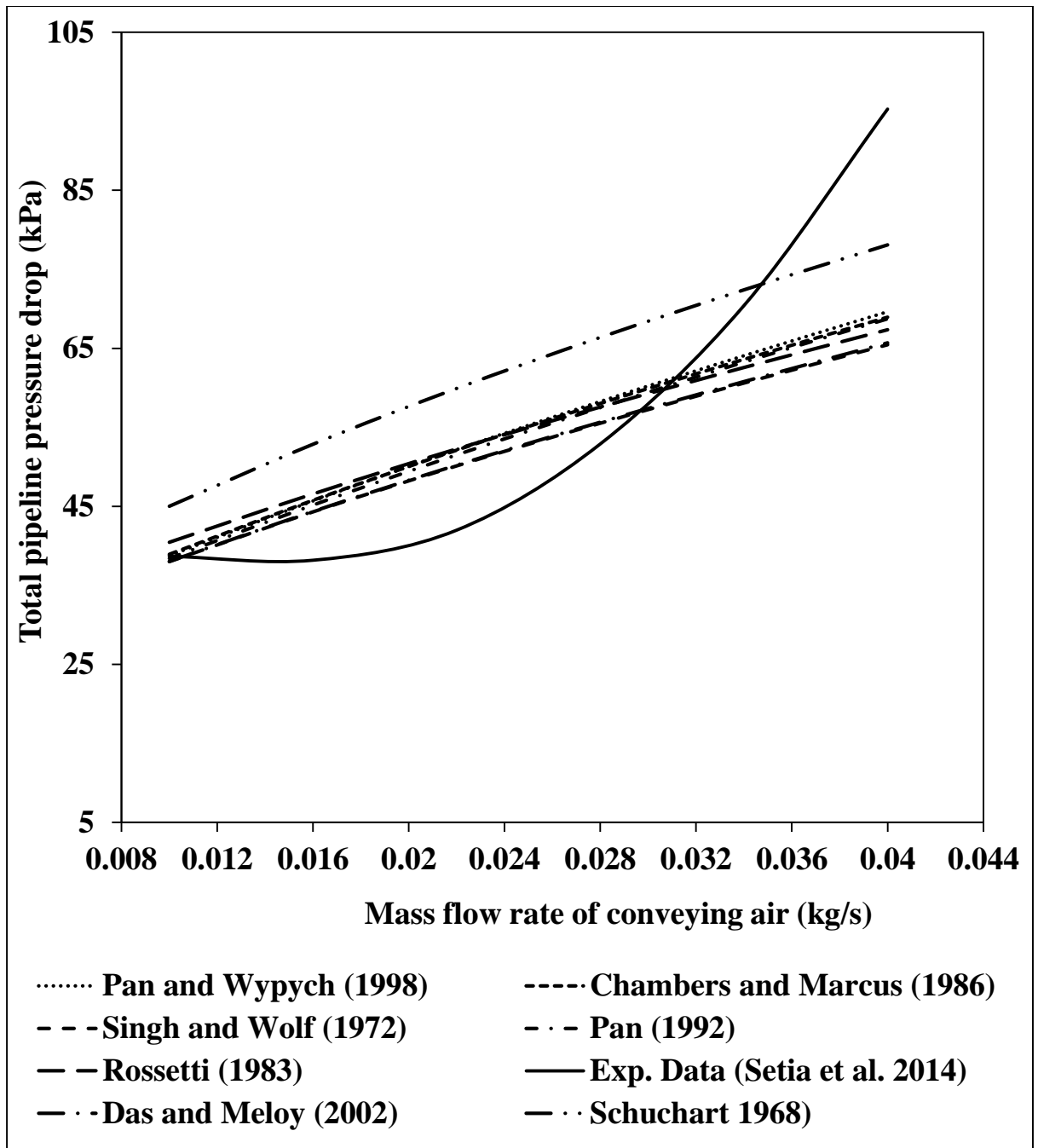


Figure 4.9: Comparison of experimental versus predicted values of total pipeline pressure drop (fly ash, $D = 50$ mm, $L = 70$ m, $m_s = 2.5$ t/h)

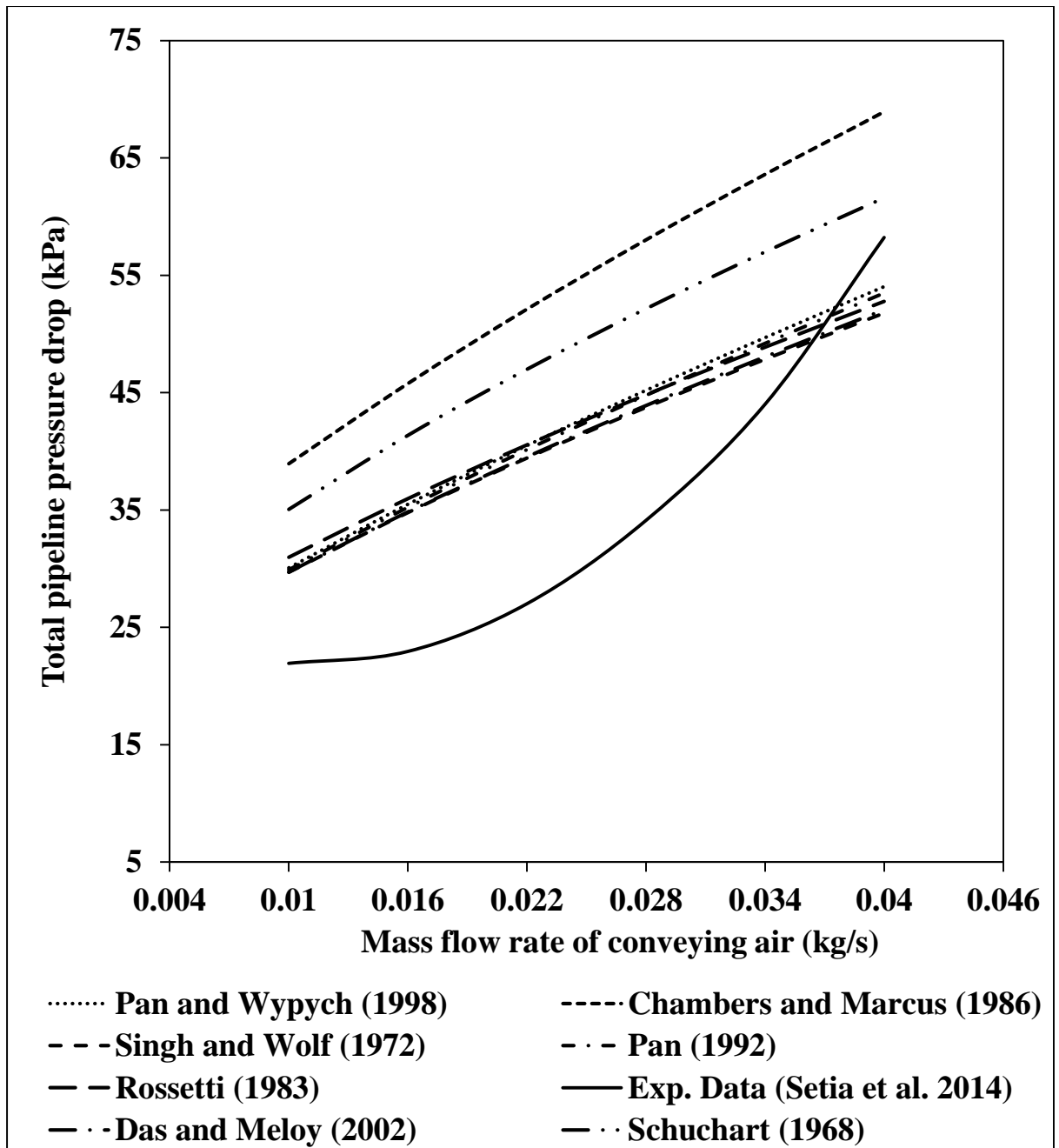


Figure 4.10: Comparison of experimental versus predicted values of total pipeline pressure drop (fly ash, $D = 50$ mm, $L = 70$ m, $m_s = 1.5$ t/h)

4.4.1 Results and discussion

The above results in Figure 4.7 to 4.10 showed that the selection of different bend models can generate significantly different predicted total pipeline conveying characteristics (even though the same solids friction factor model was used to calculate pressure drop in straight horizontal pipeline). Figure 4.7 and 4.8 (63.5 mm I.D x 24 m long) showed that in the predicted total pipeline PCC, predictions using Chamber and Marcus (1986), Pan (1992), Pan and Wypych (1998), Rossetti (1983), Schuchart (1968), Singh and Wolf (1972) and Das and Meloy (2002) models follow the similar trends as the experimental PCC. Singh and Wolf (1972) and Das and Meloy (2002) models are overlapped with each other. There was significant difference in prediction of total pipeline conveying characteristics in the dilute phase as well as in dense phase region between Schuchart (1968) and Das and Meloy (2002) model. On the other hand, the total pipeline PCC of Schuchart (1968) seem to follow the experimental trends much better. However, the model presented by other researchers is shown to under-predict in the dilute-phase region. Figure 4.9 (longer pipe) shows that there is no significant difference between predicted total pipeline pressure of drop using all above seven bend models. When the predicted total pipeline PCC were compared with the experimental plots, in dense phase region all models provided reliable estimations for total pipeline pressure drop. Whereas, in dilute phase region all bend models under predicting. There were significant difference between experimental total pipeline PCC and total pipeline pressure drop due to Das and Meloy (2002) model. From Figure 4.10, it can be seen that all bend models were over predicting with experimental total pipeline PCC in dense phase. Whereas, in dilute phase Schuchart (1968) and Chamber and Marcus (1986) models over predicting. Pan (1992), Pan and Wypych (1998), Rossetti (1983), Singh

and Wolf (1972) and Das and Meloy (2002) were under predicting with experimental total pipeline PCC and also overlapping with each other. Prediction of bend only loss for each of seven bend models in 63.5 mm I.D. x 24 m long pipeline, for a range of low velocity (dense-phase) to high velocity flow (dilute-phase) regimes are compared in Figure 4.11 for a constant solid flow rate of fly ash.

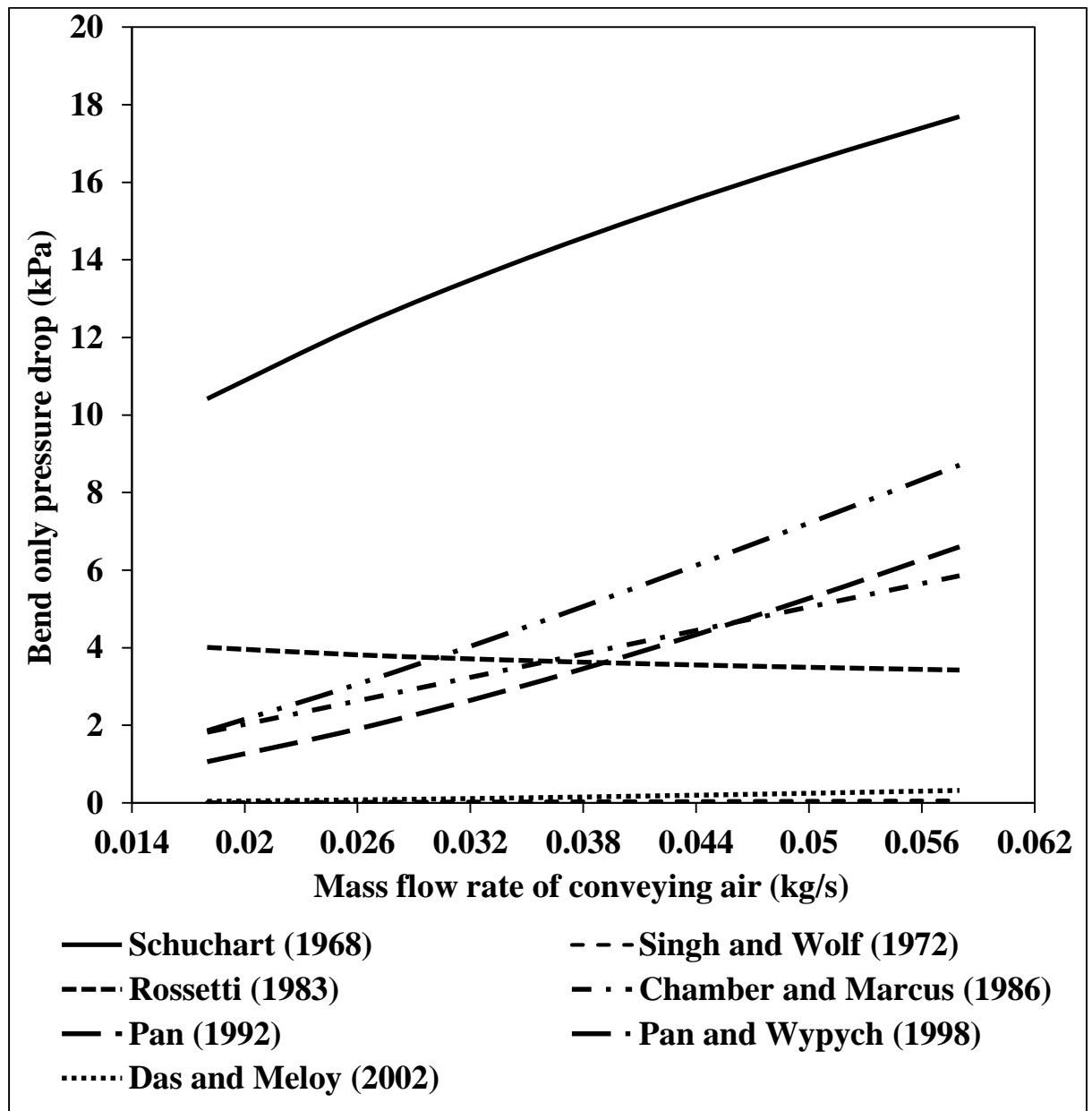


Figure 4.11: Bend loss PCC based on different bend models in dense to dilute phase (fly ash, $D = 63.5$ mm, $L = 24$ m, $m_s = 4.5$ t/h)

Figure 4.11 shows that different bend models can generate significantly different values of predicted total bend pressure drop (i.e. combined pressure drop caused by all bends in pipeline) both in low and high velocity flow. Singh and Wolf (1972) and Das and Meloy (2002) models are almost superimposing each other and predicted very low values of bend loss (which is incorrect), whereas Schuchart (1968), Chamber and Marcus (1986), Pan (1992) and Pan and Wypych (1998) have shown high pressure loss in dilute-phase as compared to dense –phase regime, which seems to be following the expected trend. Pressure loss in dense-phase is more than the dilute phase regime by using Rossetti (1983), which does not follow the expected trend (Pan, 1992). This indicates that Rossetti (1983) is not suitable for the case of fine powder conveying from dense- to dilute-phase flow.

**CHAPTER 5: MODELLING AND VALIDATION OF
SOLID FRICTION FACTOR MODEL FOR CLOSELY
COUPLED BEND**

5.1 Introduction

Previous investigations (Chapter 4) to evaluation of different “existing” bend models for bend pressure drop (Schuchart, 1968; Singh and Wolf, 1972; Rossetti, 1983; Chamber and Marcus, 1986; Marcus et.al, 1990; Pan, 1992; Pan and Wypych, 1998; and Das and Meloy, 2002 etc.) by comparing the predicted and experimental total pipeline pneumatic conveying characteristics (PCC) for a samples of fly ash have shown that the models generally can provide significant under prediction and over prediction for change of diameter and/or length. Although the above findings demonstrated the limitations of the “existing” models (derived by other researchers), it was also appreciated that the investigation would have been more fair and comprehensive if new models have been derived using the conveying data of the different fly ash and then evaluated under different diameter conditions. The very reason for which the design of a pneumatic conveying system is normally far more difficult compared to the single fluid flow is the design parameters of pneumatic conveying systems are significantly dependent on the powder/particle properties (such as the bulk and particle density, particle size, size distribution, shape, surface texture, air retention capabilities, permeability etc). A variation in any or a combination of these properties may potentially cause a significant change in the design (Wypych and Arnold, 1985). Therefore, it was felt that it would be more rational to examine the modelling procedure for its accuracy and stability. With this background, the aim of this chapter is to modelling for the bend solids friction factor.

5.2 General power function format

It was considered that the total losses due to the conveying of solids-gas mixture through a pipe can be represented as the sum of individual losses due to the solids and gas only, as given by equation (1.1) (Barth, 1958). For the purpose of modelling bend solid friction factor, the “general” power function format provided in equation (5.1) was initially employed. This relatively simple format also has been used for a wide range of fly ash of varying size range.

$$\lambda_{bs} = k(m^*)^a (Fr_{bo})^b (\rho_{bo})^c \quad (5.1)$$

For the initial modelling work using fly ash data of Thapar University, a closely coupled bend was selected for analysis on the 38 mm I.D x 24 m long pipe (Figure 3.1). Initially to derive a model for λ solution technique, based on the work of Wypych (1989) was used, from a wide range (dilute- to fluidised dense-phase) of steady state pressure drop data obtained for the P7-P8.

$$\lambda_{bs} = 0.06928(m^*)^{-0.22267} (Fr_o)^{-1.1741} (\rho_o)^{3.789257} \quad [R^2 = 0.98] \quad (5.2)$$

Models derived from P7-P8 data of the 38.1 mm I.D. x 24 m long pipe for fly ash was evaluated for accuracy and stability by using them to predict the bend pressure drop for different pipelines (50.8 mm I.D. x 24 m and 63.5 mm I.D. x 24 m) for various solids flow rates and comparing the predicted pneumatic conveying characteristics against the experimental plots. All the predicted PCC were limited to $Fr_i = 4$, as below this limit,

flow instabilities were found to occur during the experimental program. This criterion has been used throughout this chapter for all the predicted PCC.

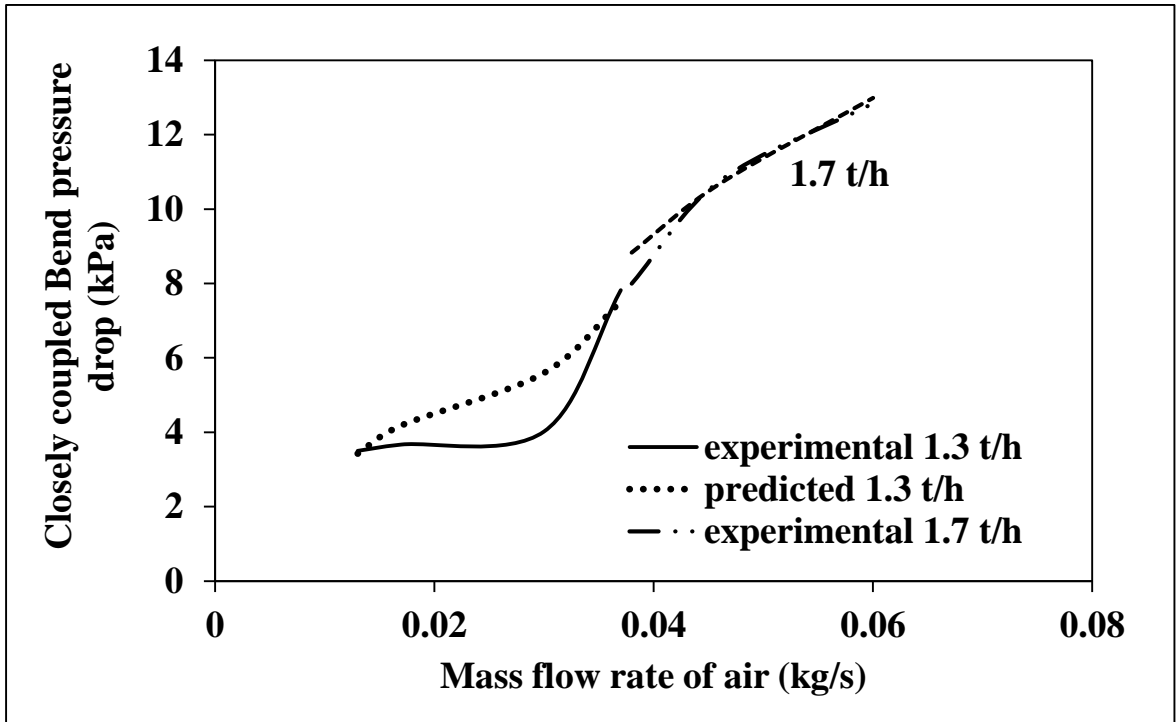


Figure 5.1: Experimental versus predicted PCC for fly ash and 38.1 mm I.D. x 24 m long Pipeline

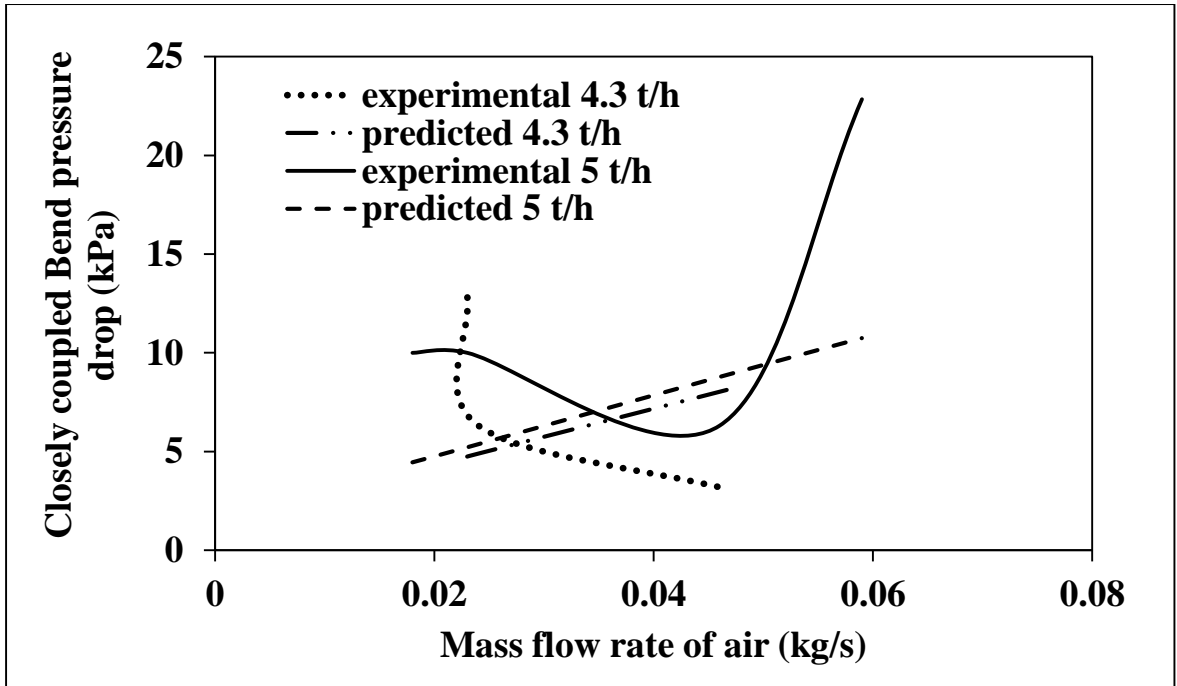


Figure 5.2: Experimental versus predicted PCC for fly ash and 38.1 mm I.D. x 24 m long Pipeline

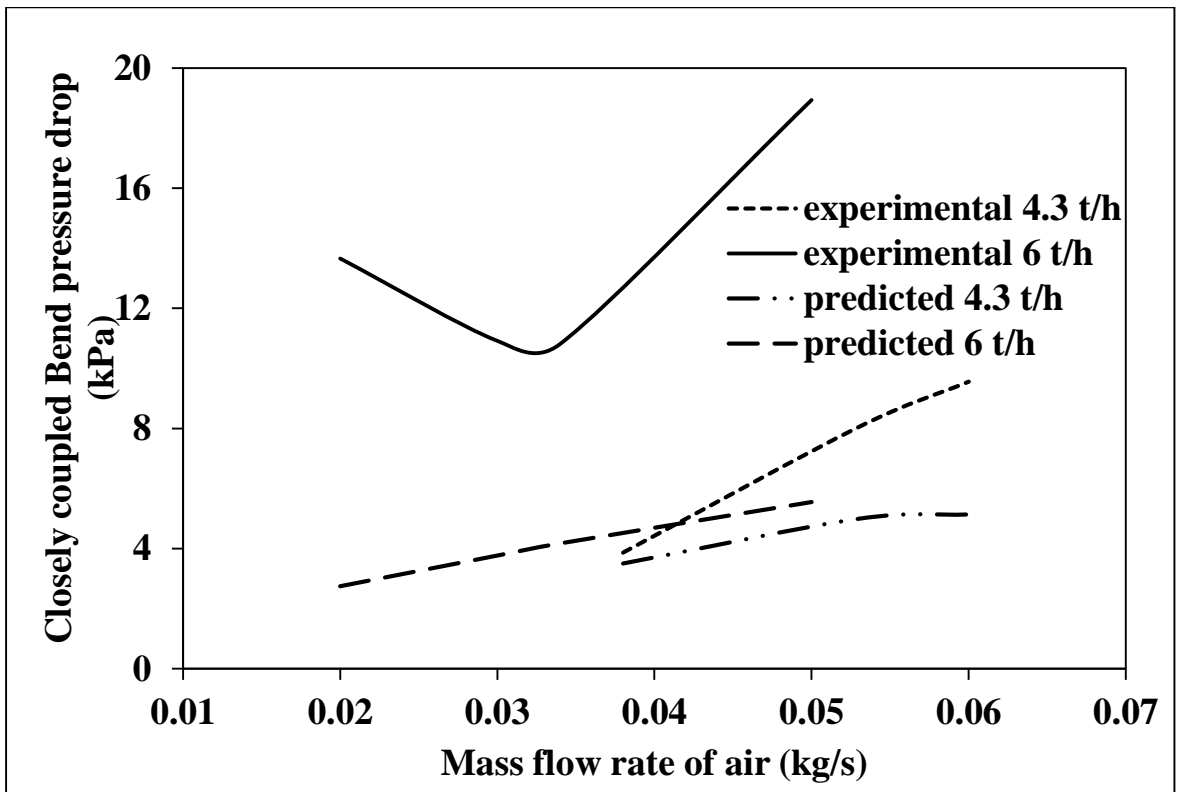


Figure 5.3: Experimental versus predicted PCC for fly ash and 63.5 mm I.D. x 24 m long Pipeline

The results show that for the 38.1 mm I.D. x 24 m pipe (Figure 5.1), the model (equation 5.2) provides much better prediction. However, for diameter scale-up (50.8 mm I.D. x 24 m long pipe and 63.5 mm I.D. x 24 m long pipe, Fig. 5.2 and 5.3 respectively), the model (i.e. equation 5.2, which was “excellent” for the smaller sized pipe) show under-predictions. This suggests that the “true” test of a model would only occur under same pipeline conditions for which model is generated.

Percentage error between experimental and predicted PCC

For 38.1 mm I.D x 24 m long pipeline, the percentage error between predicted and experimental PCC in dilute phase is 4.07 % and in dense phase 14.82 %. If same solid friction factor model which was developed for 38.1 mm I.D x 24 m long pipeline, is used for 50.8 mm I.D x 24 m long pipeline and 63.5 mm I.D x 24 m long pipeline then percentage error was increased and that was 65 % overall for 50.8 mm I.D x 24 m long pipeline and 48 % overall for 63.5 mm I.D x 24 m long pipeline.

CHAPTER 6: CONCLUSION AND FUTURE SCOPE OF WORK

6.1 Conclusion

Seven bend models were tested by predicting total pipeline PCC for particular fly ash and three different pipelines: 69 mm I.D x 168 m, 105 mm I.D x 168 m, 69 mm I.D x 554 m long pipe. Results indicate that for 69 mm I.D. x 168 m long pipeline, Pan (1992) and Pan and Wypych (1998) model better predicted pressure drop for total pipeline as compared to other bend modes. Singh and Wolf (1972) and Das and Meloy (2002) provide nearly same pressure drop for total pipe. In larger pipe 105 mm I.D. x 168 m, there is significant difference in Pan and Wypych (1998) model and Singh and Wolf (1972) and Das and Meloy (2002) model in dilute phase. Schuchart (1968), Rossetti (1983) and Chamber and Marcus (1986) models gives better total pipeline pressure drop when compared with experimental total pipeline PCC. In longer pipe 69 mm I.D. x 554 m, there is significant difference in total pipeline pressure drop of Chamber and Marcus (1986) and Singh and Wolf (1972) and Das and Meloy (2002) model. When compared with experimental PCC Singh and Wolf (1972) and Das and Meloy (2002) gives better result in dilute phase.

Based on above findings of bar charts and bend loss PCC, bend pressure drop be more in high velocity flow (dilute phase) and less in low velocity flow (dense phase). Some models (Singh and Wolf, 1972) and Das and Meloy, 2002) do not follow this trend. So, these models should not be used for 69 mm I.D. x 168 m long pipeline. For 105 mm I.D. x 168 long pipeline, Schuchart (1968) and Rossetti (1983) models give more pressure drop in dense phase compared to dilute phase. So, these models should not be used for 105 mm I.D. x 168 m long pipeline. For 69 mm I.D. x 554 m pipeline, Rossetti (1983) model provides low bend pressure drop for high velocity flow and high pressure

drop for low velocity flow. So, this model should not be used for 69 mm I.D. x 168 m long pipeline.

The results based on development of new bend solid friction factor model show that for the 38.1 mm I.D. x 24 m pipe (Figure 5.1), the model (equation 5.2) provides much better prediction. However, for diameter scale-up (50.8 mm I.D. x 24 m long pipe and 63.5 mm I.D. x 24 m long pipe, Fig. 5.2 and 5.3 respectively), the model (i.e. equation 5.2, which was “excellent” for the smaller sized pipe) show under- predictions. This suggests that the “true” test of a model would only occur under same pipeline conditions for which model is generated.

6.2 Future Scope of work

Although the results obtained in this thesis have contributed significantly to predicting and understanding the bend pressure drop in pneumatic transportation of fly ash, the following areas of investigation still require further attention:

- (i) Further research is required to be conducted to understand better the flow mechanisms of fluidised dense phase around the bends.
- (ii) Further studies are to be conducted to investigate the aspect of the pressure drops in bends, such as evaluation of the existing use of parameters in the different expressions of bend models (i.e. whether these parameters adequately describe the physical phenomenon of reacceleration of powders after the bend outlet), the dependence of bend model on product properties etc.

- (iii) There is need to facilitate the influence of bend altitude and determination of equivalent length for bend.
- (iv) Accurate estimation of acceleration length just after the bend is very essential.

REFERENCES

- Ashenden, S.J., Pittman A.N. and Bradley, M.S.A. 1995. An economic assessment of air assisted gravity conveying as an alternative to pneumatic pipeline conveying. 5th Int. Conf. on Bulk Materials Storage, Handling and Transportation, Newcastle, Australia. 249-254.
- Barth, W. 1958. Strömungsvorgänge beim transport von festteilchen und flüssigkeitsteilchen in gasen. *Chemie – Ing. – Techn.* 30 (3): 171-180.
- Bradley, M. S. A. and Mills, D. (1988). Approaches to dealing with the problem of energy loss due to bends. *In the proceedings of 13th Powder and Bulk Solids Conference.* 705-715.
- Bradley, M. S. A. 1989. An improved method of predicting pressure drop along pneumatic conveying pipelines. *In the proceedings of 3rd International Conference on Bulk Materials Storage and Transportation,* Newcastle, Australia. 282-288.
- Bradley, MSA. (1990). *Prediction of pressure losses in pneumatic conveying pipelines.* Doctoral Dissertation, Thames Polytechnic, London, UK.
- Bradley, MSA. (1990). Pressure losses caused by bends in pneumatic conveying pipelines effects of bend geometry and fittings. *Powder Handling and Processing,* 2, 315-321.
- Chambers, A.J. and Marcus, R.D. 1986. Pneumatic conveying calculations. 2nd Int. Conf. on bulk material storage, handling and transportation, Wollongong: 49-52.
- Chaudhry, A.R., Bradley, MSA, Hyder, LM, Reed, AR and Farnish, RJ. (2001). Analysis and modelling of bend pressure losses in lean phase pneumatic conveyors, for a range of particulate material. *7th International conference on bulk materials storage, handling and transportation,* Newcastle, Australia. 899-906.
- Das, P.K. and Meloy, J.R. 2002. Effect of close-coupled bends in Pneumatic Conveying. *Particulate science and Technology:* 253-266.

- Dhodapkar, S., Solt, P. and Klinzing G.. April 2009. Understanding Bends in Pneumatic Conveying Systems. *Chemical engineering*: 53-60.
- Dhodapkar, S.V. and Klinzing, G.E. 1993. Pressure fluctuations in pneumatic conveying systems. *Powder Technology*, 74: 179-195.
- Efstathios E., Michaelides and Indranil Roy. 1987. An evaluation of several correlation used for the prediction of pressure drop in particulate flow. *Int. J. Multiphase Flow* 13 (3): 433–442.
- Ito, H. 1959. Pressure losses in smooth pipe bends. *Trans. ASME*, Paper 59- Hyd-4.
- Jones, M.G., and Williams, K.C. (2003). Solids friction factors for fluidised dense phase conveying. *Particulate Science and Technology*, 21, 45-56
- Kennedy, O.C. and Wypych, P.W. 1990. Characterisation and classification of bulk solids, University of Wollongong. *Bulk Solids Handling*. 10 (4): 421-427.
- Klinzing, G.E. 1980. A comparison in pressure losses in bends between recent data and models for gas-solid flow. *The Canadian Journal of Chemical Engineering*. 58: 670-672.
- Mallick, S.S. 2010. PhD Dissertation: Modelling of Fluidised Dense-Phase Pneumatic Conveying of Powders , University of Wollongong.
- Mallick, S.S., Wypych, P.W. and Rizk, F. 2010. Effect of bend model on prediction of pressure drop for pneumatic conveying systems. *International Conference for Bulk Materials Storage, Handling and Transportation*: 1-6.
- Marcus, R.D., Hilbert, J.D. and Klinzing, G.E. 1983. The flow through bends in pneumatic conveying systems. *Journal of pipeline*, Netherlands: Elsevier Science Publishers. Volume 4: 103-112.
- Marcus, R. D., Hilbert Jr, J.D. and Klinzing, G.E. 1984. The flow through bends in pneumatic conveying systems. *Journal of Pipelines*. (4), 103-112.

- Marcus, R.D., Leung, L.S, Klinzing, G.E. and Rizk, F. 1990. Pneumatic conveying of solids - A theoretical and practical approach. Publ. Chapman and Hall.
- Mills, D. and Mason, J.S. 1985. The influence of bend geometry on pressure drop in pneumatic conveying system pipelines. *In the proceedings of 10 International Conference Powder and Bulk Solids Handling*, Chicago, IL, USA. Cahners Exhibition Group, Des Plaines, IL. 203-214.
- Mills, D. (2004). *Pneumatic conveying design guide* (2nd ed.).Oxford: Elsevier/Butterworth-Heinemann.
- Mills, D. and Mason, J.S. 1985. The influence of bend geometry on pressure drops in pneumatic conveying system pipelines. In the proceedings of 10th International Conference Powder and Bulk Solids Handling, Chicago, IL, USA. Cahners Exhibition Group, Des Plaines, IL: 203-214.
- Mills, D. 2004. An investigation of the unstable region for dense phase conveying in sliding bed flow, *Granular Matter* (6): 173–177.
- Mainwaring, N.J. and Reed, A.R. 1987. Permeability and air retention characteristics of bulk solid materials in relation to modes of dense phase pneumatic conveying. *Bulk Solids Handling*. 7(June No. 3): 415 - 425.
- Moody, L.F. and Princeton, N.J. 1944. Friction factor for pipe flows. *Trans ASME*. 66 (8): 671-684.
- Pan, R. 1999. Material properties and flow modes in pneumatic conveying. *Powder technology*. 104(2): 157-163.
- Pan, R., and Wypych, P.W. (1998) Dilute and dense phase pneumatic conveying of fly ash, *6th International Conference on Bulk Materials Storage and Transportation*. Wollongong, NSW, Australia. 183-189.

- Rossetti, S.J. (1983) Concepts and criteria for gas-solids flow, Handbook of fluids in motion, Ed. Nicholas P. Cheremisinoff and Remesh Gupta. *Ann Arbor: Ann Arbor Science Publishers.* 635-652.
- Stegmaier, W. 1978. Zur berechnung der horinentalen pneumatischen forderung feinkorniger feststoffe - for the calculation of horizontal pneumatic conveying of fine grained solids. *Fordern and Heben.* 28: 363-366.
- Schuchart, P. (1968). Widerstansgesetze beim pneumatischen Transport in Rohrkrummern. *Symposium series no. 27 (The Institution of Chemical Engineers).* 65 – 72.
- Singh, B., and Wolfe, R.R. (1972). Pressure losses due to bends in pneumatic forage handling. *Transaction of the ASAE.* 246-248.
- Weber, M. (1981). Principles of hydraulic and pneumatic conveying in pipes. *Bulk Solids Handling, 1,* 57-63.
- Williams, K.C. and Jones, M.G. (2004), Numerical model velocity profile of fluidised dense phase pneumatic conveying. *8th International Conference on Bulk Materials Storage and Transportation,* Wollongong, NSW, Australia. 354-358.
- Wypych, P.W. 1989. PhD Dissertation: Pneumatic conveying of bulk solids, University of Wollongong.
- Wypych, P.W. and Arnold, P.C. 1989. Plug-phase pneumatic transportation of bulk solids and the importance of blow tank air injection, *Powder Handling and Processing,* Vol. 1, No. 3: 271-275.
- Wypych, P.W. and Hauser, G. 1990. Design considerations for low-velocity conveying systems & pipelines. *Int. Conf. on Pneumatic Conveying Technology.* 241-260.
- Wypych, P.W., Hastie, D.B. and Yi, J. 2005. Prediction of optimal operating conditions for dense-phase pneumatic conveying systems. Final research report for the International Fine Particle Research Institute, In. USA:1-92.

Wypych, P.W. 2006. Course note written on pneumatic conveying of bulk solids and dust control, University of Wollongong.

Yi, J. 2001. PhD Dissertation: Transport boundaries for pneumatic conveying, University of Wollongong.

Appendix-A1

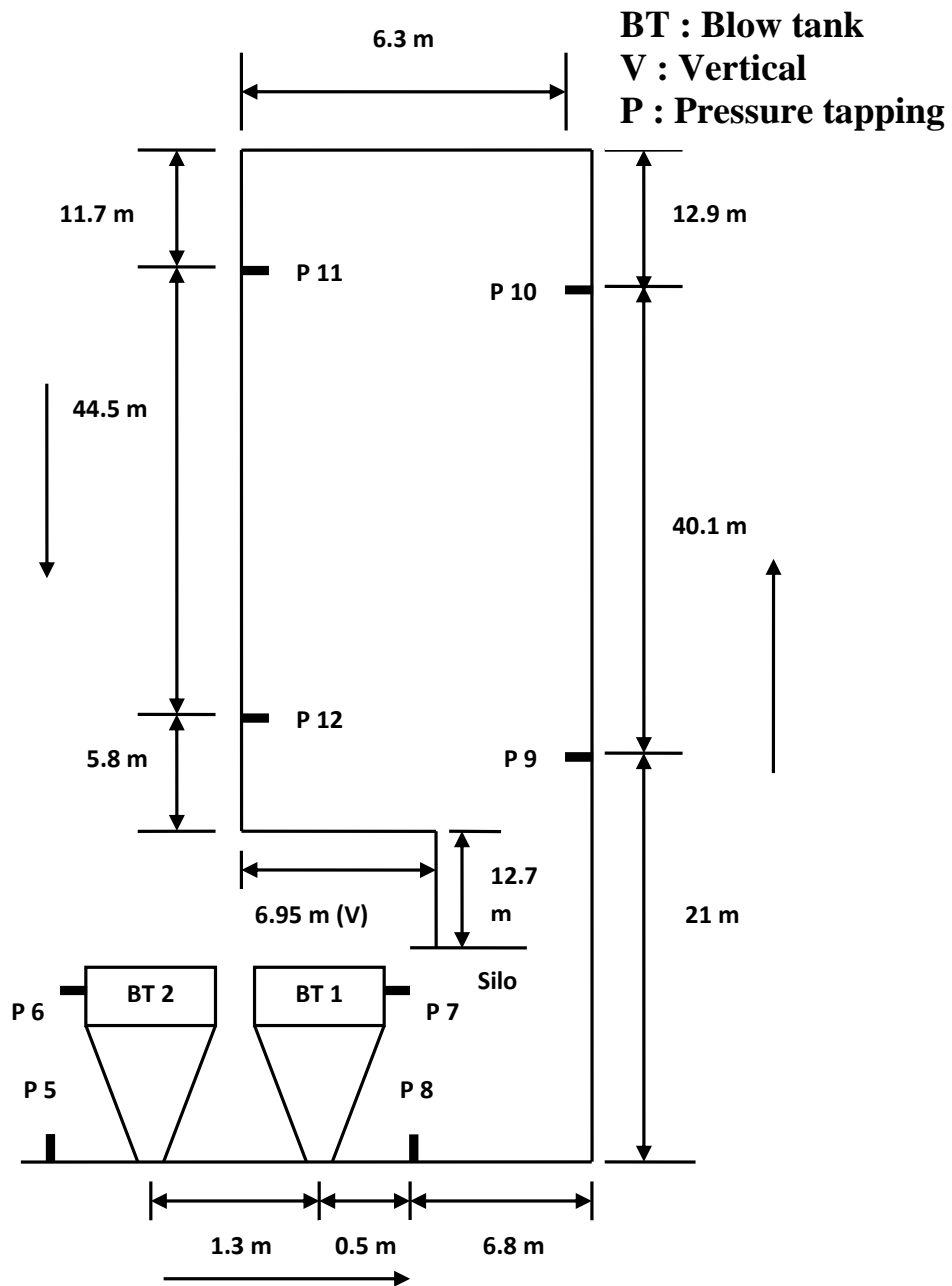


Figure A1.1: Schematic of the 105 mm I.D. × 168 m Long Test Rig (for Fly Ash)

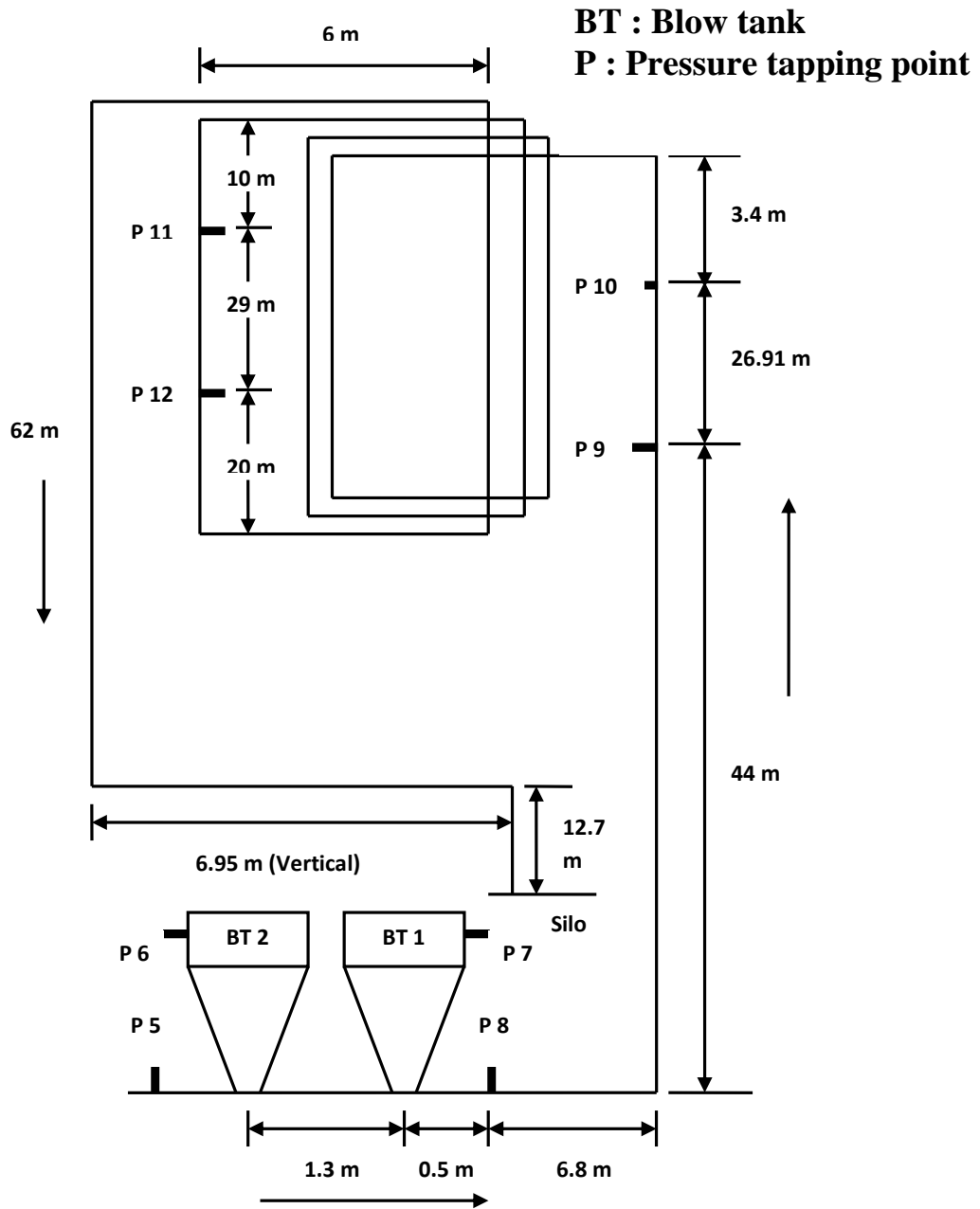


Figure A1.2: Schematic of the 69 mm I.D. × 554 m Long Test Rig (for Fly Ash)

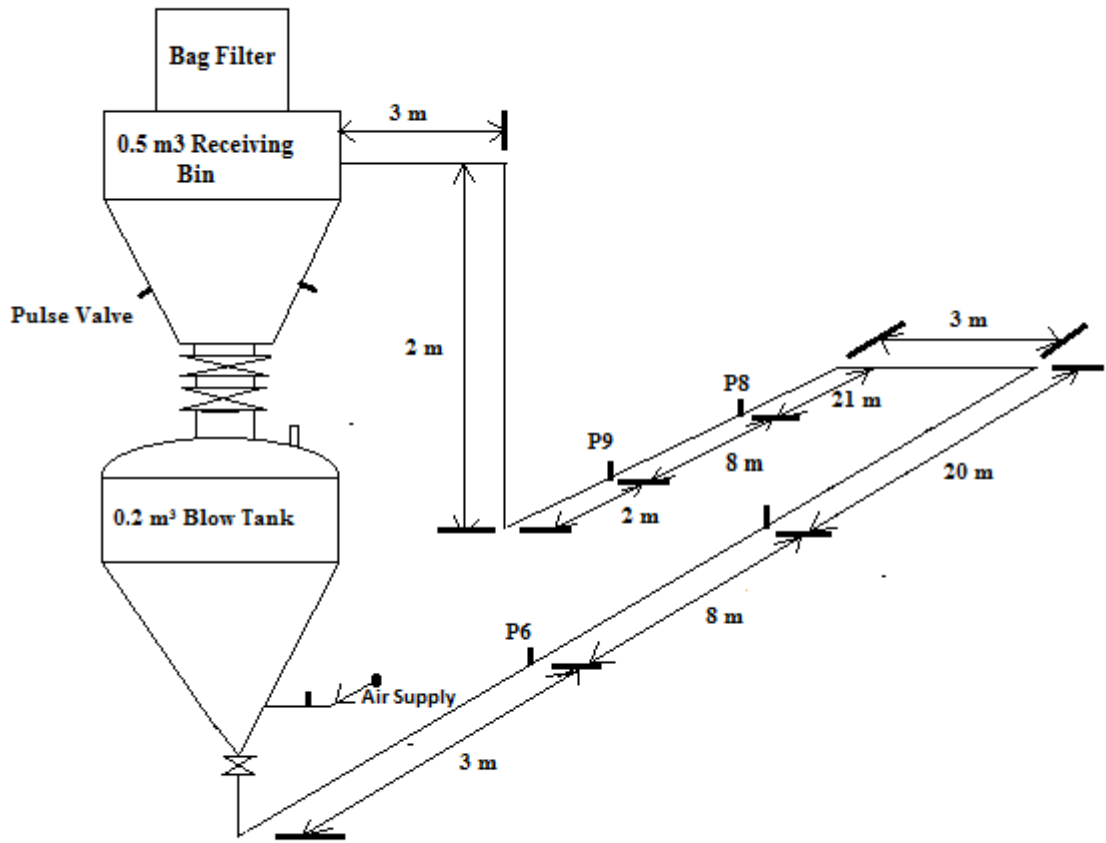


Figure A1.3: Schematic of the 50 mm I.D. ×70 m Long Test Rig (for Fly Ash)

Appendix-A2

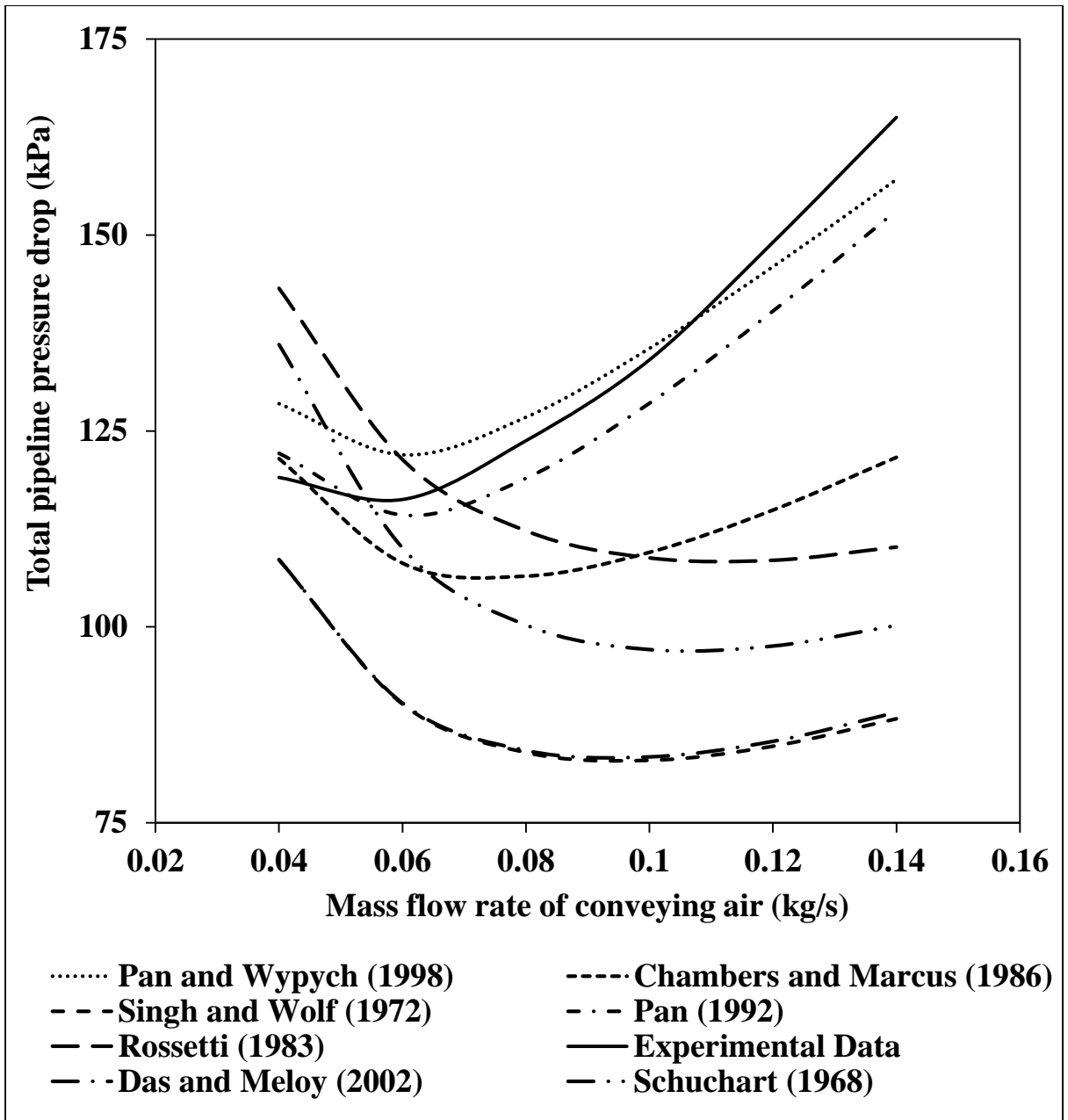


Figure A2.1: Comparison of experimental and predicted values of total pipeline pressure drop (fly ash, $D = 69$ mm, $L = 168$ m, $m_s = 14$ t/h)

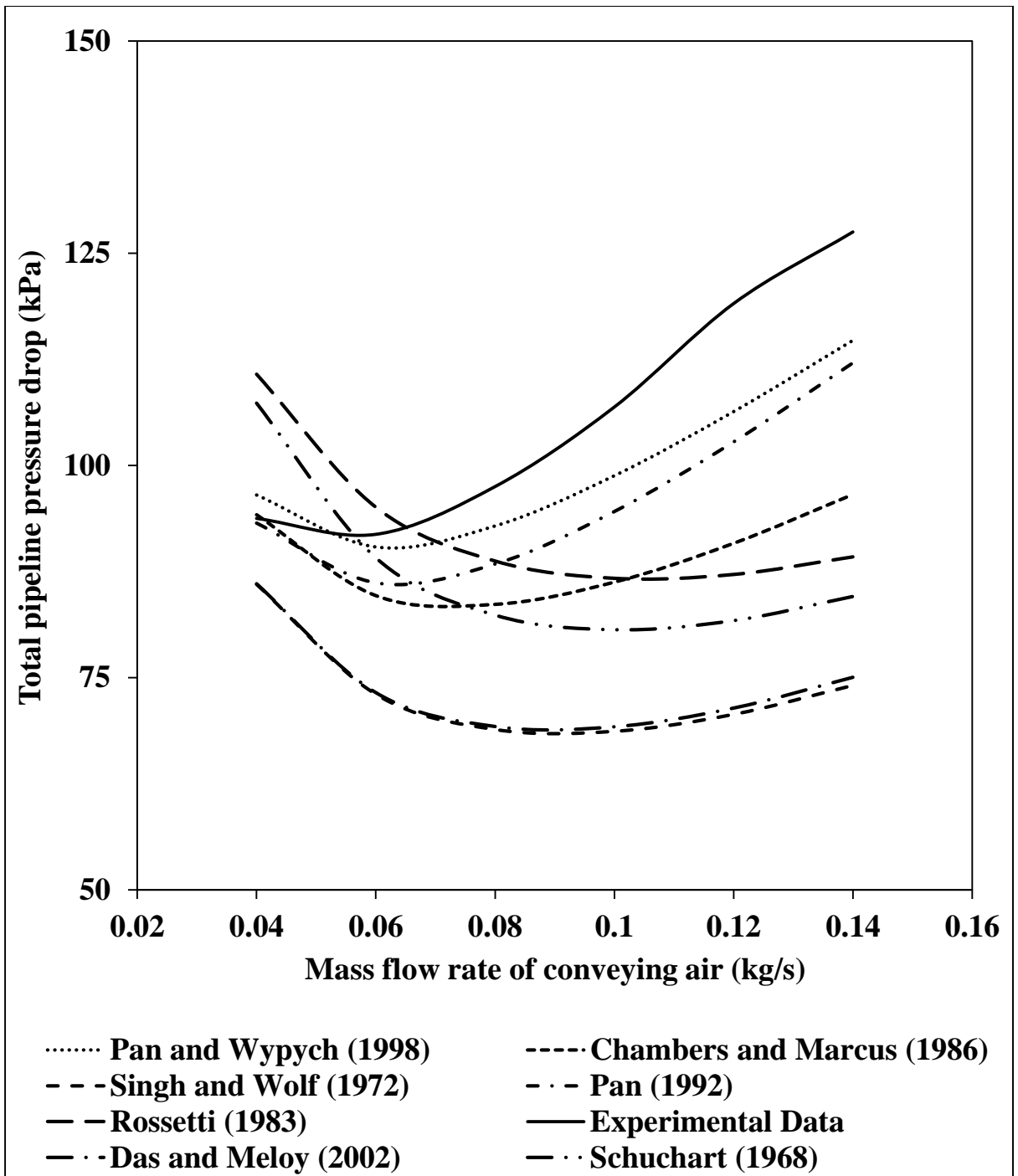


Figure A2.2: Comparison of experimental and predicted values of total pipeline pressure drop (fly ash, $D = 69$ mm, $L = 168$ m, $m_s = 9$ t/h)

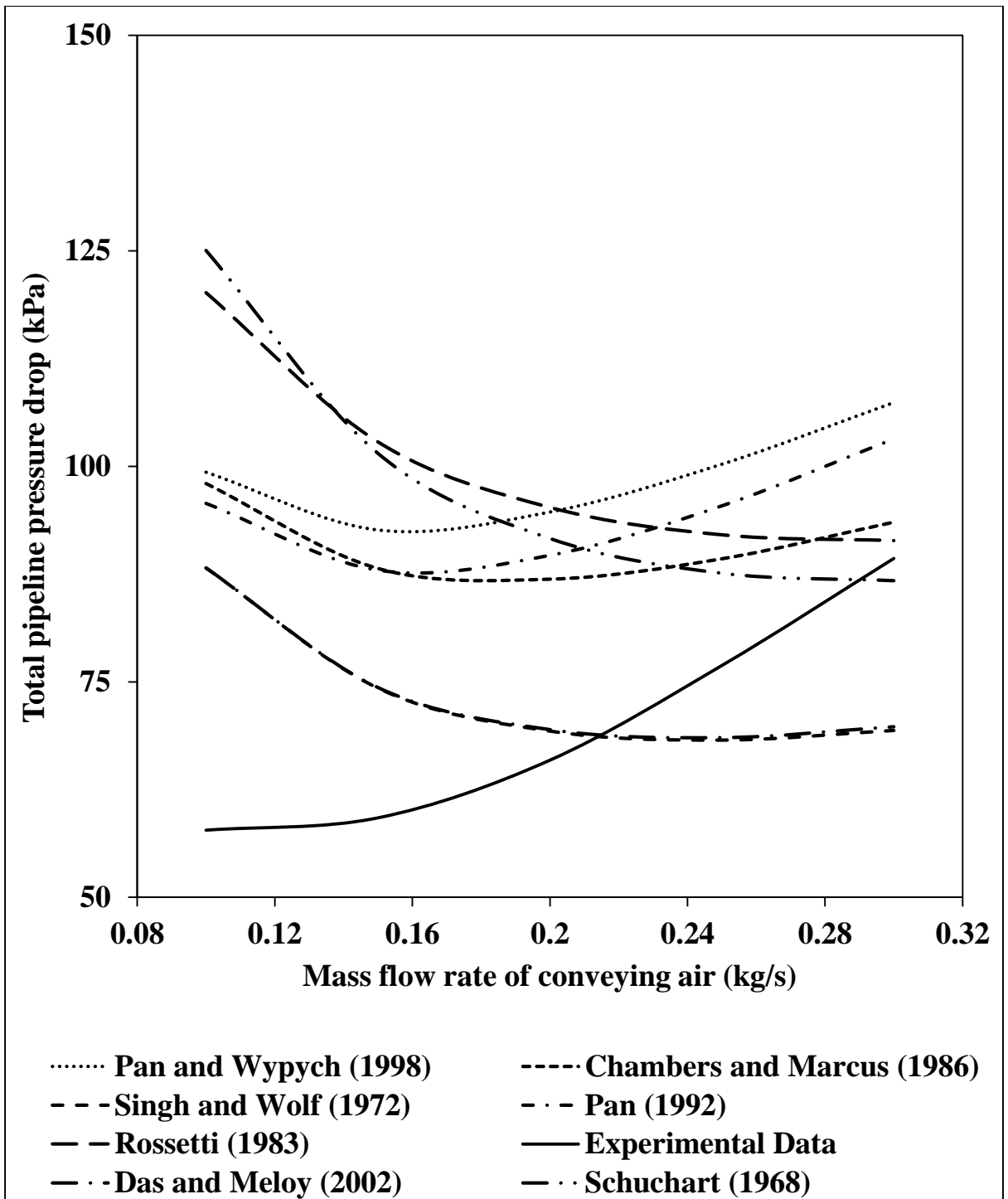


Figure A2.3: Comparison of experimental and predicted values of total pipeline pressure drop (fly ash, $D = 105$ mm, $L = 168$ m, $m_s = 23$ t/h)

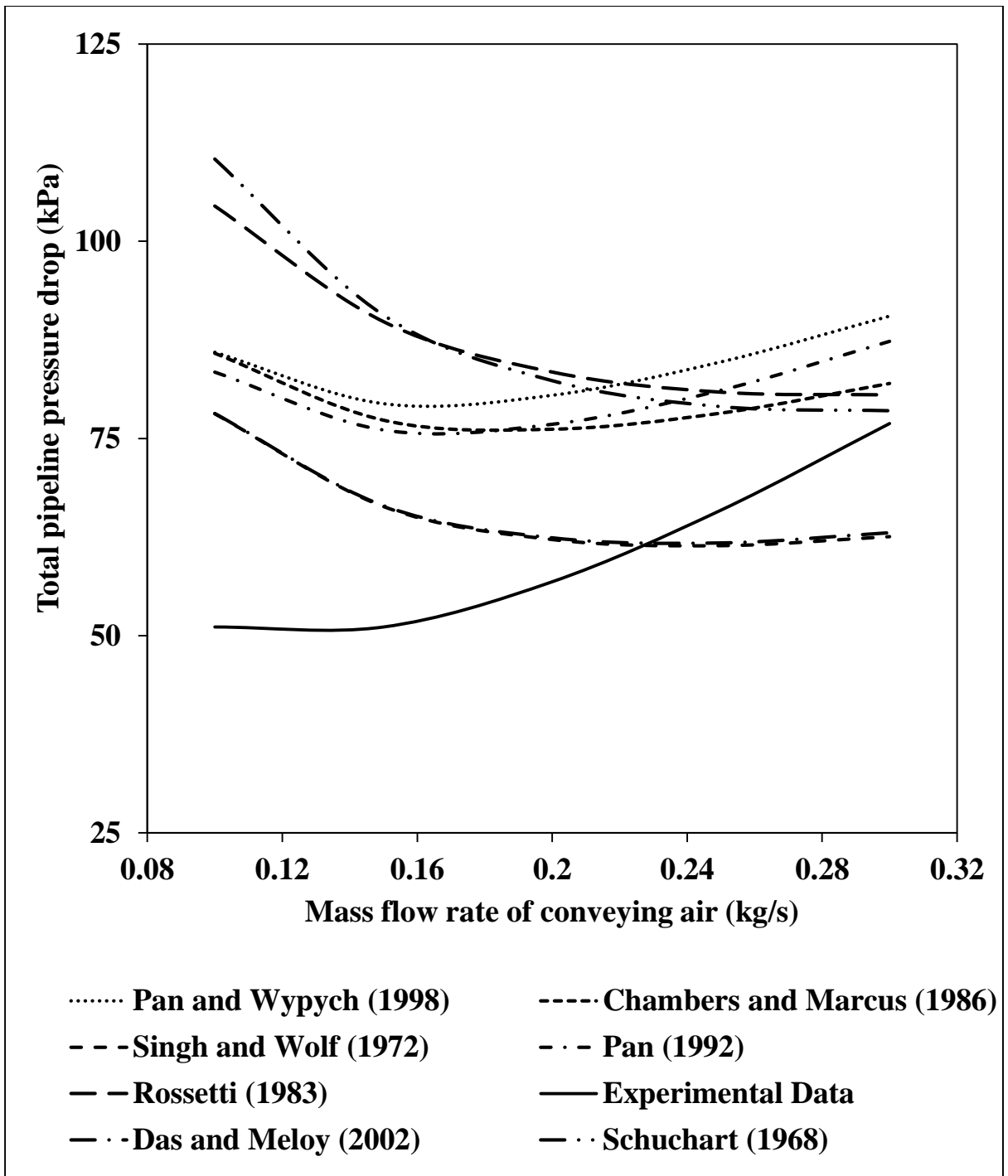


Figure A2.4: Comparison of experimental and predicted values of total pipeline pressure drop (fly ash, $D = 105$ mm, $L = 168$ m, $m_s = 18$ t/h)

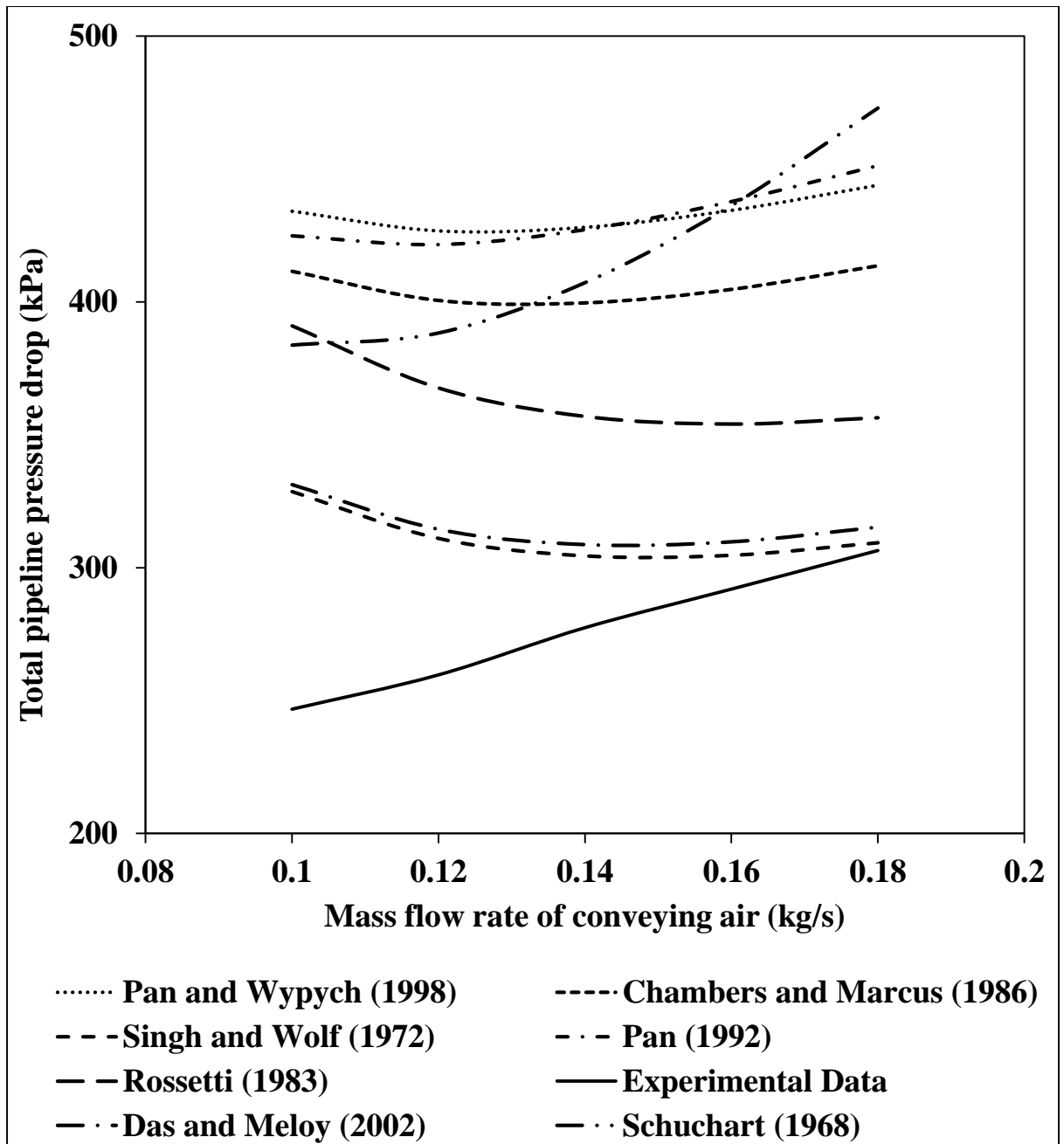


Figure A2.5: Comparison of experimental and predicted values of total pipeline pressure drop (fly ash, $D = 69$ mm, $L = 554$ m, $m_s = 9$ t/h)

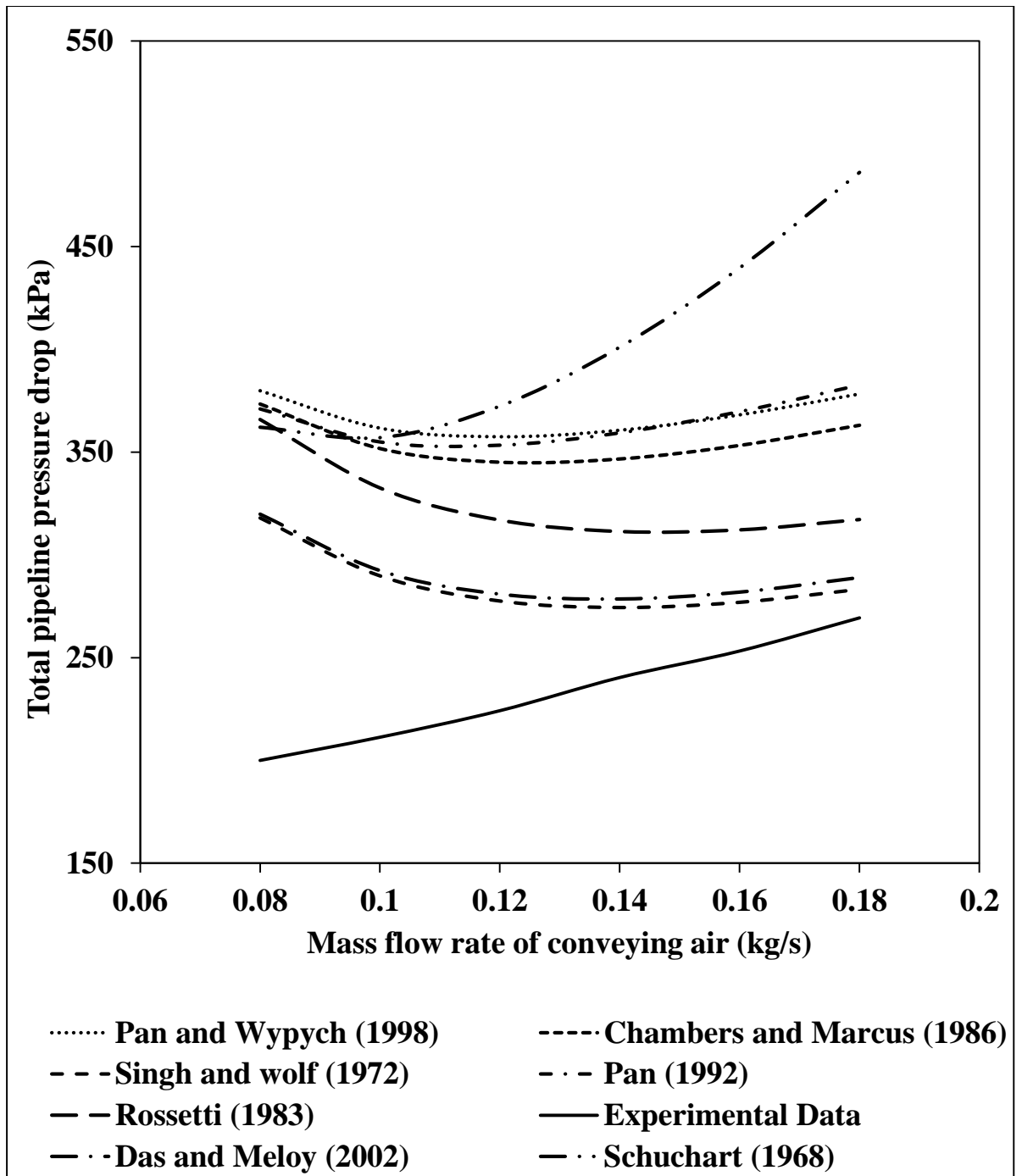


Figure A2.6: Comparison of experimental and predicted values of total pipeline pressure drop (fly ash, $D = 69$ mm, $L = 554$ m, $m_s = 7$ t/h)

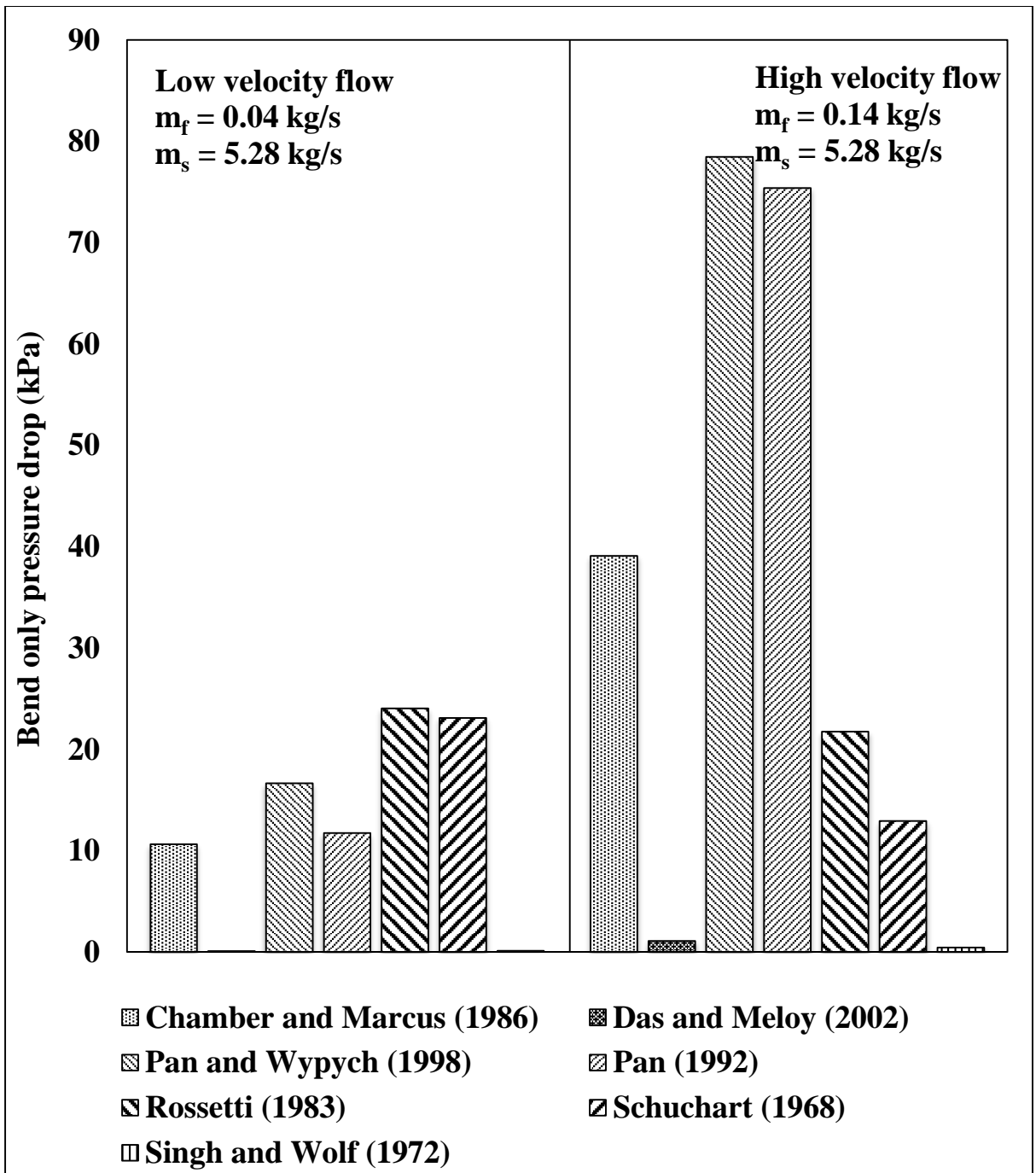


Figure A2.7: Comparison of bend only pressure drop between low velocity flow and high velocity (fly ash, $D = 69 \text{ mm}$, $L = 168 \text{ m}$, $m_s = 19 \text{ t/h}$)

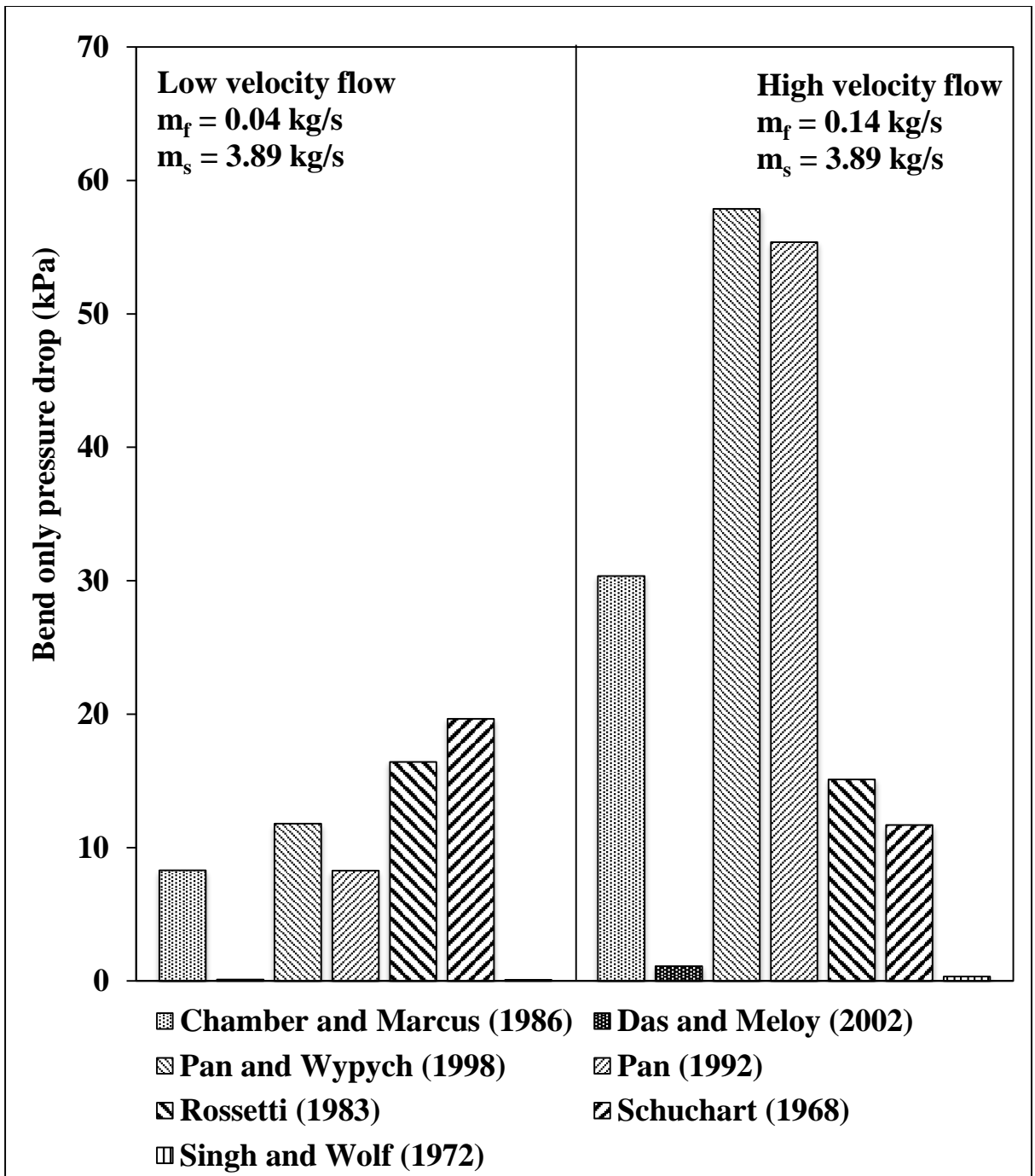


Figure A2.8: Comparison of bend only pressure drop between low velocity flow versus high velocity flow (fly ash, $D = 69 \text{ mm}$, $L = 168 \text{ m}$, $m_s = 14 \text{ t/h}$)

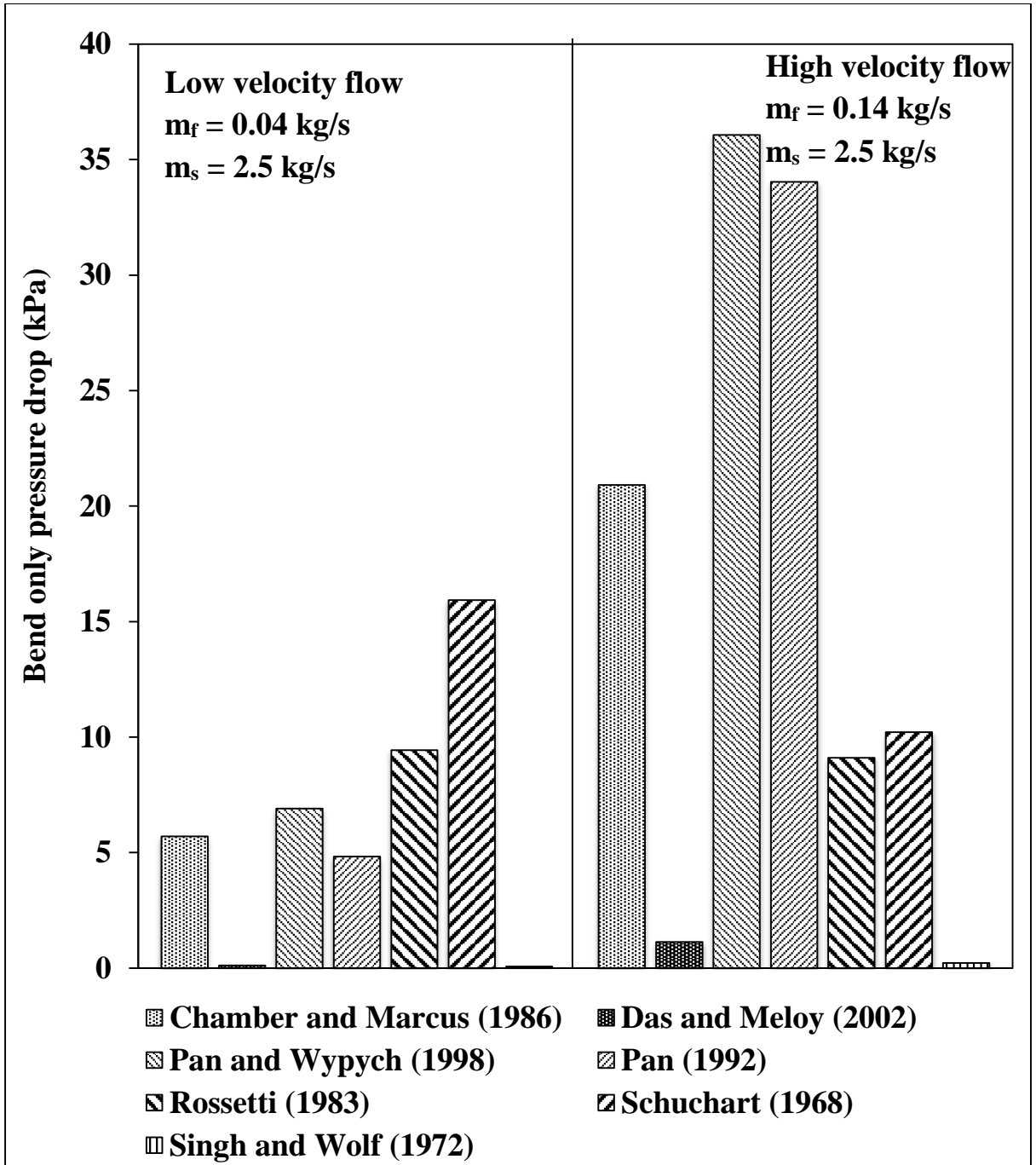


Figure A2.9: Comparison of bend only pressure drop between low velocity flow and high velocity flow (fly ash, $D = 69 \text{ mm}$, $L = 168 \text{ m}$, $m_s = 9 \text{ t/h}$)

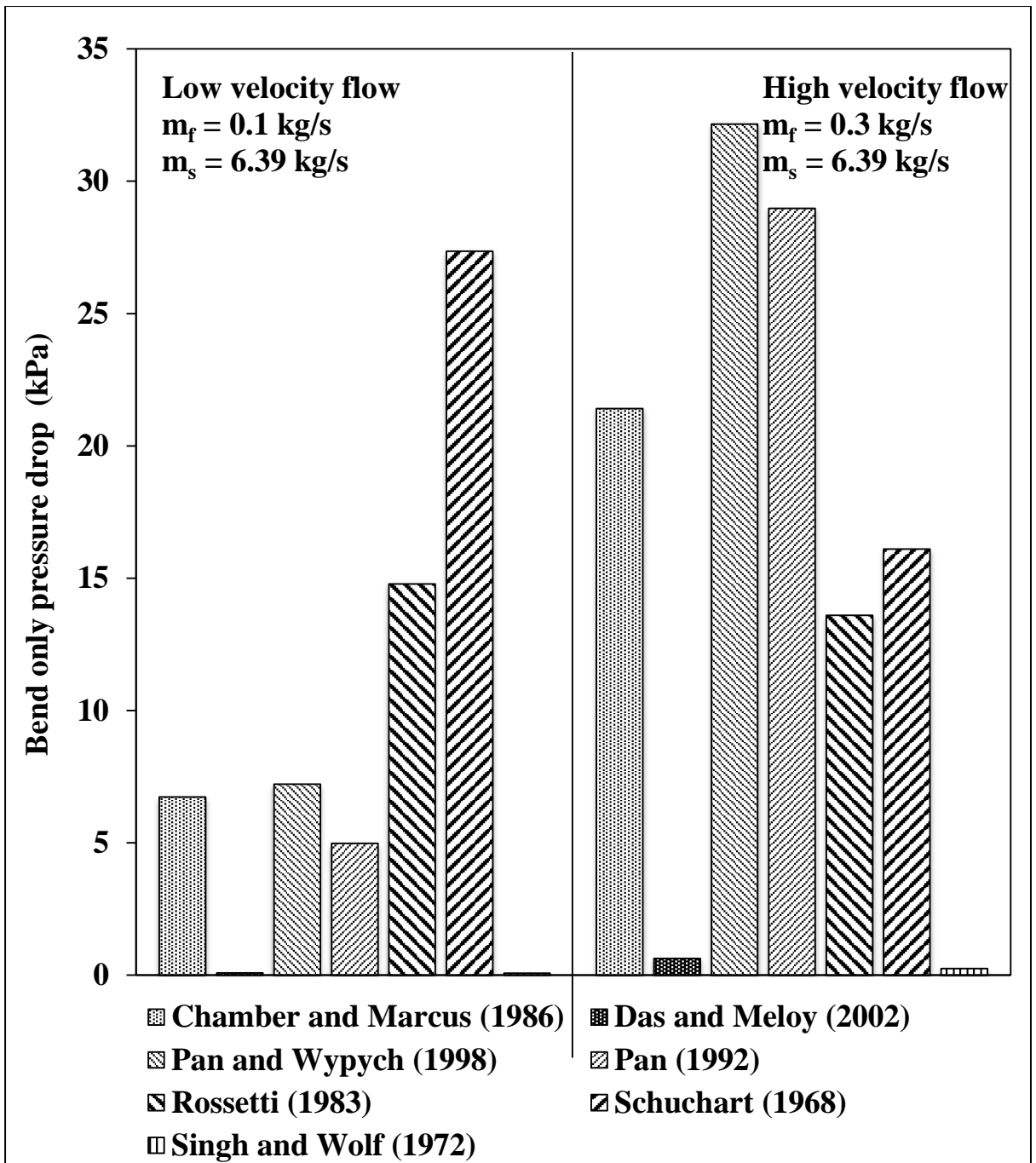


Figure A2.10: Comparison of bend only pressure drop between low velocity flow versus high velocity flow (fly ash, $D = 105 \text{ mm}$, $L = 168 \text{ m}$, $m_s = 23 \text{ t/h}$)

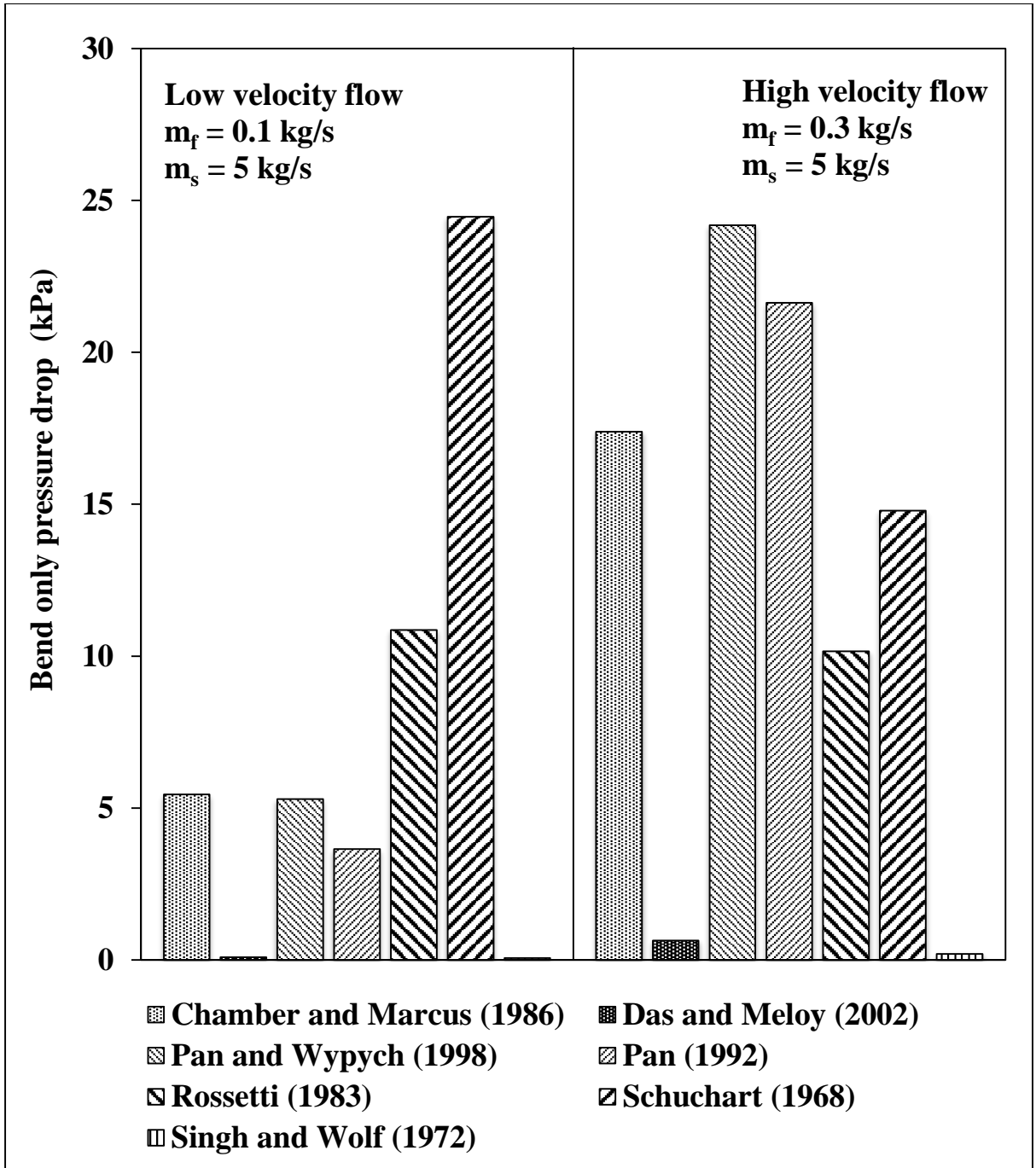


Figure A2.11: Comparison of bend only pressure drop between low velocity flow and high velocity flow (fly ash, $D = 105 \text{ mm}$, $L = 168 \text{ m}$, $m_s = 18 \text{ t/h}$)

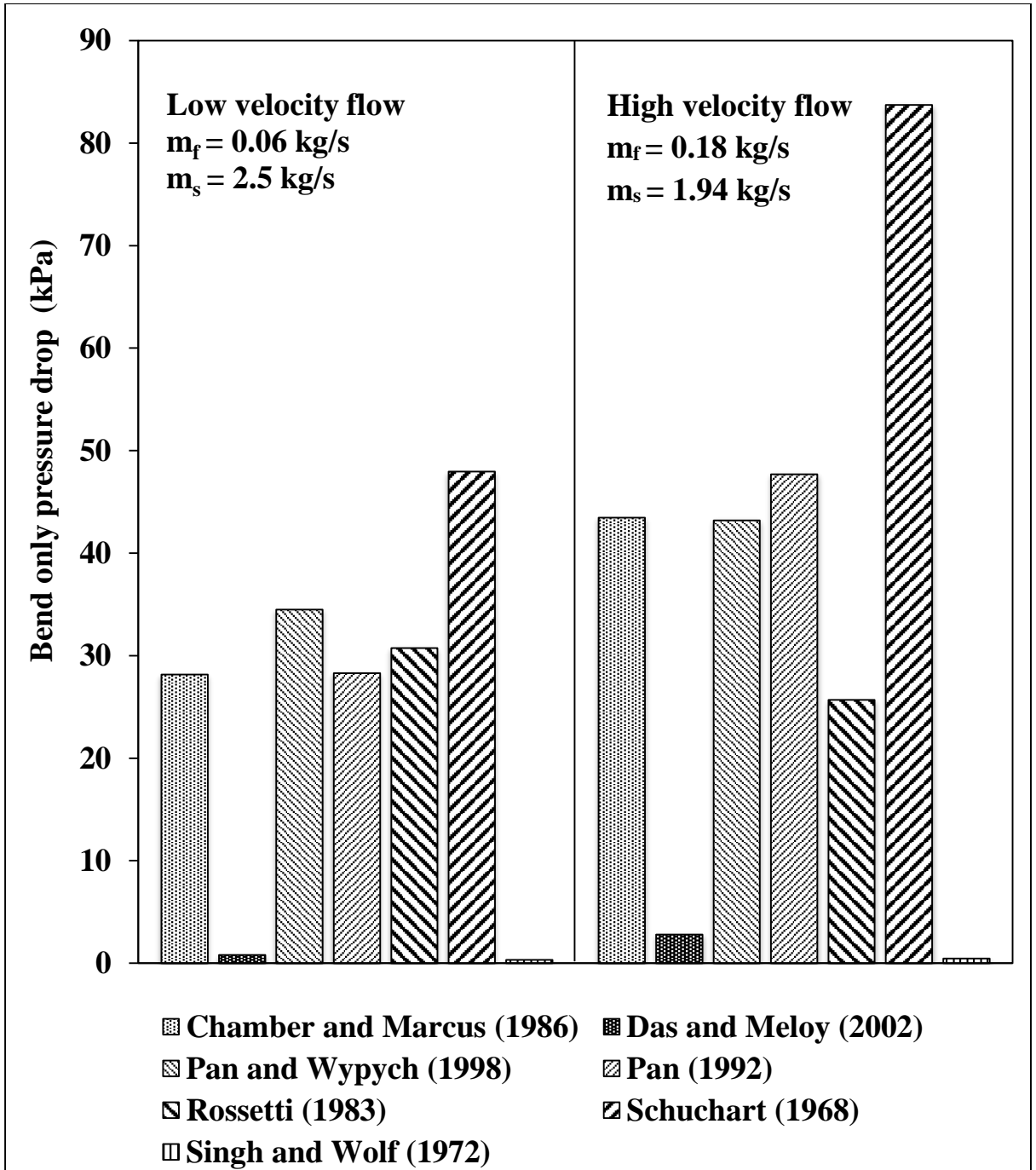


Figure A2.12: Comparison of bend only pressure drop between low velocity flow and high velocity flow (fly ash, $D = 69 \text{ mm}$, $L = 554 \text{ m}$, $m_s = 9 \text{ t/h}$)

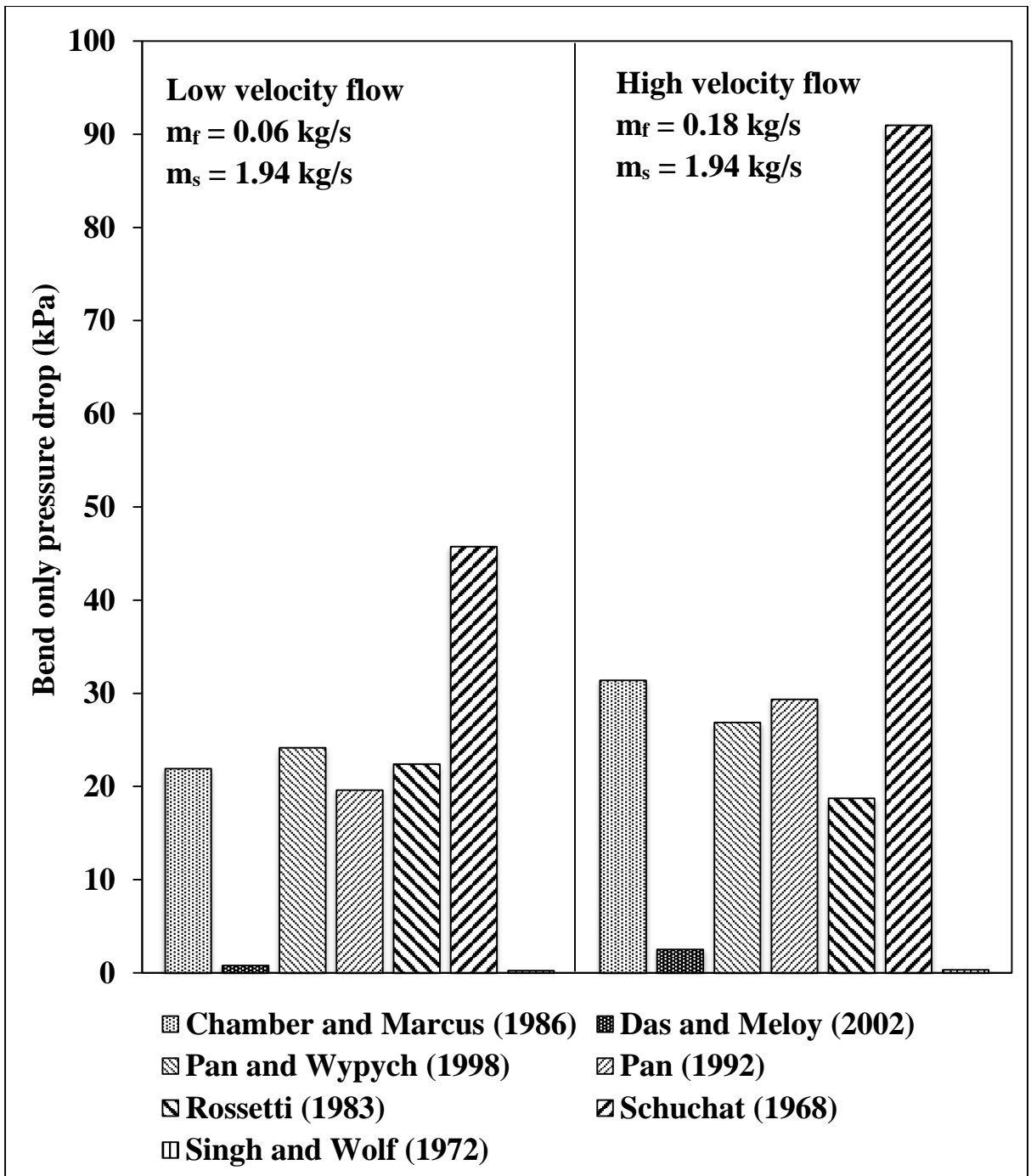


Figure A2.13: Comparison of bend only pressure drop between low velocity flow and high velocity (fly ash, $D = 69 \text{ mm}$, $L = 554 \text{ m}$, $m_s = 7 \text{ t/h}$)

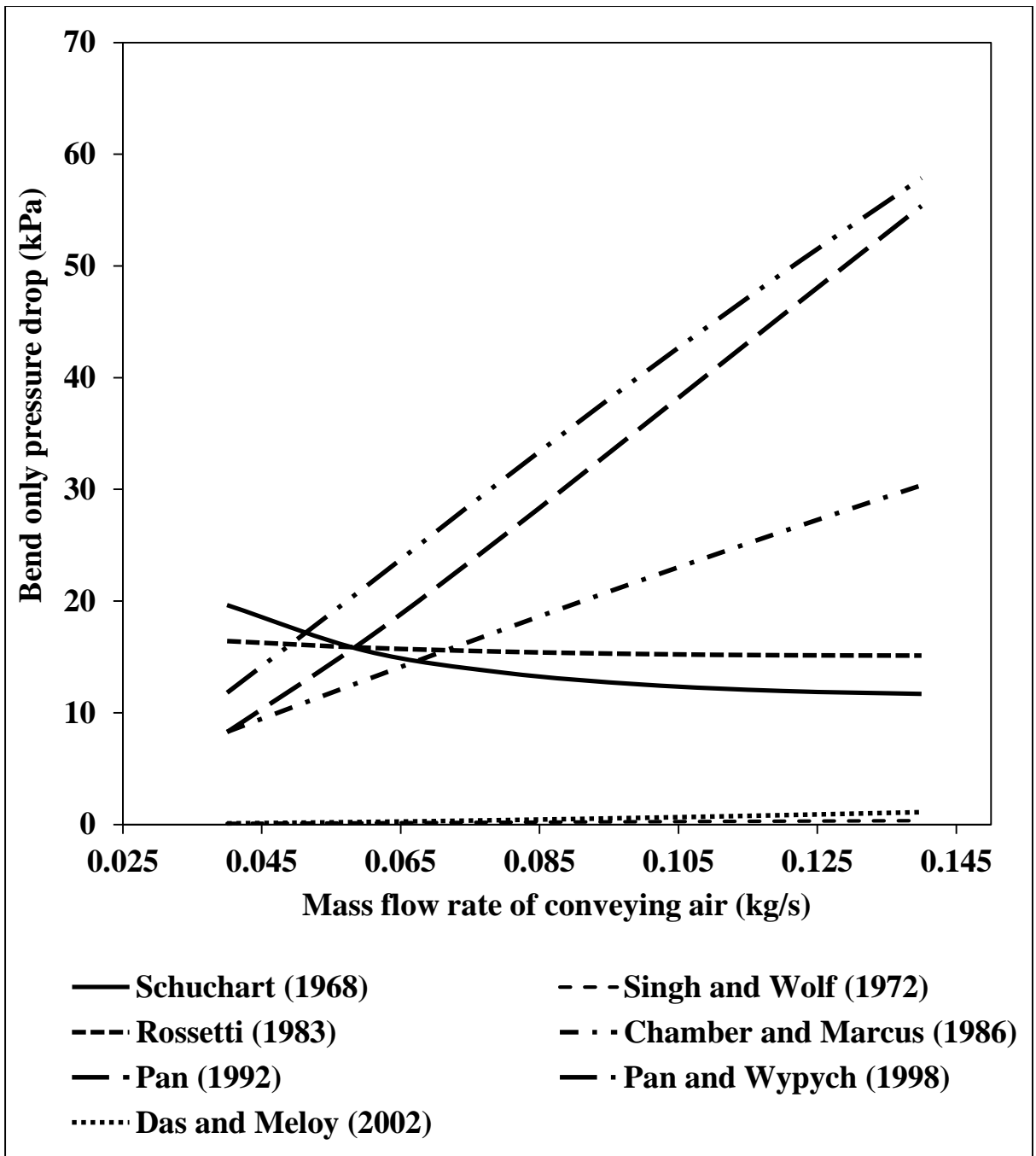


Figure A2.14: Bend loss PCC based on different bend models

(fly ash, $D = 69$ mm, $L = 168$ m, $m_s = 14$ t/h)

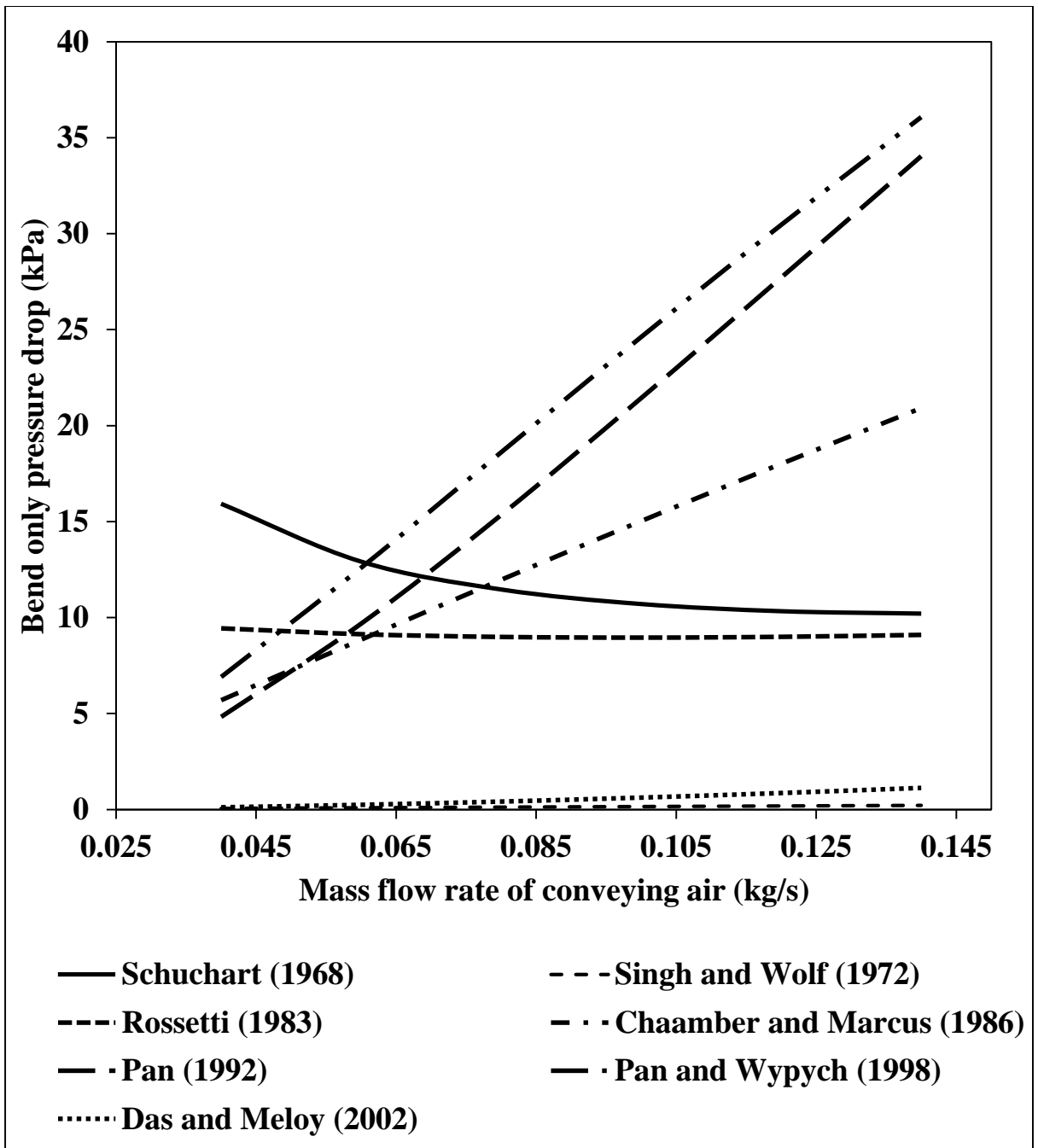


Figure A2.15: Bend loss PCC based on different bend models

(fly ash, $D = 69$ mm, $L = 168$ m, $m_s = 9$ t/h)

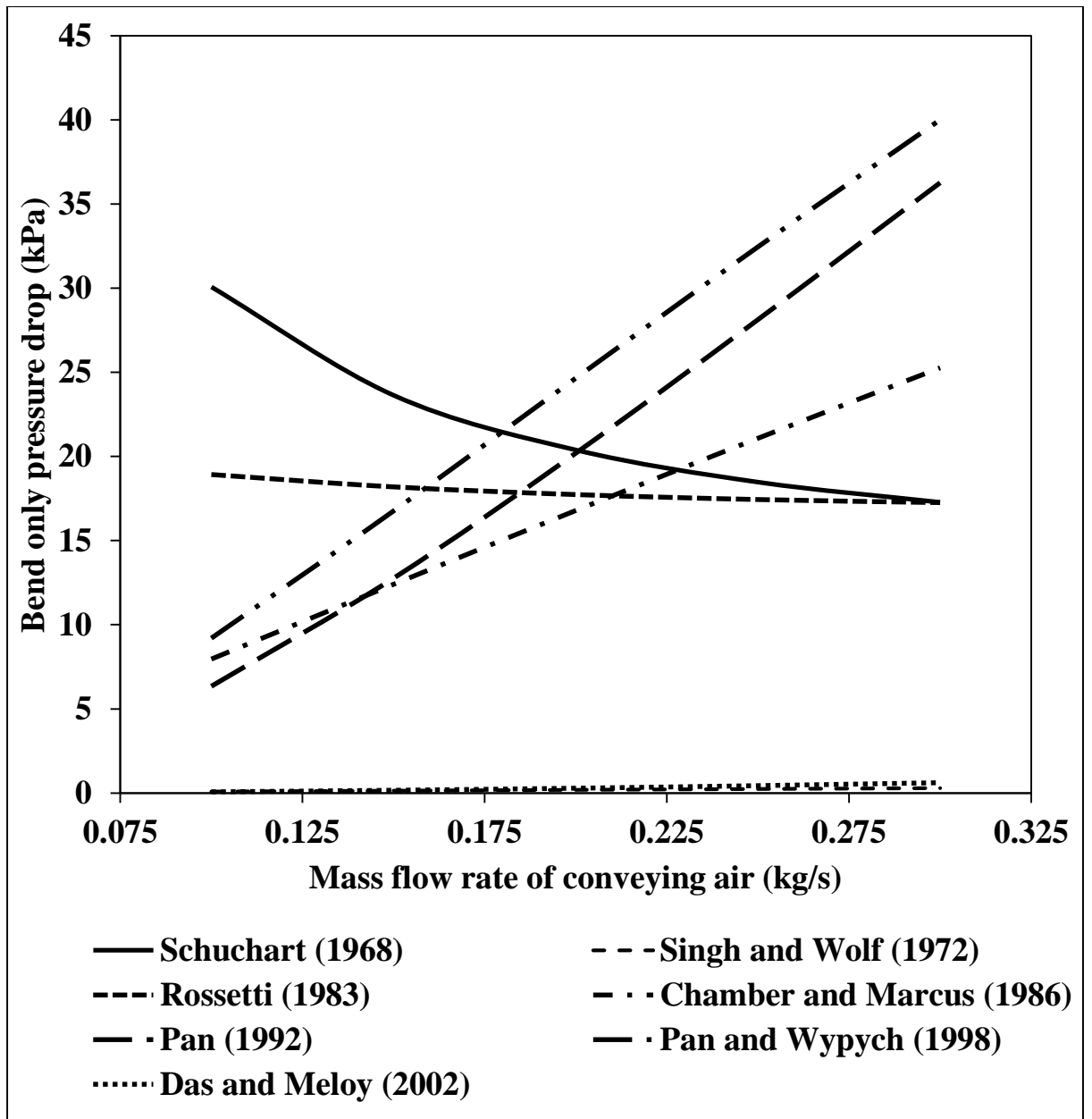


Figure A2.16: Bend loss PCC based on different bend models

(fly ash, $D = 105$ mm, $L = 168$ m, $m_s = 28$ t/h)

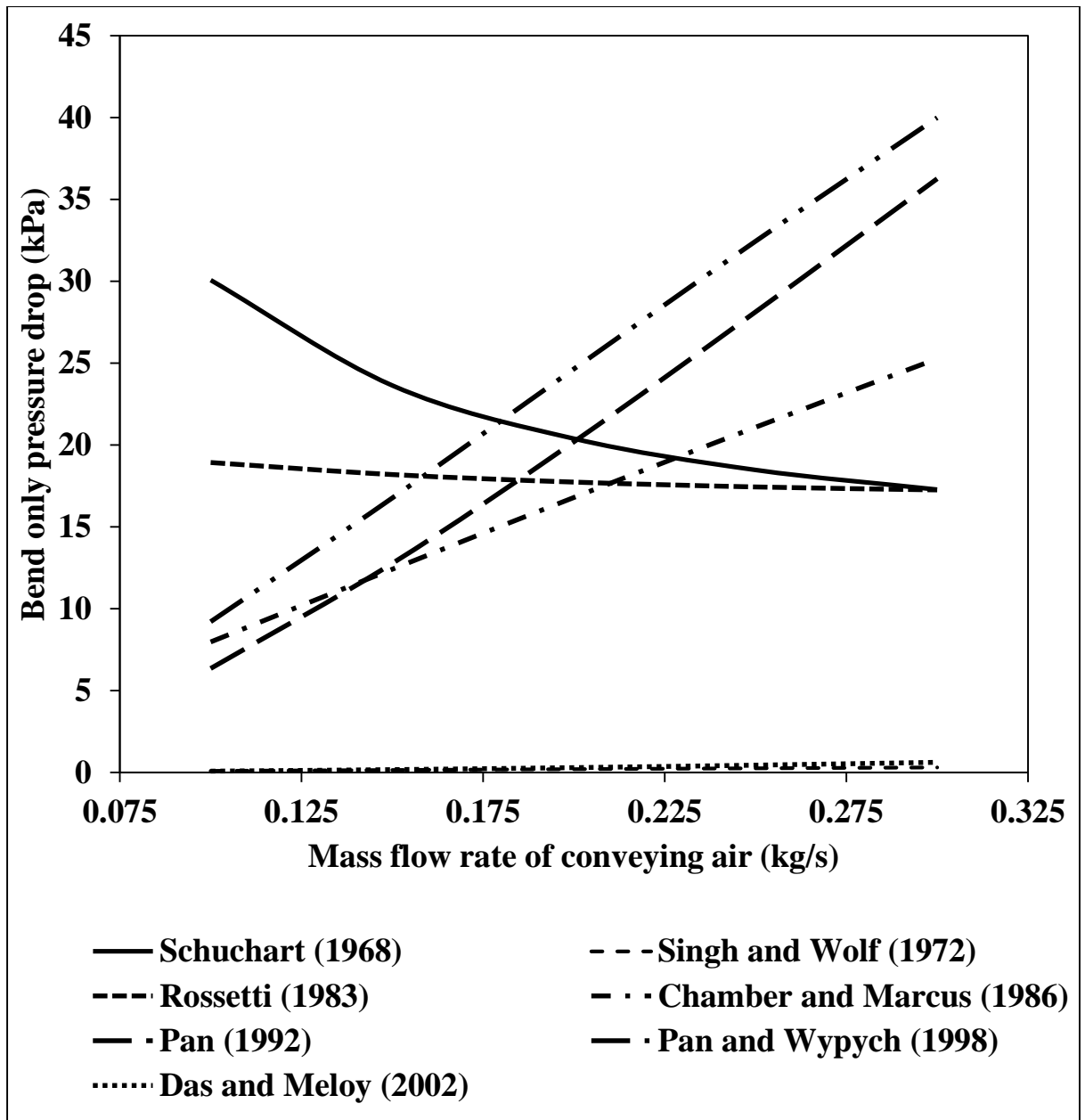


Figure A2.17: Bend loss PCC based on different bend models

(fly ash, $D = 105$ mm, $L = 168$ m, $m_s = 23$ t/h)

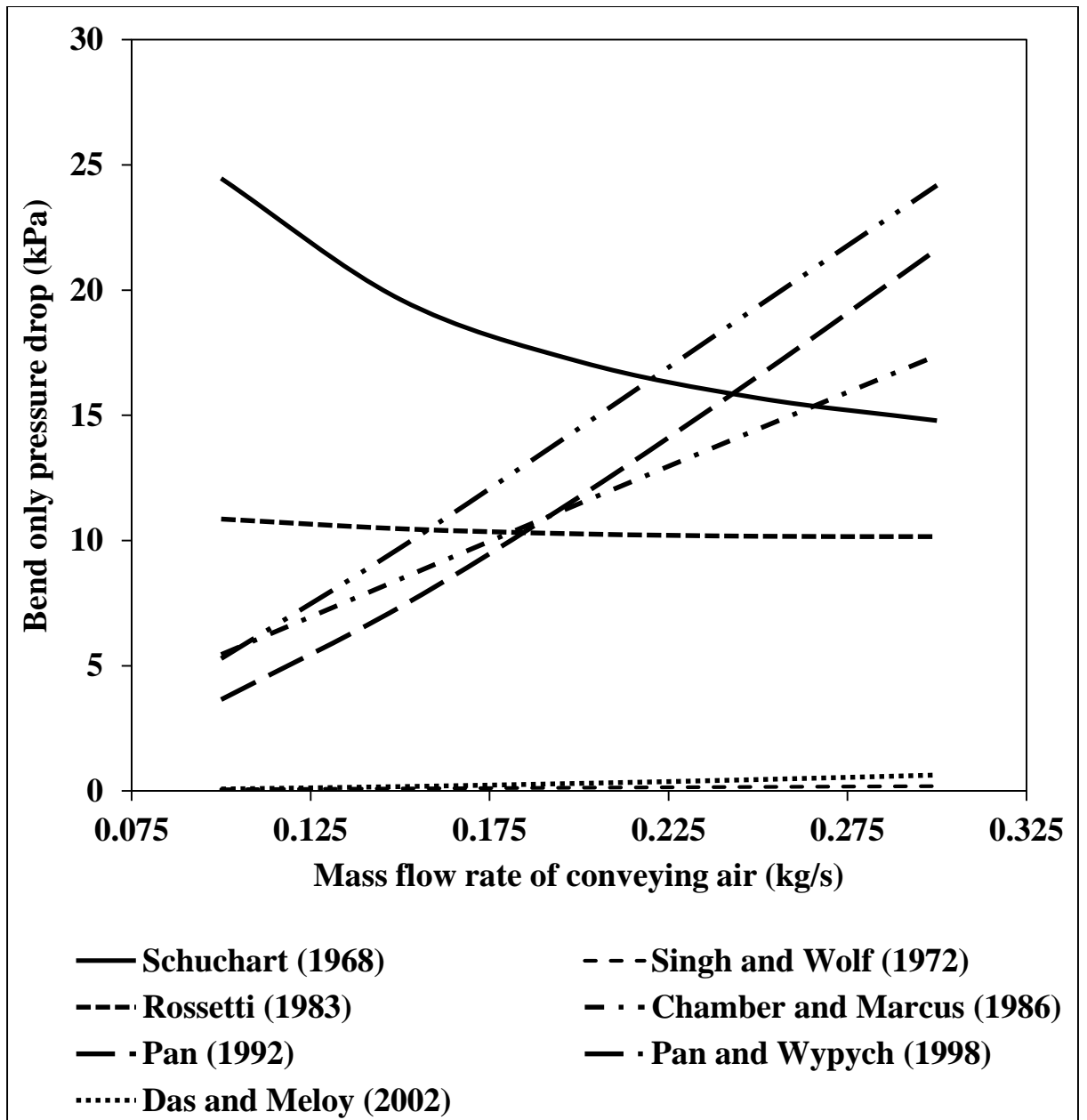


Figure A2.18: Bend loss PCC based on different bend models

(fly ash, $D = 105 \text{ mm}$, $L = 168 \text{ m}$, $m_s = 18 \text{ t/h}$)

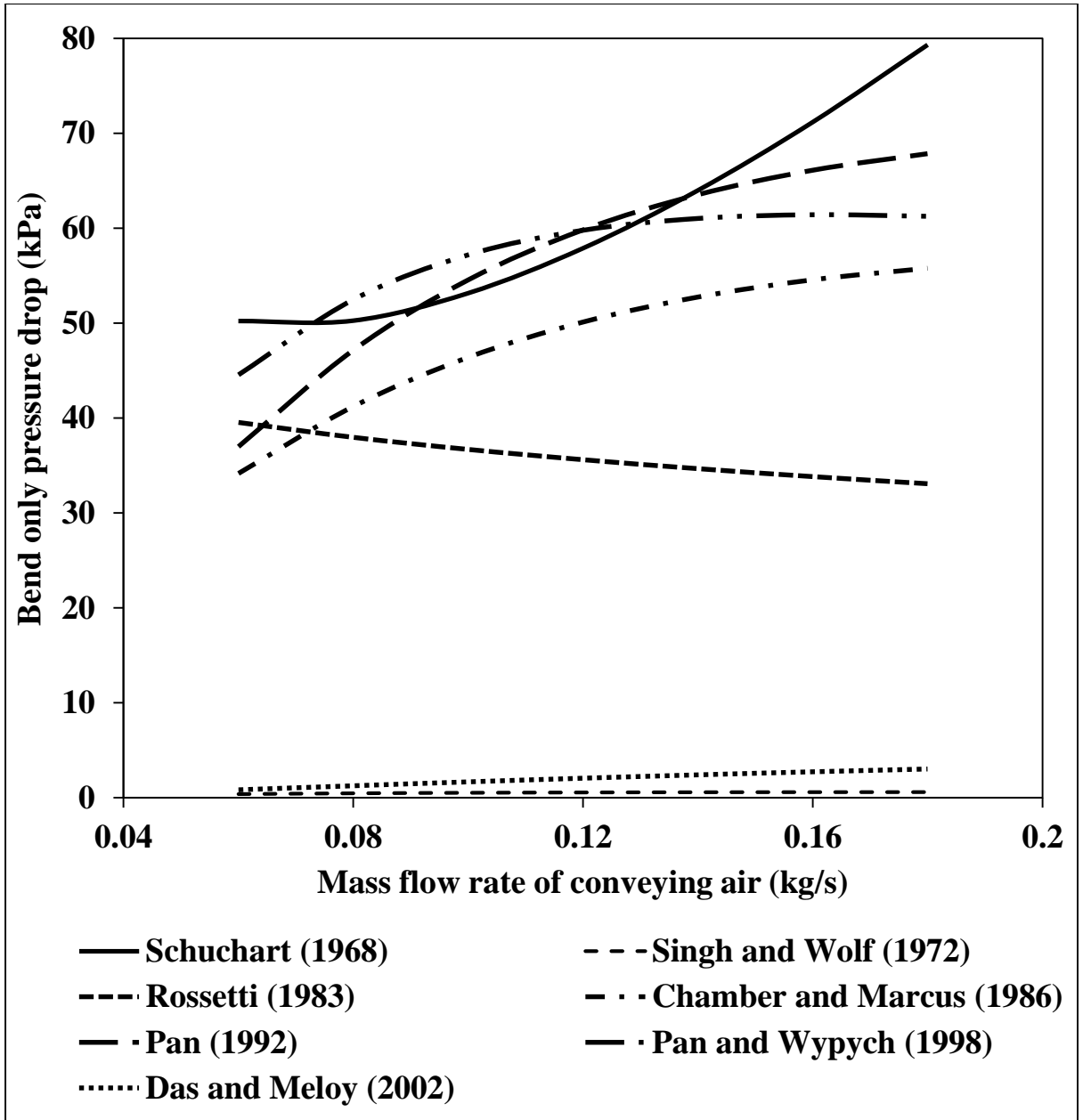


Figure A2.19: Bend loss PCC based on different bend models

(fly ash, $D = 69 \text{ mm}$, $L = 554 \text{ m}$, $m_s = 11 \text{ t/h}$)

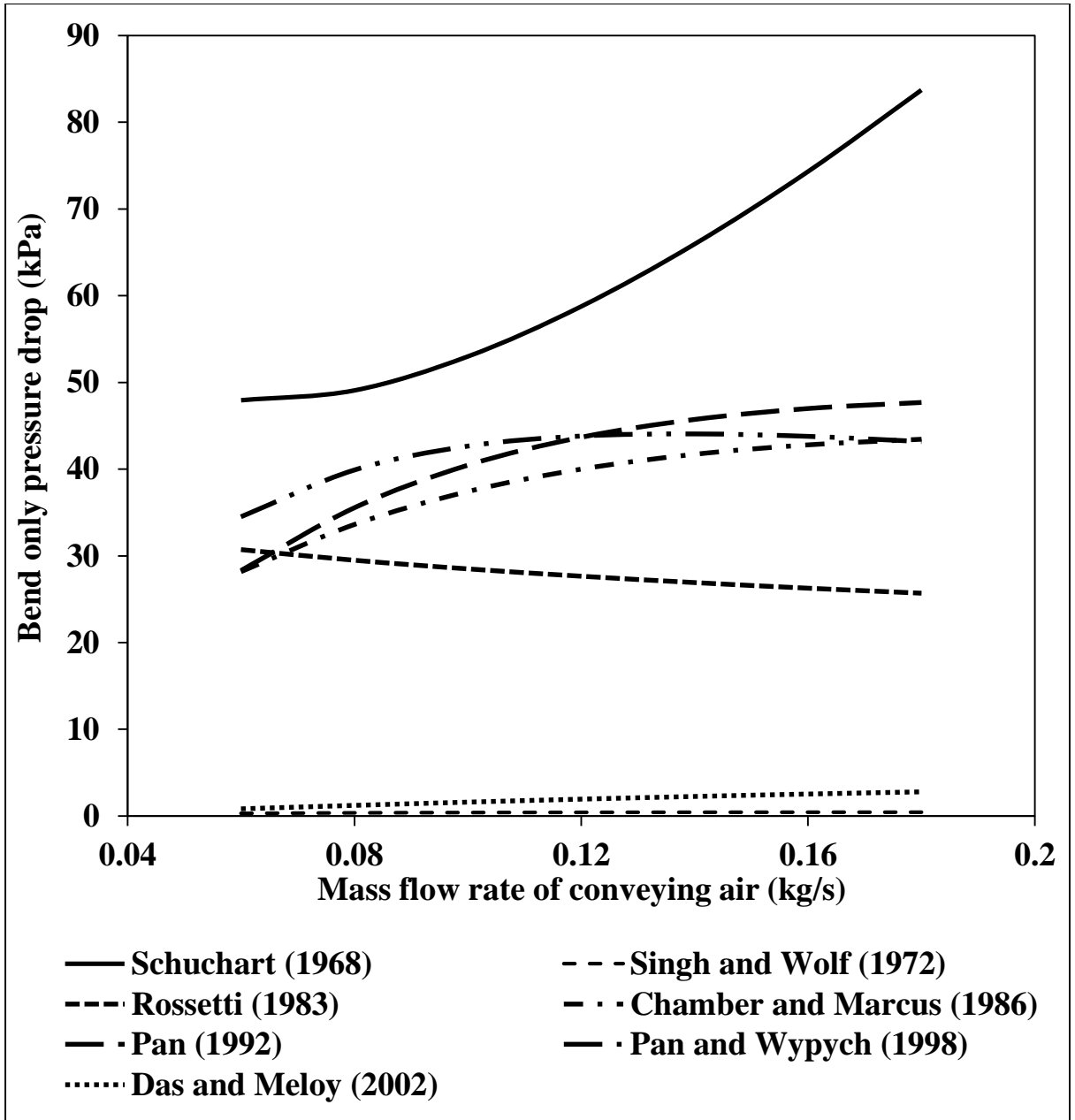


Figure A2.20: Bend loss PCC based on different bend models

(fly ash, $D = 69 \text{ mm}$, $L = 554 \text{ m}$, $m_s = 9 \text{ t/h}$)

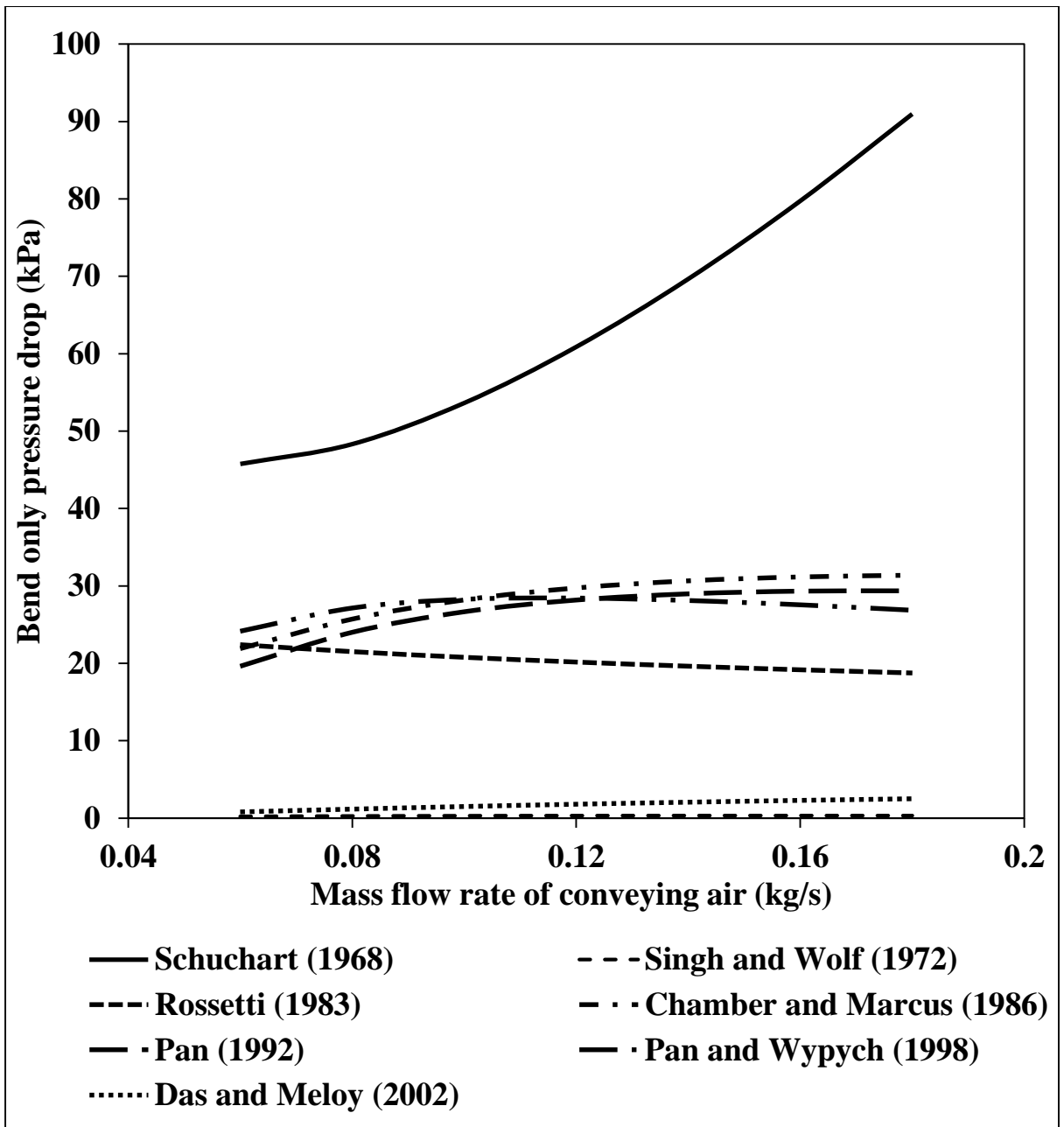


Figure A2.21: Bend loss PCC based on different bend models

(fly ash, $D = 69 \text{ mm}$, $L = 554 \text{ m}$, $m_s = 7 \text{ t/h}$)

Appendix- A3

Table A3.1: Closely coupled bend data (P7-P8)

Exp No.	m_f	m_s	P7	P8	ΔP	Pipe dia (d)	ρ_7	ρ_8	V_7	V_8	Fr7	Fr8	Re	λ_f	λ_{bs}	$\log_{10} \lambda_{bs}$	$\log_{10} m^*$	$\log_{10} Fr_o$	$\log_{10} \rho_o$
	kg/s	kg/s	kPa	kPa	kPa	m	kg/m ³	kg/m ³	m/s	m/s			at bend outlet		Pan and Wypych (1998)				
1	0.06	0.66	34.6	21.0	13.5	0.03	1.61	1.45	34.6	38.4	56.3	62.627	118237	0.84125	0.00122	-2.913	1.0132	1.7968	0.1629
2	0.051	0.62	29.7	17.3	12.4	0.03	1.55	1.41	28.1	31.0	45.8	50.662	92689.1	0.88323	0.00148	-2.828	1.0898	1.7047	0.1492
3	0.061	0.59	33.2	18.6	14.5	0.03	1.59	1.42	32.6	36.6	53.2	59.696	110452	0.85279	0.00154	-2.811	0.993	1.7759	0.1541
4	0.047	0.53	25.7	15.0	10.7	0.03	1.51	1.38	27.1	29.6	44.1	48.26	86613.0	0.89529	0.00156	-2.804	1.0527	1.6836	0.1409
5	0.046	0.48	22.8	12.6	10.1	0.03	1.47	1.35	26.9	29.3	43.9	47.845	84108.9	0.90055	0.00163	-2.786	1.0262	1.6798	0.1319
6	0.039	0.46	21	13	8	0.03	1.45	1.35	23.0	24.6	37.5	40.214	70906.7	0.93184	0.00163	-2.788	1.0739	1.6044	0.1332
7	0.057	0.47	28.9	16.0	12.8	0.03	1.54	1.39	31.5	34.9	51.3	56.982	103187	0.86448	0.00178	-2.75	0.9273	1.7557	0.1448
8	0.027	0.43	18.2	11.2	6.98	0.03	1.42	1.33	16.7	17.7	27.2	28.901	50175.4	0.99857	0.00211	-2.674	1.1954	1.4609	0.1264
9	0.031	0.38	16.5	10.5	5.94	0.03	1.40	1.33	19.0	20.0	30.9	32.618	56301.6	0.97583	0.00177	-2.752	1.1004	1.5135	0.1239
10	0.013	0.36	13.2	9.70	3.52	0.03	1.36	1.31	8.21	8.48	13.3	13.818	23662.8	1.16055	0.00262	-2.58	1.4515	1.1404	0.1205
11	0.011	0.38	11.7	7.64	4.05	0.03	1.34	1.29	7.27	7.54	11.8	12.297	20666.6	1.19241	0.00326	-2.486	1.5271	1.0898	0.1123
12	0.023	0.43	16.9	11.3	5.62	0.03	1.40	1.33	14.0	14.7	22.8	23.987	41672.4	1.03636	0.00205	-2.688	1.2757	1.38	0.1267
13	0.006	0.30	13	4.25	8.75	0.03	1.35	1.25	3.49	3.78	5.69	6.1668	10041.1	1.37760	0.01756	-1.755	1.7436	0.7901	0.0986
14	0.017	0.37	7.84	4.17	3.66	0.03	1.29	1.25	11.5	11.9	18.8	19.505	31737.3	1.09437	0.00191	-2.718	1.3283	1.2901	0.0983

15	0.03	0.39	16.6	9.38	7.27	0.03	1.40	1.31	18.7	20	30.5	32.585	55638.9	0.97814	0.00214	-2.668	1.1097	1.513	0.1192
16	0.037	0.36	18.0	10.2	7.82	0.03	1.41	1.32	22.5	24.1	36.8	39.383	67768.4	0.94031	0.00204	-2.689	0.9943	1.5953	0.1226
17	0.027	0.35	15.2	11.2	4.01	0.03	1.38	1.33	16.5	17.1	27.0	27.973	48552.5	1.00516	0.00152	-2.817	1.1261	1.4467	0.1263
18	0.013	0.33	12.1	7.4	4.72	0.03	1.34	1.29	8.01	8.36	13.0	13.629	22854.1	1.16865	0.00393	-2.406	1.4242	1.1345	0.1114
19	0.009	0.26	12.2	7.20	5.02	0.03	1.34	1.29	5.45	5.70	8.88	9.2979	15563.7	1.26199	0.00770	-2.113	1.4918	0.9684	0.1106
20	0.009	0.24	11.3	8.03	3.28	0.03	1.33	1.29	5.62	5.79	9.17	9.4467	15932.7	1.25609	0.00543	-2.265	1.4412	0.9753	0.1139
21	0.03	0.32	19.5	13	6.58	0.03	1.43	1.35	20.1	21.2	32.7	34.661	61116.0	0.95995	0.00219	-2.659	0.9892	1.5398	0.1332

Table A3.2: Summary output of Regression Analysis for Closely coupled bend data (P7-P8)						
<i>Regression Statistics</i>						
Multiple R	0.896301					
R Square	0.803355					
Adjusted R Square	0.768653					
Standard Error	0.133907					
Observations	21					
<i>ANOVA</i>						
	<i>df</i>	<i>SS</i>	<i>MS</i>	<i>F</i>	<i>Significance F</i>	
Regression	3	1.245323	0.415108	23.15013	3.09E-06	
Residual	17	0.304829	0.017931			
Total	20	1.550152				
	<i>Coefficients</i>	<i>Standard Error</i>	<i>t Stat</i>	<i>P-value</i>	<i>Lower 95%</i>	<i>Upper 95%</i>
Intercept	-1.15938	1.1052	-1.04902	0.308852	-3.49115	1.172386
X Variable 1	-0.22267	0.508236	-0.43813	0.666809	-1.29496	0.849611
X Variable 2	-1.1741	0.462878	-2.53653	0.021291	-2.15069	-0.19752
X Variable 3	3.789257	3.516342	1.077613	0.296261	-3.62958	11.20809

LIST OF PUBLICATIONS

Referred Journals (Under Review) – 2 No.

Tripathi, N.M., Sharma, A., Mallick, S.S. and Wypych, P.W. An Investigation into Energy Loss in Bends for Pneumatic Conveying of Fly Ash. **Particuology, Elsevier** (*Under Review*).

Tripathi, N.M., Kumar, D., Mehta, E., Setia, G., and Mallick, S.S. An Investigation into pressure drop across bends for fluidised dense phase pneumatic conveying systems. **Powder Technology, Elsevier** (*Under Communication*).

Poster Presentation – 1 No.

Tripathi, N.M. and Mallick, S.S. **International Conference on Powder, Granule and Bulk solids: Innovations and Applications**, Thapar University, Patiala, Punjab, November 28-30th, 2013.

